ASE EXPERT CONSENSUS STATEMENT

American Society of Echocardiography Clinical Recommendations for Multimodality Cardiovascular Imaging of Patients with Pericardial Disease

Endorsed by the Society for Cardiovascular Magnetic Resonance and Society of Cardiovascular Computed Tomography

Allan L. Klein, MD, FASE, Chair, Suhny Abbara, MD, Deborah A. Agler, RCT, RDCS, FASE, Christopher P. Appleton, MD, FASE, Craig R. Asher, MD, Brian Hoit, MD, FASE, Judy Hung, MD, FASE, Mario J. Garcia, MD, Itzhak Kronzon, MD, FASE, Jae K. Oh, MD, FASE, E. Rene Rodriguez, MD, Hartzell V. Schaff, MD, Paul Schoenhagen, MD, Carmela D. Tan, MD, and Richard D. White, MD, *Cleveland and Columbus, Ohio; Boston, Massachusetts; Weston, Florida; Scottsdale, Arizona; Rochester, Minnesota; Bronx and New York, New York*

(J Am Soc Echocardiogr 2013;26:965-1012.)

Keywords: Pericardial disease, Echocardiography, Cardiovascular magnetic resonance, Cardiac computed tomography

TABLE OF CONTENTS

From the Cleveland Clinic, Cleveland, Ohio (A.L.K., D.A.A., E.R.R., P.S., C.D.T.); Massachusetts General Hospital, Boston, Massachusetts (S.A., J.H.); the Cleveland Clinic, Weston, Florida (C.R.A.); the Mayo Clinic, Scottsdale, Arizona (C.P.A.); the Mayo Clinic, Rochester, Minnesota (J.K.O., H.V.S.); University Hospitals Case Medical Center, Cleveland, Ohio (B.H.); Montefiore-Einstein Center for Heart and Vascular Care, Bronx, New York (M.J.G.); Lenox Hill Hospital, New York, New York (I.K.); and The Ohio State University Medical Center, Columbus, Ohio (R.D.W.).

The following authors reported no actual or potential conflicts of interest in relation to this document: Deborah A. Agler, RCT, RDCS, FASE, Christopher P. Appleton, MD, FASE, Judy Hung, MD, FASE, E. Rene Rodriguez, MD, Hartzell V. Schaff, MD, Paul Schoenhagen, MD, Carmela D. Tan, MD, and Richard D. White, MD. The following authors reported relationships with one or more commercial interests: Allan L. Klein, MD, FASE, receives honoraria for books from Elsevier and Lippincott Williams & Wilkins and serves on a multicenter trial steering committee for Bayer. Suhny Abbara, MD, serves as a consultant for Perceptive Informatics. Craig R. Asher, MD, coedited a book published by Lippincott Williams & Wilkins. Brian Hoit, MD, FASE, has served as a speaker for Philips Medical Systems. Mario J. Garcia, MD, receives royalties from Lippincott Williams & Wilkins and Elsevier and owns stock in Pfizer. Itzhak Kronzon, MD, FASE, has received an honorarium from Philips Medical Systems. Jae K. Oh, MD, FASE, has received a research grant from Toshiba and core laboratory funding from Medtronic.

Reprint requests: American Society of Echocardiography, 2100 Gateway Centre Boulevard, Suite 310, Morrisville, NC 27560 (E-mail: ase@asecho.org).

0894-7317/$36.00

http://dx.doi.org/10.1016/j.echo.2013.06.023

Abbreviations

CMR = Cardiovascular magnetic resonance

CP = Constrictive pericarditis

CT = Computed tomography

ECG = Electrocardiographic

IVC = Inferior vena cava

LGE = Late gadolinium enhancement

LV = Left ventricular

MR = Magnetic resonance

NSAID = Nonsteroidal anti-inflammatory drug

PEff = Pericardial effusion

PET = Positron emission tomography

PW = Pulsed-wave

RA = Right atrial

RV = Right ventricular

SE = Spin-echo

SSFP = Steady-state free precession

STIR = Short-tau inversion recovery

SVC = Superior vena cava

TEE = Transesophageal echocardiography

T1W = T1-weighted

TTE = Transthoracic echocardiography

T2W = T2-weighted

2D = Two-dimensional

ORGANIZATION OF THE WRITING COMMITTEE

The writing committee was made up of experts in pericardial diseases and imaging of the pericardium from the American Society of Echocardiography (ASE), the Society for Cardiovascular Magnetic Resonance Imaging, and the Society of Cardiovascular Computed Tomography. The document was reviewed by the ASE Guidelines and Standards Committee and official reviewers nominated by the Society for Cardiovascular Magnetic Resonance Imaging and the Society of Cardiovascular Computed Tomography.

The objective of this document is to provide a consensus expert opinion on the appropriate use of multimodality imaging in the diagnosis and management of pericardial diseases. This document will allow clinicians to weigh the evidence on the strengths and weaknesses of a particular imaging modality in the evaluation and management of pericardial diseases. Of note, there have been only a small number of randomized clinical trials on pericardial diseases[1-3]; thus, we use a consensus of expert opinions in this report and do not attempt to use the standard level-of-evidence grading system (Levels A–C). The document focuses on multimodality imaging of pericardial diseases, including echocardiography, computed tomography (CT), and cardiovascular magnetic resonance (CMR), and is not comprehensive with regard to clinical presentation and treatment, which have been discussed in recent reviews.[4,5]

I. INTRODUCTION

A. Clinical Perspective

Pericardial diseases are very common worldwide, encountered in various settings (including primary care, emergency room, and subspecialty settings such as rheumatology, infectious diseases, oncology, and cardiology), and can have significant morbidity as well as

Table 1 Comparison of multimodality imaging modalities in the evaluation of pericardial diseases

	Echocardiography	CT	CMR
Main strengths	• First-line imaging test in the diagnostic evaluation of pericardial disease • Readily available • Low cost • Safe • Can be performed at bedside or urgent situations • Portable • TEE available for better evaluation • High frame rate • Can be performed with respirometer	• Second-line for better anatomic delineation • Evaluation of associated/ extracardiac disease • Preoperative planning • Evaluation of pericardial calcification	• Second-line for better anatomic delineation • Superior tissue characterization • Evaluation of inflammation
Main weaknesses	• Limited windows, narrow field of view • Technically limited with obesity, COPD, or postoperative setting • Relatively operator dependent • Low signal-to-noise ratio of the pericardium • Limited tissue characterization	• Use of ionizing radiation • Use of iodinated contrast • Functional evaluation only possible with retrospective gated studies (higher radiation dose, suboptimal temporal resolution) • Difficulties in case of tachycardia or unstable heart rhythm (particularly for prospective gated studies) • Need for breath-hold • Hemodynamically stable patients only	• Time-consuming, high cost • Preferably stable heart rhythms • Relatively contraindicated in case of pacemaker or ICD • Lung tissue less well visualized • Calcifications not well seen • Use of gadolinium contrast contraindicated in case of advanced renal dysfunction (glomerular filtration rate <30 mL/min) • Use of some breath-hold sequences • Hemodynamically stable patients only

COPD, Chronic obstructive pulmonary disease; *ICD*, implantable cardioverter-defibrillator.
Adapted with permission from Verhaert.[8]

mortality.[5,6] Patients can present with variable symptoms of chest pain, shortness of breath, ascites, leg swelling, and hypotension. Pericardial diseases can be grouped into a constellation of clinical syndromes, including acute pericarditis, recurrent pericarditis, pericardial effusion (PEff) or tamponade, constrictive pericarditis (CP), pericardial masses, and congenital anomalies of the pericardium. The etiologic classification of pericardial diseases includes infectious, autoimmune, post–myocardial infarction, and autoreactive causes, as reported in the European pericardial guidelines.[7] In a substantial subset of patients, etiology is not apparent and is classified as idiopathic. However, the diagnosis as well as the management of pericardial diseases can be complex, with such conditions as mixed CP with myocardial and/or valvular heart disease, transient CP, effusive CP, or localized postoperative tamponade.[8] Clearly, the evaluation of these pericardial conditions can be difficult to detect clinically; therefore, there is an increasing role for the use of imaging techniques including echocardiography, CMR, and CT,[9,10] in the diagnosis and management of these conditions.

B. Role of Integrated Multimodality Imaging

Multimodality imaging is an integral part of modern management for most, if not all, cardiovascular conditions, including pericardial diseases. Although imaging is often performed to confirm an initial clinical suspicion, it sometimes provides a clinically unsuspected diagnosis as well as a complementary approach to the clinical assessment. Therefore, imaging should follow a careful history and physical examination, electrocardiography (ECG), and chest x-ray and then be focused toward the clinical working diagnosis. This stepwise approach is important to avoid unnecessary testing with its potential risk for side effects, false-positive diagnoses, and inappropriate allocation of resources, thus avoiding excessive costs. Among multimodality imaging tests, echocardiography is most often the first-line test, followed by CMR[11] and/or CT.[12,13] Each of the tests can be useful in the evaluation of the structure and hemodynamic and/or functional disturbances of pericardial diseases. For example, echocardiography with respirometric recording would be considered the first-line modality to evaluate the anatomic and physiologic features of CP. CMR and CT would be second-line tests to further assess the degree of increased pericardial thickness, functional effects of the constrictive process, inflammation, as well as the distribution of calcium in the pericardium.[8] It is important to note that all three tests are rarely necessary in the diagnosis of CP unless there are technically poor or diagnostically uncertain transthoracic echocardiographic studies, there is mixed CP and restriction, being evaluated for pericardiectomy, or there is a concern for transient constriction with ongoing inflammation, as an example. Sometimes, an invasive hemodynamic study is necessary to evaluate myocardial versus pericardial diastolic heart failure, especially in the setting of atrial fibrillation.

C. Which Test to Choose?

The strengths and weaknesses of each modality are shown in Table 1.[8] A description of the pericardial disease–specific protocol for each modality is shown in Table 2 and the Appendix (available at www.onlinejase.com). Echocardiography remains as an initial imaging test in most scenarios because of its ease of use, wide availability, bedside

Table 2 Protocols and findings for the multimodality imaging modalities in the evaluation of pericardial diseases (see Appendix)

Echocardiography	Prospective or retrospective electrocardiographically gated multidetector CT	CMR
2D echocardiography • PEff (size, location, free flowing vs organizing, suitability for pericardiocentesis vs window) • Pericardial thickness (particularly TEE) • Collapse of right-sided chambers (duration of diastole and relation with respiration) • Early diastolic septal bounce, respiratory shift of the ventricular septum • IVC plethora • Pleural effusion/ascites • RA tethering (best seen by TEE) • Stasis of agitated saline contrast in right atrium (sluggish flow)	Axial imaging • Pericardial calcification and thickening • Localization and characterization of PEffs, cysts, or masses • Evaluation of lungs (pleural effusion, postradiation fibrosis, malignancy), and liver (cirrhosis, ascites) • Proximity of bypass grafts and/or other vital structures to the sternum (preoperative planning)	Bright-blood single-shot SSFP and black-blood axial stacks* (half Fourier SSTSE, electrocardiographically gated) • Presence of pleural effusion, ascites, distension of the IVC, assessment of pericardial thickening
Doppler + simultaneous respirometry† • Restrictive mitral inflow pattern • Reciprocal respiratory changes of mitral (and tricuspid) inflow • Reciprocal respiratory changes of diastolic forward flow velocity and end-diastolic flow reversal in hepatic veins • Tissue Doppler velocities of mitral annulus, color Doppler M-mode of mitral inflow • 2D strain of longitudinal and circumferential deformation	Multiplanar reconstruction • Chamber dimensions (RA enlargement, conical ventricular deformity) • Assess coronary patency	Black-blood images‡ (T1W + T2W fast SE); optional: T2W STIR (edema-weighted) fast SE • Tissue characterization, measurement of pericardial thickness • Assessment of pericardial inflammation and masses (STIR sequence)
M-mode • Flattening of the posterior wall during diastole • Respiratory variation of ventricular size	Volume-rendered imaging • Extent and distribution of pericardial calcification	Tagged cine images§ (T1W gradient-echo) • Epicardial/pericardial tethering
	Cine imaging (retrospectively gated study only) • Functional evaluation (septal bounce, pericardial tethering)	Bright-blood cine images‖ (SSFP) • Atrial/ventricular size and function • Diastolic restraint • Conical deformity of the ventricles • Myocardial tethering • Diastolic septal bounce • Pericardial thickening and/or effusion
		LGE images¶ (phase-sensitive inversion-recovery sequence) • Detection of pericardial inflammation
		Real-time gradient-echo cine image# • Monitor respiratory variation of ventricular septal motion and interventricular dependence

SSTSE, Single-shot turbo SE.
*Orientation: axial.
†Doppler measurements should be repeated in the sitting position (reducing preload) in case of nondiagnostic findings and suspicion for constriction to lower the preload.
‡Orientation: two-chamber, three-chamber, and four-chamber views plus three short-axis LV slices (basal, mid, and distal).
§Orientation: three short-axis LV slices (basal, mid, and distal); optional: two-chamber, three-chamber, and four-chamber views.
‖Orientation: two-chamber, three-chamber, and four-chamber views plus 3 short-axis LV slices.
¶Orientation: two-chamber, three-chamber, and four-chamber views plus short-axis stack.
#Orientation: basal and mid short-axis slice with diaphragm in view.
Adapted with permission from Verhaert.[8]

availability, cost-effectiveness, and comprehensive assessment of both anatomy and physiology. After review of the results of transthoracic echocardiography (TTE) and integration with other available data, such as the clinical examination and ECG, additional imaging is often not necessary in many patients. However, the use of additional imaging modalities should be justified by the expected incremental information complementary to the physiologic and structural information obtained from TTE.

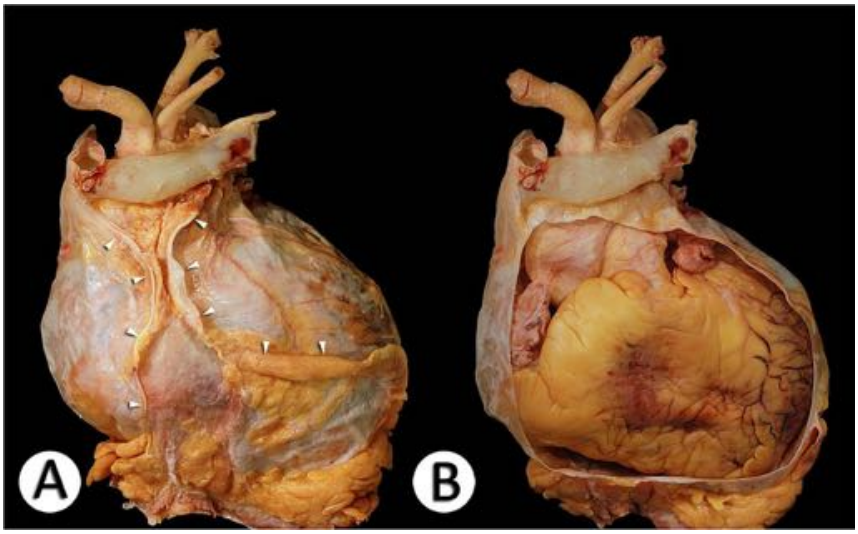

Figure 1 **(A)** Anterior view of the intact parietal pericardial sac. The attachment of the fibrous sac to the diaphragm is seen at the base. Abundant epipericardial fat is conspicuously present at the pericardial-diaphragm junction. The mediastinal pleura invest the lateral portion of fibrous pericardium. The anterior reflections of the mediastinal pleura are indicated by the *white arrowheads*. The space between the *arrowheads* corresponds to the attachment of the pericardium to the posterior surface of the sternum. Superiorly, the left innominate vein is seen merging with the SVC. The arterial branches of the aortic arch are just dorsal to the innominate vein. **(B)** The anterior portion of the pericardial sac has been removed to show the heart and great vessels in anatomic position. It distinctly shows how the proximal segments of the great arteries are intrapericardial. At that point, there is fusion of the adventitia of the great vessels with the fibrous pericardium.

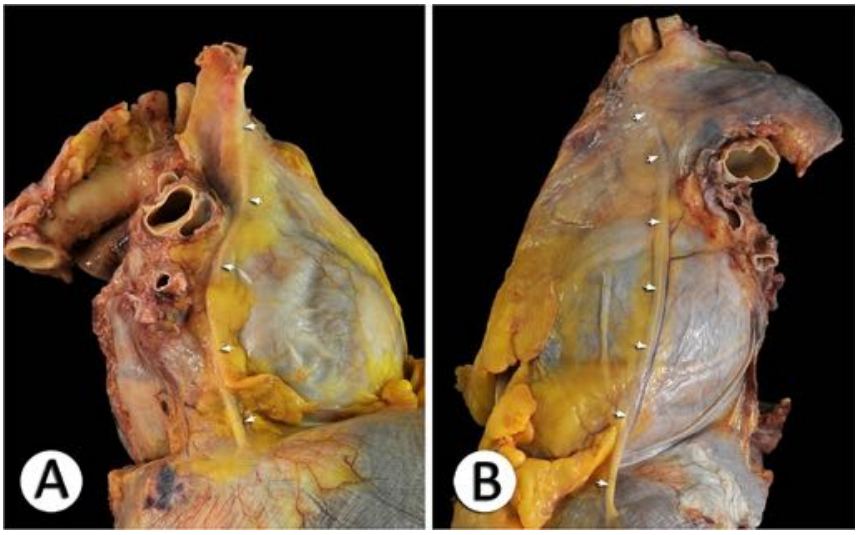

Figure 2 **(A)** *Right lateral view* of the pericardium shows the right phrenic nerve (*arrows*). It courses parallel and lateral to the SVC and continues downward, anterior to the right pulmonary hilum, toward the diaphragm. **(B)** *Left lateral view* shows the left phrenic nerve (*arrows*) descending over the *left atrial* appendage and anterolateral LV before reaching the diaphragm.

D. Limitations

We acknowledge several limitations of this report. Obviously, the recommendations for the groups of clinical scenarios may not fit individual situations and may therefore require us to deviate from the proposed decision trees. Current published data are limited and based on relatively small, single-center experience, with a lack of large randomized prospective trials. The clinical presentation, diagnostic considerations, and therapeutic interventions for pericardial diseases described in this report would apply only in part to the care of patients in developed countries[14] and not necessarily developing countries.

II. ANATOMY OF THE PERICARDIUM

A. Fibrous and Serosal Pericardium

The pericardium, a roughly flask-shaped sac that contains the heart, consists of a fibrous and a serosal component. The outer fibrous sac is composed primarily of collagen fibers with interspersed short elastic fibrils.[15] The fibrous envelope is continuous with the adventitia of the great vessels superiorly and is attached to the central tendon of the diaphragm inferiorly. It is attached anteriorly to the sternum by

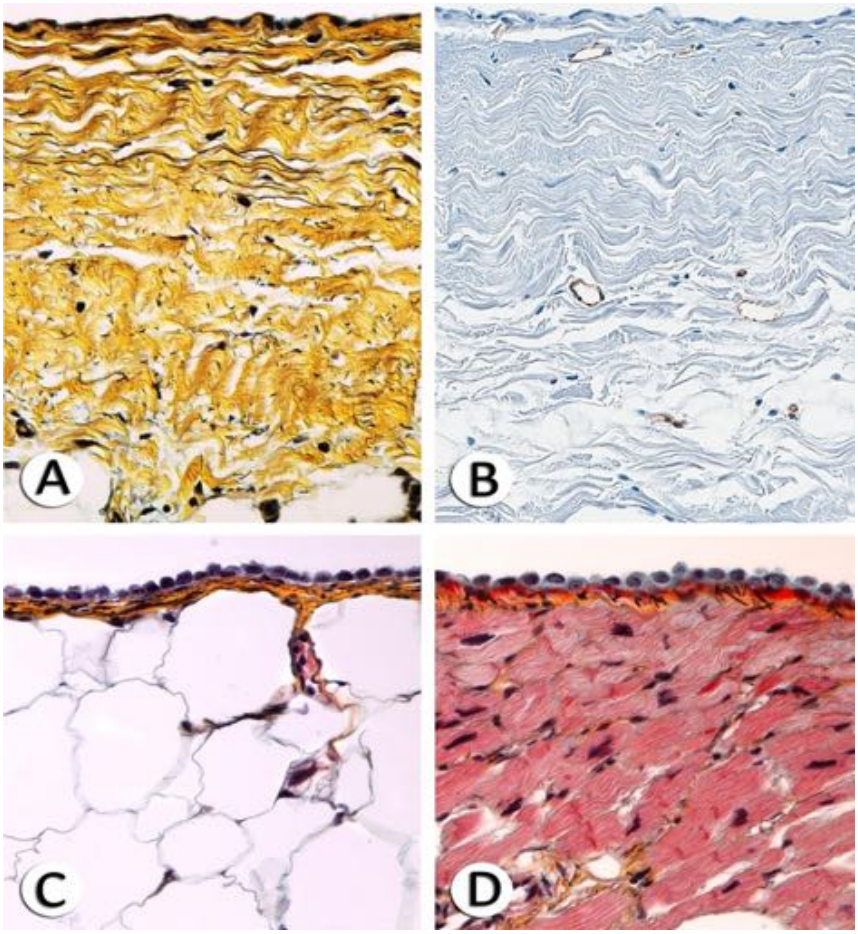

Figure 3 **(A)** Normal, full-thickness parietal pericardium is shown. It consists of a layer of mesothelial cells and compact layers of dense wavy collagen (*yellow*) with interspersed short elastic fibers (*black*). **(B)** Fibroblasts with elongated nuclei and scant thin blood vessels are normally present in the parietal pericardium. CD34 immunostaining highlights the endothelial cells of capillaries. **(C)** The visceral pericardium (also called epicardium) consists of a mesothelial cell layer and a thin subepithelial layer of collagen with elastic fibers. The mesothelial cells show distinct microvilli. Beneath the visceral pericardium is epicardial adipose tissue. **(D)** In other areas of the visceral pericardium (or epicardium), only a thin layer of fibrous tissue (*yellow*) separates the mesothelial cells from the myocardium with absence of epicardial fat. Original magnifications 400×; A, C, and D: Movat pentachrome stain; B: CD34 immunoperoxidase.

sternopericardial ligaments. In the anteroinferior portion, the pericardium may come in direct contact with the costal cartilages of the left fourth to sixth ribs. The lateral surfaces are invested by the mediastinal part of the parietal pleura (Figure 1). Posteriorly, it is related to the major bronchi, esophagus, and descending thoracic aorta.

The phrenic nerves and pericardiophrenic vessels are contained in a bundle between the fibrous pericardium and the mediastinal pleura anterior to the pulmonary hilum (Figure 2). The serosal component consists of a single layer of mesothelium that forms a parietal and a visceral layer enclosing the pericardial cavity. The parietal layer lines the fibrous pericardium, and together, these structures form the parietal pericardium (Figures 3A and 3B). The visceral layer is also known as the epicardium and covers the heart (Figures 3C and 3D). Between the visceral pericardium and the myocardium is a variable amount of epicardial adipose tissue (Figure 4). Epicardial fat is most abundant along the atrioventricular and interventricular grooves and over the right ventricle, especially at the acute border. The epicardial fat contains the coronary arteries and veins, lymphatics, and nerve tissue. The parietal pericardium can be visualized as a curvilinear density on CT and low-intensity signal on CMR delineated by epipericardial and epicardial fat (Figures 5–7). The parietal pericardium exhibits a normal variation in thickness from region to region and is between 0.8 and 1 mm thick as measured in anatomic studies but appears slightly thicker on imaging.[16] The thinnest segments of the pericardium ranged from 0.7 to 1.2 mm in width when measured by CT and 1.2 to 1.7 mm on CMR.[17,18] The discrepancy in pericardial thickness may be partially explained by including small amounts of physiologic pericardial fluid in the measured thickness.[18] TTE is unreliable for measuring pericardial thickness; however, TEE has been shown to be reproducible, compared with CT, for pericardial thickness measurements in normal controls and patients with CP.[19]

B. Pericardial Sinuses and Recesses

The visceral pericardium is reflected to become continuous with the parietal pericardium as it invests the proximal segments of the great arteries, the venae cavae, and the pulmonary veins (Figure 8). The aorta and main pulmonary artery together are completely ensheathed

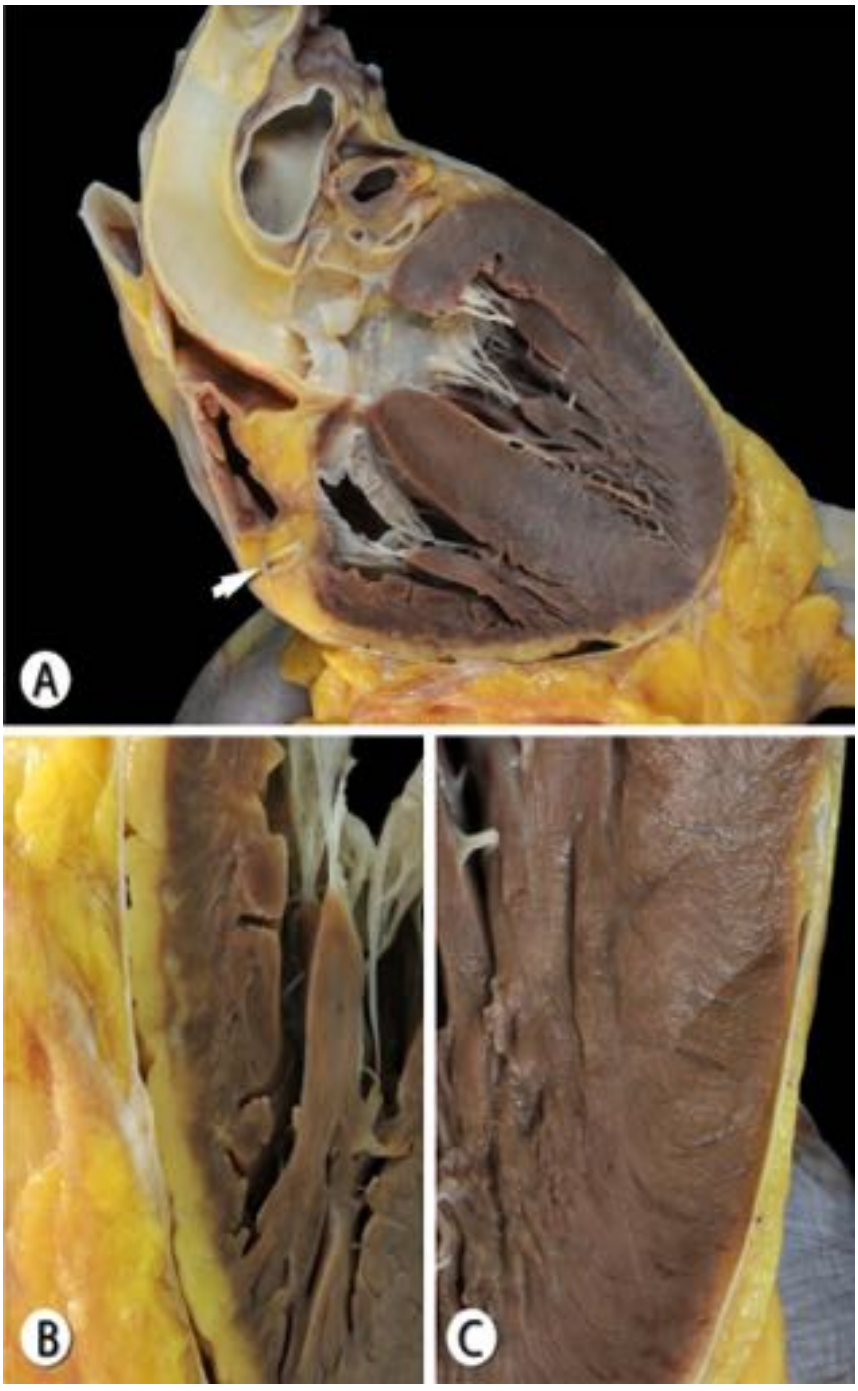

Figure 4 **(A)** Coronal section of the heart showing that the epicardial fat is abundant in the right atrioventricular sulcus where a cross-section of the right coronary artery is seen (*arrow*). The RV free wall also contains a variable amount of epicardial fat that helps outline the pericardium. Note the abundance of epipericardial fat at the angle between the pericardium and diaphragm anteriorly. **(B)** The parietal pericardium is well delineated by the epipericardial fat on the anterior diaphragmatic surface and epicardial fat over the right ventricle. **(C)** The left ventricle contains little epicardial fat, resulting in poor visualization of the pericardium in this area on imaging.

in one investment with a bare area between them. A second investment separately covers the veins. These reflections of the serous pericardium between the arteries and the veins at the base of the heart form the pericardial sinuses and recesses.

The transverse sinus is a passage that separates the arteries located anteriorly from the atria and veins posteriorly (Figure 9). This space lies behind the ascending aorta and main pulmonary artery and above the roof of the left atrium. It extends upward along the right side of the ascending aorta, where it forms the superior aortic recess between the aorta and the superior vena cava (SVC; Figure 10). It extends downward to the level of the aortic valve; the space between the ascending aorta and the right atrium is called the inferior aortic recess of the transverse sinus (Figure 11).[20] The lateral extensions of the transverse sinus inferior to the proximal left and right

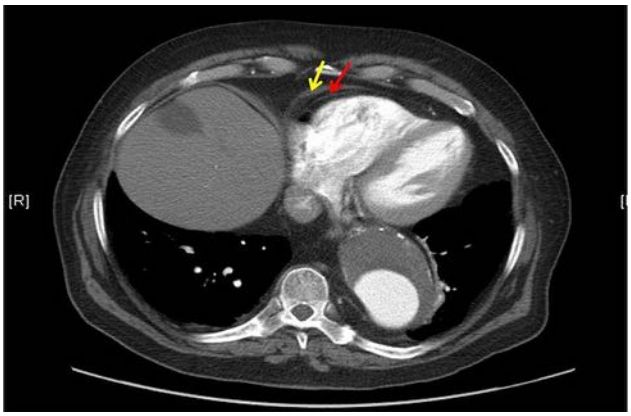

Figure 5 Contrast-enhanced computed tomographic nongated axial image showing the pericardium anterior to the right ventricle (*yellow arrow*), surrounded by layers of epicardial (*red arrow*) and pericardial fat.

pulmonary arteries are called the left and right pulmonic recesses, respectively. The postcaval recess is an extension of the pericardial cavity proper that lies behind and on the right lateral aspect of the SVC. It is separated from the transverse sinus by the reflection of the serous pericardium that covers the SVC across the right pulmonary artery and right superior pulmonary vein. The oblique sinus is a cul-de-sac located behind the left atrium delineated by the pulmonary veins and the inferior vena cava (IVC) and directly abuts the carina (Figure 12).

C. Lymphatic Drainage, Vascular Supply, and Innervation

The pericardial cavity normally contains <50 mL of serous fluid that can be detected in the superior aortic recess and transverse sinuses on CT.[21] The pericardial fluid is an ultrafiltrate of plasma that comes from epicardial and parietal pericardial capillaries. It also contains prostaglandins secreted by mesothelial and endothelial cells that modulate cardiac reflexes and coronary tone.[22,23] Pericardial fluid is drained by the lymphatic system on the surface of the heart and in the parietal pericardium.

The arterial supply of the pericardium comes from the pericardiophrenic and musculophrenic arteries, which are branches of the internal thoracic artery, and the descending thoracic aorta. Venous drainage is provided by pericardiophrenic veins that drain directly into or via the superior intercostal veins and internal thoracic veins to the innominate veins.[24]

The parasympathetic nerve supply of the pericardium is from the vagus and left recurrent laryngeal nerves as well as branches from the esophageal plexus. Sensory fibers from the phrenic nerve supply sensation to the pericardium. Sympathetic innervation is derived from the first dorsal ganglion, stellate ganglion and the aortic, cardiac, and diaphragmatic plexuses.[25]

D. Pericardial Response to Injury

The pericardium has a limited response to injury, which is manifested as exudation of fluid, fibrin, and inflammatory cells (Figure 13). Healing with organization may result in focal or diffuse obliteration of the pericardial cavity by adhesions between the visceral and parietal pericardium. Fibrous proliferation of the pericardium may predominantly involve only one of the serosal components or may involve both the parietal and visceral pericardium. Chronic effusions may be associated with pericardial thickening. At times, loculated accumulation of fluid may result in cardiac compression and a constrictive clinical picture. Calcific deposits may be focal or extensive and likely represent end-stage reaction to injury.

The histologic features of excised pericardium for CP are generally nonspecific in terms of etiologic diagnosis and most often reflect a spectrum from organizing fibrinous pericarditis to organized fibrocalcific pericarditis. Pericardial late gadolinium enhancement (LGE) on CMR shows an association with the presence of granulation tissue and active inflammation with increased fibroblastic proliferation and neovascularization (Figure 14).[26]

III. PATHOPHYSIOLOGY OF THE PERICARDIUM

A. Introduction

Although not essential for life, the pericardium performs important anatomic and physiologic functions (Table 3). The pericardium partitions the heart from the pulmonary space lessening the chance for contiguous infections from the lungs. Both pericardial layers help limit distension of the cardiac chambers if there is acute volume overload that prevents anatomic deformation of both the chambers and the mitral and tricuspid apparatus, which may prevent valvular regurgitation and further distension. The pericardium also facilitates interaction and coupling of the ventricles and atria, with the thin-walled right atrium and right ventricle more subject to the influence of changes in pericardial pressure than the thicker walled left ventricle, with its higher filling pressures.[27]

B. Mechanical Effects of the Pericardium

When cut, the relatively inelastic parietal pericardium retracts, indicating that it exerts pressure on the underlying myocardial chambers. This effect is greatest on the thinner walled right atrium and right ventricle, in which ≥50% of normal diastolic pressure is due to this pericardial influence. The effect on cardiac chamber pressures is magnified by either a rapid increase in total cardiac volume, as is seen with exercise, hypervolemia, or acute severe valvular regurgitation, or with an increase in pericardial fluid above the normal "reserve volume," which increases cardiac pressures and reduces cardiac filling. Conversely, the mechanical effects of the pericardium on the heart are diminished by hypovolemia.

C. Pericardial Reserve Volume and Pressure-Volume Relations without PEff

As noted, because of the many potential spaces and sinuses in the pericardial sac, there is a small pericardial reserve volume of approximately <50 mL. Although relatively small, this amount is adequate to allow increased right heart filling with normal inspiration without increased pericardial restraint and increased right heart chamber pressures. However, with marked swings in intrathoracic pressures due to acute dyspnea, right heart filling during inspiration can exceed the pericardial reserve volume, causing pericardial constraint and cardiac pressures to increase. This "overfilling" of the right heart may decrease left heart filling through ventricular interdependence, the process by which physical changes of one ventricle affect the other (Figure 15). These interactions occur chiefly in diastole and are due to the inelastic parietal pericardium. Ventricular interdependence

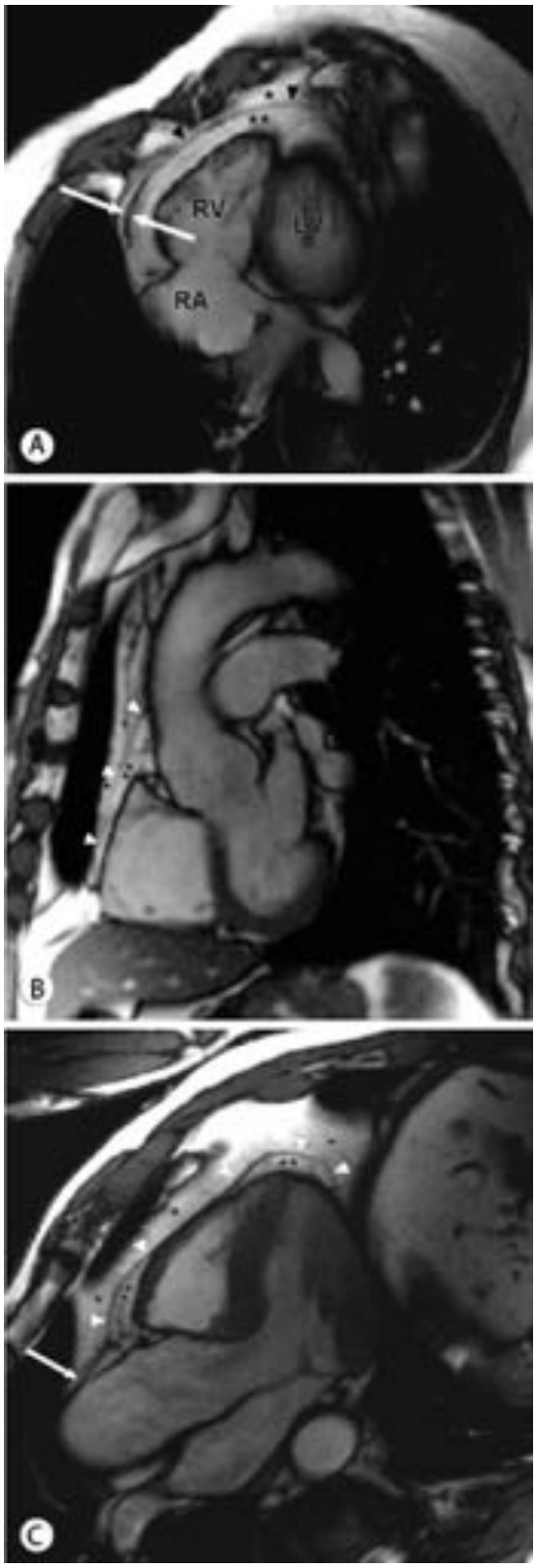

Figure 6 SSFP gradient-echo white blood cine images in modified four-chamber view (inferior image from a four-chamber stack): **(A)** basilar LV short axis view, **(B)** three-chamber view, and **(C)** pericardial fat (*asterisk*) between chest wall and pericardial layers (*arrowheads*), and epicardial fat between pericardium and myocardium (*double asterisk*). Note that the visceral (also known as epicardium, serous) and parietal (fused serous and fibrous layers) pericardium are indistinguishable from each other and appear as one single thin line (*arrowheads*). The epicardium and parietal pericardium are visible as separate structures (*white arrows*) where the layers are separated by a small physiologic pocket of fluid as demonstrated in **A**. Each individual layer artificially appears thicker than the sum of the two because of an artifact whereby voxels containing both fluid and fat become black, thus creating black artificial lines that do not reflect the true anatomy. Another example of this artifact is noted between epicardial fat and the RV anterior free wall, where the separating artificial black line has no anatomic correlate. Note the pericardial reflection at the ascending aorta referred to as the superior aortic sinus (*arrow* in **C**).

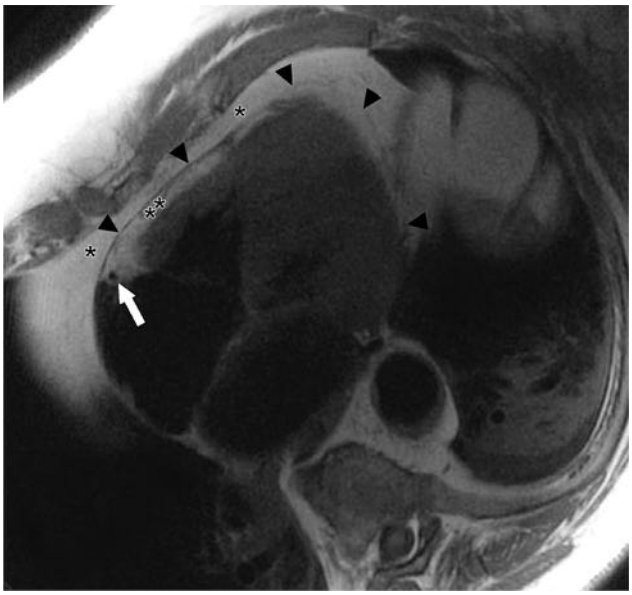

Figure 7 Black-blood fast SE sequence without fat suppression shows pericardial (*asterisk*) and epicardial (*double asterisks*) fat separated by epicardial and parietal pericardial layers (*arrowheads*) that appear inseparable as one thin line. The epicardial fat contains the coronary arteries and cardiac veins. Note that the right coronary artery (*arrow*) is surrounded by right atrioventricular groove fat.

and interaction play a prominent role in the physiology of acute cardiac dilation, cardiac tamponade, and CP.

The parietal pericardium exhibits a nonlinear pressure-volume relation. There is an initial flat portion in the pressure-volume relation whereby small changes in pericardial volume produce either no or minimal change in pericardial pressure. However, once the pericardial reserve volume is exceeded, there is an upward bend in pressure. With additional volume, the curve rapidly steepens so that even small increases in pericardial fluid result in large changes in pericardial pressure. Thus, an acute, relatively small PEff may inhibit cardiac filling and cause cardiac tamponade. On the other hand, a very large, chronic PEff is seen with minimal hemodynamic effect if the fluid accumulation is slow enough to enable the pericardium to stretch and grow, which causes an increase in compliance by shifting its pressure-volume relation to the right (Figure 16).[28]

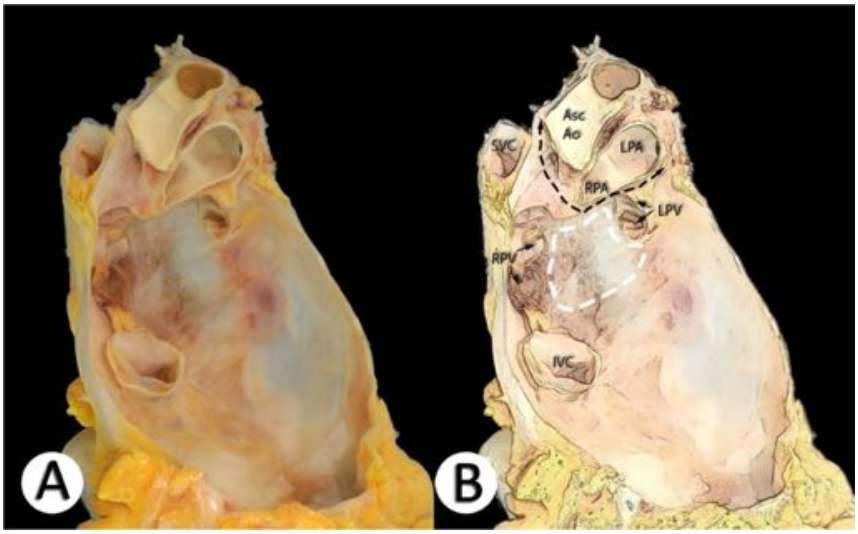

Figure 8 **(A)** The anterior portion of the pericardial sac and the heart has been removed. This view exposes the lateral, dorsal, and diaphragmatic aspects of the pericardial sac. The visceral and parietal pericardium is continuous at the basal region of the heart, where the great arteries and veins are located. The aorta (Ao) and pulmonary trunks are enclosed in one sheath, while the pulmonary veins and venae cavae are covered separately. **(B)** The transverse sinus (*black arrow path*) is the space between the arterial and venous pericardial reflections that forms an access between the right and left sides of the pericardial cavity. The cul-de-sac behind the left atrium bounded by the pulmonary veins is called the oblique sinus (*white interrupted line area*). *LPA*, Left pulmonary artery; *LPV*, left pulmonary veins; *RPA*, right pulmonary artery; *RPV*, right pulmonary veins.

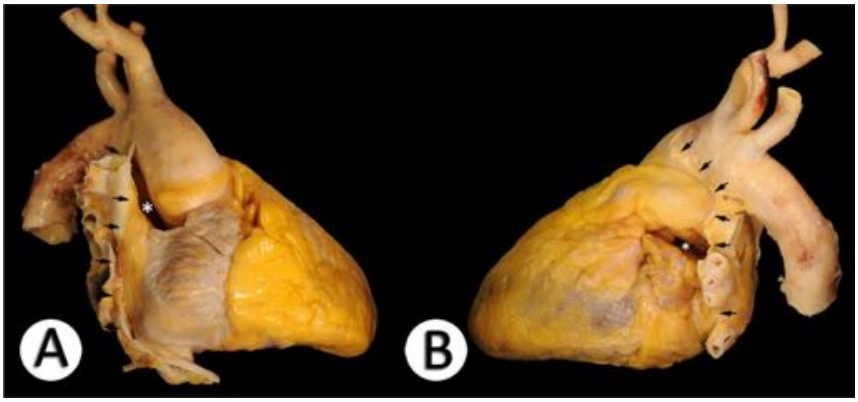

Figure 9 The heart is shown with only a rim of the pericardium left and marked by the *arrows*. The transverse sinus is indicated by the *asterisks* as shown from the right and left sides of the heart.

IV. PERICARDIAL DISEASES

A. Acute Pericarditis

1. Introduction. Acute pericarditis is a pericardial syndrome that is characterized by infiltration of inflammatory cells into the pericardium. There are a multitude of causes of acute pericarditis; in general, most cases are self-limited. The etiology of acute pericarditis is quite variable and can result from a primary pericardial process or secondary to a number of systemic illnesses, such as lupus, acute myocardial infarction, and malignancy.[29,30] Most cases of acute pericarditis are idiopathic or viral. It usually lasts <3 months, after which time it can be referred to as chronic pericarditis.[7] Acute pericarditis typically presents with characteristic chest pain that is described as substernal and sharp, often acute in onset, and often radiating to the trapezius ridge. Pericarditic pain is pleuritic, worse when lying down, and better when sitting forward. The positional nature of the pain is a distinguishing feature from myocardial ischemia.[31,32] Physical signs include a pericardial friction rub and characteristic ECG changes as shown in Figure 17.[32] Table 4 shows criteria for the diagnosis of acute pericarditis. Altogether, the diagnosis of acute pericarditis is based on the presence of (1) typical chest pain, (2) a pericardial rub, (3) typical ECG changes, and (4) new or worsening PEff. In most cases, two or more of these findings are present. However, if not, ancillary supportive data should be sought, including elevations in inflammatory markers (Westergren sedimentation rate, C-reactive protein) or ultrasensitive C-reactive protein, white blood count or troponin levels or a fever.[4] In selective equivocal or refractory cases in which definitive diagnoses are required, imaging by CMR with T2-weighted (T2W) images and LGE may be used to identify pericardial edema and inflammation.[8]

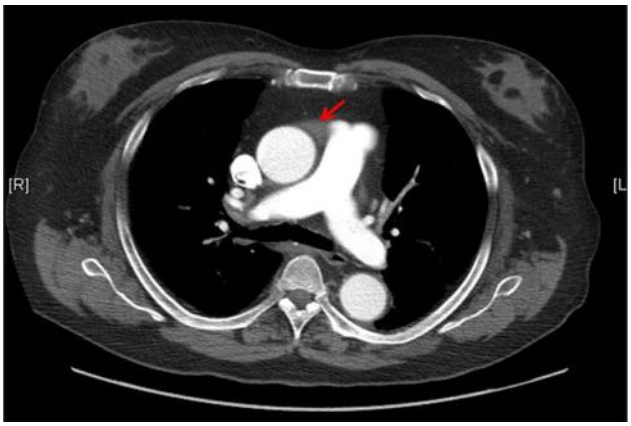

Figure 10 Contrast-enhanced computed tomographic nongated axial image shows the superior aortic recess of the transverse sinus (*arrow*).

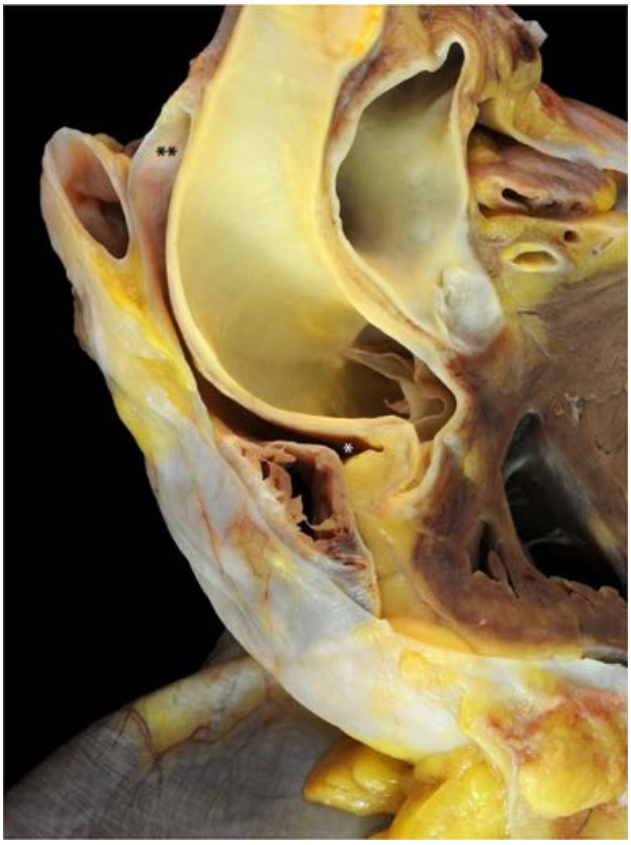

Figure 11 The superior aortic recess is indicated by the *double asterisks*. It is a space between the ascending aorta and SVC. The inferior aortic recess (*asterisk*) is a space between the aorta and the right atrium.

Treatment includes exercise restriction, aspirin or nonsteroidal anti-inflammatory drugs (NSAIDs),[33] and colchicine.[4] In some cases, because of poor prognostic predictors, intensive anti-inflammatory therapy is initiated with NSAIDs, colchicine, and steroids, which can be guided by imaging.[8]

2. General Indications for Imaging. Echocardiography is recommended as an initial noninvasive imaging test for all patients with acute pericarditis because it is an accurate diagnostic method to assess

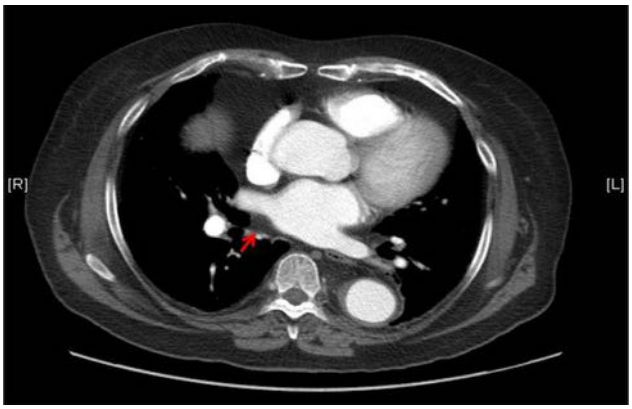

Figure 12 Contrast-enhanced computed tomographic nongated axial image shows the oblique sinus (*arrow*).

for PEff[7,31,32] and tamponade physiology. It should be done within 24 hours of presentation. CT and CMR should be considered when there are associated poor prognostic features. A summary of imaging findings in acute pericarditis is shown in Table 5.

3. Echocardiography. TTE is the first-line imaging test to detect PEff[7,31,32] and tamponade physiology (Figure 18). Although many patients with acute pericarditis may appear to have normal echocardiographic results, the presence of a PEff is consistent with acute pericarditis. Other findings may include increased pericardial brightness, pericardial thickening, and abnormal septal bounce, suggesting early constriction. A PEff can be trivial to large and localized, loculated, or circumferential. Importantly, tamponade physiology can be seen in 3% of patients. Intrapericardial fibrinous strands suggest either an inflammatory etiology or clotted blood. Intrapericardial masses may be seen with primary or secondary pericardial tumors or with inflammatory processes. TTE may also help differentiate acute pericarditis from myocardial ischemia or injury by excluding wall motion abnormalities, even though a small percentage of patients with acute pericarditis (5%) will demonstrate segmental wall motion abnormalities. This is an important indication for acute pericarditis because not infrequently, these patients are referred directly to coronary angiography for suspected ST-segment elevation myocardial infarction.[34]

4. CT. On CT, noncalcified pericardial thickening with a PEff is suggestive of acute pericarditis.[9] As the duration and severity of pericardial inflammation worsens, increasing pericardial irregularity is detected on CT.[35] With the administration of iodinated contrast media, enhancement of the thickened visceral and parietal surfaces of the pericardial sac confirms the presence of active inflammation (Figure 19).[36-38] Computed tomographic attenuation values of PEff can help in the differentiation of exudative fluid (20–60 Hounsfield units), as found with purulent pericarditis, and simple transudative fluid (<10 Hounsfield units).[8,39,40]

5. CMR. As on CT, noncalcified pericardial thickening, combined with PEff, is suggestive of acute pericarditis on CMR.[9,39] With pericarditis, signal intensity on spin-echo (SE) images tends to be inversely related to chronicity of the pericardial inflammation.[9] In the acute and subacute forms of pericarditis, the thickened pericardium and adhesions typically have elevated signal intensity on SE images.[36,42] The presence of a significant signal in pericardial tissue on T2W short-tau inversion recovery (STIR) images correlates with pathologic findings of edema, neovascularization, and/or granulation tissue.[41,43,44]

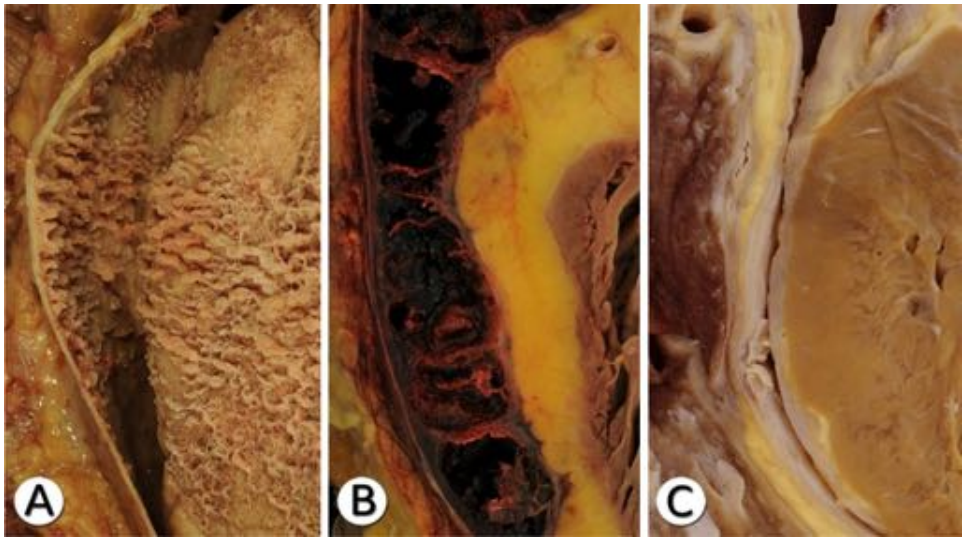

Figure 13 **(A)** Fibrinous pericarditis shows diffuse fibrin deposits over the parietal and visceral surfaces as commonly seen in the setting of uremia. **(B)** Fibrinohemorrhagic exudate is most commonly associated with neoplasms. **(C)** Fibrous pericarditis with thickening of both parietal and visceral pericardium causes constriction in a case of radiation pericarditis. Collagen deposition is evident as a thick gray continuous line over the LV myocardium. There are fibrous adhesions between the parietal pericardium, mediastinal pleura, and visceral pleura of the lung.

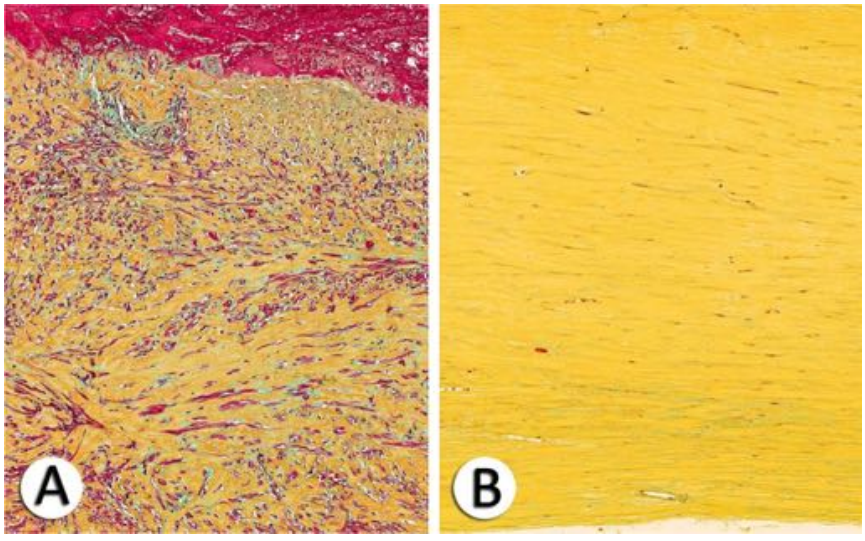

Figure 14 **(A)** Organizing pericarditis shows fibrin on top and granulation tissue with proliferation of elongated fibroblasts, capillaries and collagen matrix. **(B)** Organized healed pericarditis is hypocellular with dense fibrosis. Original magnification 400×, Movat pentachrome stain.

Enhancement of thickened pericardium on T1-weighted (T1W) SE images or LGE images after the administration of gadolinium-based contrast media confirms active inflammation (Figure 20).[9,26,36,41,45-51] Sensitivity for LGE detection of pericardial inflammation has been reported to range from 94% to 100%,[43,45] with much lesser degrees (extent and intensity) also seen in many patients with CP responsive to medical therapy due to underlying ongoing inflammation.[43] In the setting of acute myocardial infarction, CMR detection of early pericardial injury as shown by the finding of inflammation and PEff has emerged as a marker of the severity of the myocardial infarction. It may also have a role in patients with atypical chest pain or in the setting of ECG findings after infarction that may be related to either from ongoing ischemia or from pericarditis.[52] On the other hand, chronic fibrotic pericarditis, characterized by avascular pericardial layers with an abundance of collagen fibers and fibroblasts in the absence of vascularized granulation tissue, shows pericardial thickening without enhancement.[45]

An exudative PEff, as might be found in acute pericarditis, has a high protein and cell content as well as relative immobility, leading to relatively higher T1W signal intensity on SE images.[8,9,37,42,53-57] Cine images, such as with balanced SSFP, are able to demonstrate the full extent of the abnormal PEff and altered cardiac motion.[58]

Pericardial adhesions between inflamed visceral and parietal pericardial surfaces may be further assessed using dynamic tagging demonstrating loss of the normal slippage of the outer pericardium over the epicardial surface during the cardiac cycle[48,56,59] (Figure 21).

Table 3 Functions of the pericardium

Mechanical
Effects on chambers
Limits short-term cardiac distention
Facilitates cardiac chamber coupling and interaction
Maintains pressure-volume relation of the cardiac chambers and output from them
Maintains LV geometry
Effects on whole heart
Lubricates, minimizes friction
Equalizes gravitation and inertial, hydrostatic forces
Mechanical barrier to infection
Immunologic
Vasomotor
Fibrinolytic
Modulation of myocyte structure and function and gene expression
Vehicle for drug delivery and gene therapy

Adapted with permission from Hoit.[214]

6. When to Consider Added Imaging. TTE should be performed in all cases of acute pericarditis to assess for effusion, tamponade physiology, and myocardial involvement as in myopericarditis. If the results of TTE are negative or equivocal in a patient suspected to have acute pericarditis with poor prognostic signs, including fever >38°C, indolent course, failure of response to therapy, or evidence of hemodynamic compromise, the most sensitive subsequent test is CMR, which shows edema and inflammation as well as features of constrictive physiology.

Imaging with CT or CMR should be considered in limited clinical scenarios with complex clinical presentation or inconclusive echocardiographic findings. The choice of CT or CMR should be based on the specific clinical question according to the strength of these modalities. The following are scenarios in which additional imaging with CT or CMR may be considered:

- inconclusive echocardiographic findings and ongoing clinical concern;
- failure to respond promptly to anti-inflammatory therapy;
- atypical clinical presentation;
- search for a specific cause (i.e., malignancy or tuberculosis);
- suspicion of CP or effusive CP;
- associated trauma (penetrating injury, chest injury); and
- acute pericarditis in the setting of acute myocardial infarction, neoplasm, lung or chest infection, or pancreatitis.

B. Recurrent Pericarditis

1. Introduction. Recurrent pericarditis is a pericardial syndrome that is defined as a recurrence of episodes of pericarditis after a latent or asymptomatic period of ≥6 weeks. It is a common complication of acute pericarditis, with up to one third of patients with acute pericarditis developing repeat episodes.[6,60,61] The pathophysiology for recurrent episodes may be related to repeat episodes of primary acute pericarditis (i.e., viral reactivation) or autoimmune-mediated inflammation initiated by pericardial injury from the initial or prior episodes.[61]

Symptoms associated with recurrent episodes are similar to those of the initial episode, although often not as severe. However, pericardial rubs, ECG changes, and PEff occur less commonly with recurrent pericarditis.[61] Inflammatory markers may be elevated. Risk factors for recurrence are fever, subacute presentation, immunosuppressed host, myopericarditis, large PEff effusion or tamponade physiology, prior chest trauma, coexisting anticoagulant medications, incomplete anti-inflammatory treatment course, steroid therapy, and failure to respond promptly to initial treatment. Recurrent pericarditis can generally be treated with a prolonged course of NSAIDs. Colchicine can be added to NSAIDs or as monotherapy. Corticosteroids provide rapid symptomatic relief but are generally avoided initially, as there is evidence that they exacerbate episodes of recurrent pericarditis.[61] Recently, corticosteroids have been used with the combination of NSAIDs and colchicine on the basis of severe inflammation noted on CMR.[8] Finally pericardiectomy can be considered for rare cases of severely symptomatic and refractory recurrent pericarditis,[56,57] but caution is necessary in the setting of ongoing inflammation, which can cause adhesions.

2. General Indications for Imaging. Similar to acute pericarditis, echocardiography is used as the initial imaging in cases of suspected recurrent pericarditis, and additional imaging could be used for complicated cases, especially in the setting of features associated with worse outcomes, as listed previously.

3. Echocardiography. The echocardiographic features of recurrent pericarditis include many of the same present in acute pericarditis, including PEff with and without tamponade physiology (Figure 22) and segmental wall motion abnormalities. With recurrent events, additional features may also include signs of CP, such as septal bounce and respirophasic shift of the interventricular septum.

4. CT and CMR. CT and CMR are not used as the initial imaging modalities for the diagnosis of recurrent pericarditis however, enhancement of the pericardium can be demonstrated with both modalities and indicates pericardial inflammation as in acute pericarditis (Figures 19 and 20). Enhancement of the pericardium, inflammatory changes in pericardial fat and epicardium, and the presence of blood in the pericardial space provide supportive evidence for recurrent pericarditis. CMR (Figure 21) and CT (Figure 23) may be useful in ruling out significant CP in the presence of recurrent pericarditis. CMR may have good negative predictive value in terms of the absence of pericardial thickening or inflammation for a patient with a history of recurrent pericarditis with atypical chest pain, when the objective findings of pericarditis are lacking.

5. When to Consider Added Imaging. Additional imaging with CT or CMR may be used if TTE is not achievable or its results are inconclusive or if other entities need to be excluded, such as metastatic disease. For example, in patients with malignancy and suspected metastatic disease to the pericardium, there may be a smooth enhancing pericardium with small effusions in the absence of enhancing nodules. Although this presentation is suggestive of nonmalignant pericarditis, diffuse tumor infiltration is a possibility, and CT or positron emission tomography (PET) may be indicated. In recurrent pericarditis, serial CMR examinations may be used to follow pericardial inflammation during treatment course and to guide therapy (Figure 24).[62] Further studies are needed to verify the benefits of this approach.

C. PEff

1. Introduction. As mentioned, there is usually a small pericardial reserve volume present.[63] Accumulation of transudative or exudative fluid >50 mL is abnormal and occurs in disorders that selectively

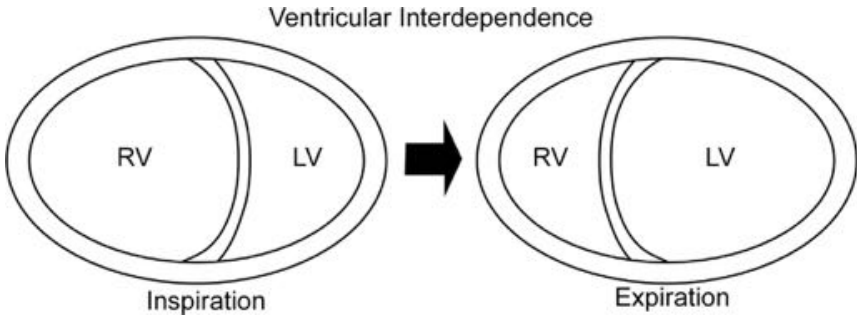

Figure 15 Schematic diagram showing interventricular dependence. On inspiration (*left*), there is a shift of the ventricular septum toward the left ventricle; and on expiration (*right*), there is a shift of the ventricular septum toward the right ventricle. Adapted with permission from Atherton.[215]

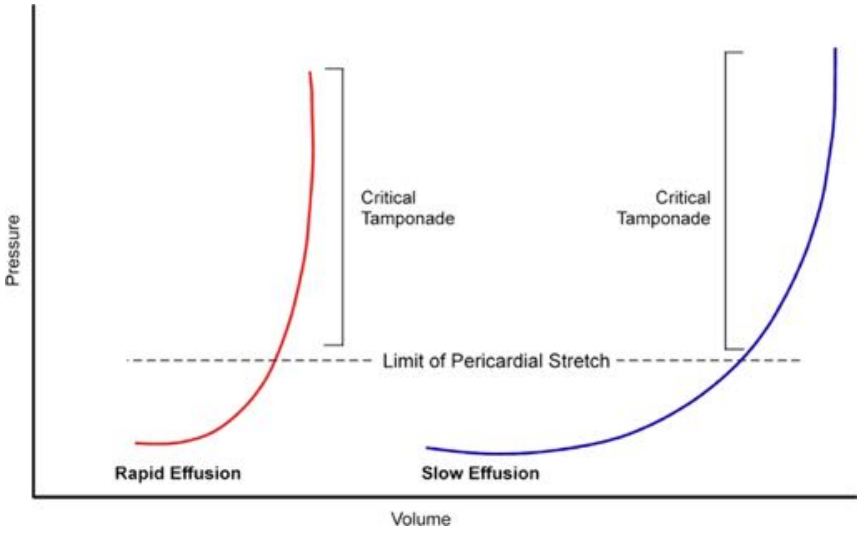

Figure 16 Pericardial pressure-volume (or strain-stress) curves are shown in which the volume increases slowly or rapidly over time. (*Left*) Rapidly increasing pericardial fluid first reaches the limit of the pericardial reserve volume (the initial flat segment) and then quickly exceeds the limit of parietal pericardial stretch, causing a steep rise in pressure, which becomes even steeper as smaller increments in fluid cause a disproportionate increase in the pericardial pressure. (*Right*) A slower rate of pericardial filling takes longer to exceed the limit of pericardial stretch, because there is more time for the pericardium to stretch and for compensatory mechanisms to become activated. Adapted with permission Spodick.[28]

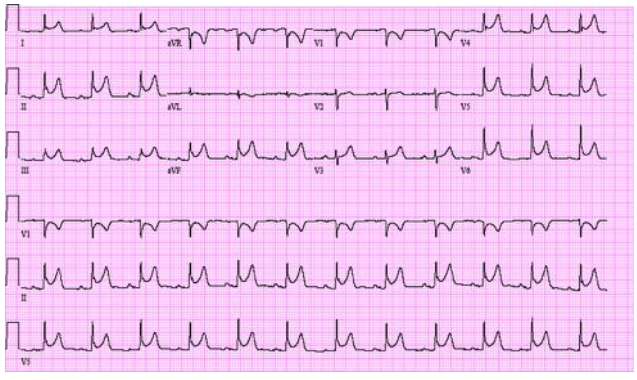

Figure 17 ECG changes showing diffuse concave ST-segment elevations consistent with acute pericarditis. Note that lead aVR shows reciprocal ST-segment depression and reciprocal PR-segment elevation.

Table 4 Criteria for acute pericarditis (the presence of two criteria is considered diagnostic)

Typical chest pain
Pericardial friction rub
ECG changes consistent with pericarditis
New or worsening PEff
*Elevated C-reactive protein or ultrasensitive C-reactive protein/ Westergren sedimentation rate is a confirmatory finding
*LGE on CMR may be a new confirmatory finding

Adapted from Imazio.[4]

affect the pericardium and in general medical conditions such as hypothyroidism, end-stage renal disease, and neoplastic disease.[63] PEff can present as transudates, exudates, hemopericardium, or pyopericardium.[7] Although the definition is arbitrary, small effusions are generally defined as 50 to 100 mL, moderate as 100 to 500 mL, and large

Table 5 Summary of imaging features of acute pericarditis

Echocardiographic features
• PEff with or without tamponade physiology
• Segmental wall motion abnormality (if myocardial involvement)
• Normal findings in some patients
• Increased pericardial brightness
CT features
• Noncalcified pericardial thickening
• Enhancement of the thickened visceral and parietal surfaces of the pericardial sac with contrast
• CT attenuation values of PEff can help distinguish between exudative and transudative fluid
CMR features
• Enhancement of thickened pericardium on T1W SE images or LGE images is consistent with active inflammation
• Significant signal in pericardial tissue on T2W images correlates with edema, neovascularization, and/or granulation tissue
• High T1W signal intensity on SE images is suggestive of exudative effusions
• Loss of the normal slippage of the outer pericardium over the epicardial surface during the cardiac cycle by dynamic tagging is consistent with the presence of pericardial adhesions between inflamed visceral and parietal pericardium

as >500 mL. The size of a PEff correlates poorly with its hemodynamic effect on the heart but is sometimes a clue to its etiology and chronicity.

In developed countries, acute pericarditis is most often associated with a minimal or small PEff and is commonly idiopathic or due to a viral infection.[65] Moderate-sized effusions have a variety of medical causes, while large PEffs may have neoplasia, tuberculosis and hypothyroidism as etiologies.[66-68] Rapidly accumulating blood in the pericardial space can result from blunt trauma, ascending aortic dissection, cardiac rupture as a complication of myocardial infarction, or invasive cardiac procedures (i.e., electrophysiology ablations or pacemaker implantations).[67,69] In these cases, a PEff may be only small to moderate size but often results in acute cardiac tamponade because of rapid accumulation of blood in a limited space.

A PEff should be suspected in any patient with symptoms of pericarditis and in any patient who becomes tachycardic, dyspneic, or hemodynamically unstable with an elevated central venous pressure. On the other hand, an asymptomatic PEff is often discovered during the evaluation of an unrelated medical complaint or disorder. A PEff may be clinically silent, apparent only during the evaluation of unrelated complaints as an incidental finding by echocardiography or CT, or it may be detected in patients with either acute pericarditis or systemic diseases that involve the pericardium (see above).[6]

In patients presenting to the emergency room with chest pain, acute pericarditis is often underdiagnosed. Those patients with suspicious findings for pericarditis should undergo TTE, on which a small PEff is the most common finding, confirming the diagnosis. In the majority of these cases, the patients are labeled "idiopathic" and can be treated with NSAIDs and followed up in an outpatient setting. Patients who present with dyspnea and moderate or large effusions should be admitted for evaluation of cardiac tamponade and possible drainage for diagnostic and/or therapeutic purposes.

Drainage of a moderate or large PEff by pericardiocentesis or pericardial window is usually unnecessary unless symptoms occur, purulent pericarditis is suspected, or cardiac tamponade supervenes,

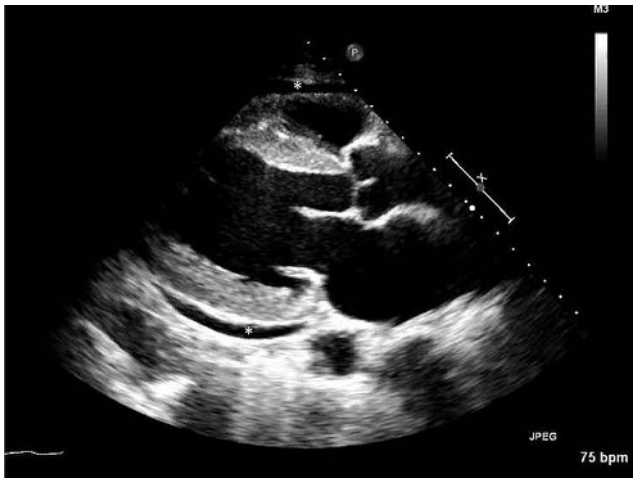

Figure 18 Acute pericarditis: 2D echocardiographic long-axis view, diastolic frame. Note small PEff around the heart (*asterisk*).

although pericardiocentesis is sometimes needed to establish the etiology of a hemodynamically insignificant PEff.

In general, the prognosis of PEff is related to etiology. In the Framingham study,[70] the finding of asymptomatic PEff increased with age, especially in elderly women, in whom it was >10% in patients aged > 80 years. If metabolic causes and hypothyroidism are excluded and the effusion is stable on follow-up examination, it is labeled idiopathic, and no further investigation or treatment is warranted.[71] If the effusion is large and initially asymptomatic, the prognosis is less favorable, because these patients often have occult malignancies or pericardial inflammation warranting diagnostic studies such as CT or MR imaging and diagnostic pericardiocentesis.[71]

2. General Indications for Imaging. Cardiac imaging should be performed whenever a PEff is suspected, because a physical examination or chest x-ray cannot make a definitive diagnosis. Cardiac imaging is therefore recommended in all patients with chest pain consistent with pericarditis or aortic dissection,[2] a chest x-ray that shows an enlarged cardiac silhouette (classically "flask shaped"), and systemic diseases associated with PEff and jugular venous distension. In addition, cardiac imaging is recommended for patients after myocardial infarctions or invasive (surgical or percutaneous) cardiac procedures that develop hypotension or hemodynamic instability.

3. Echocardiography. Echocardiography is the initial procedure of choice to detect the presence of a PEff because it can be performed with minimal delay and has an accuracy of nearly 100%. It is also the best diagnostic tool for assessing the physiologic and hemodynamic effects of a PEff. The proper performance of an examination for both detecting a PEff and assessing whether cardiac tamponade is present is listed in Table 2 and the Appendix.

M-mode echocardiography shows the persistence of an echo-free space between the epicardium and parietal pericardium throughout the cardiac cycle.[72] A separation of the two layers that is seen only in systole represents a normal or clinically insignificant amount of pericardial fluid (trivial PEff), whereas a separation that is present in both systole and diastole is associated with effusions of >50 mL (small PEff). A left pleural effusion may mimic a PEff. In these cases, a two-dimensional (2D) parasternal long-axis view that shows fluid between the descending aorta and heart establishes the fluid as

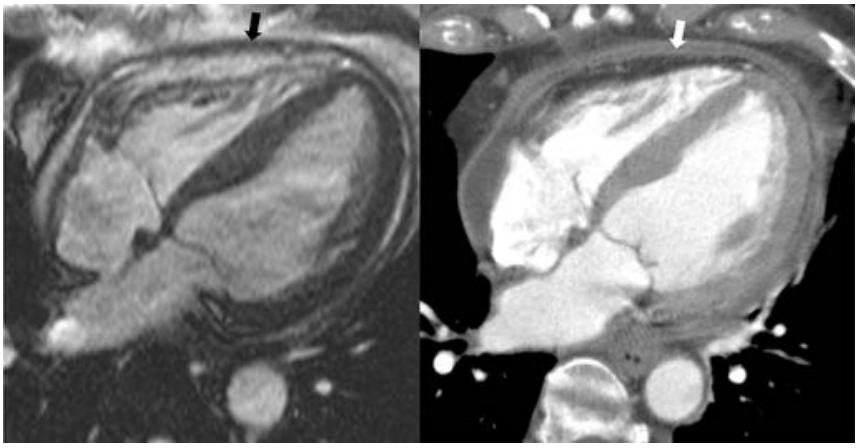

Figure 19 Inflammation-related pericardial surface enhancement on contrast-enhanced CT (four chamber). Compared with cine (SSFP) CMR (*left*; Video 1; available at www.onlinejase.com), which shows nonspecific overall thickening of the pericardium (*black arrow*), corresponding post–iodinated agent CT (*right*; Video 2; available at www.onlinejase.com) reveals enhancement of both outer parietal and inner visceral layers of the pericardium due to inflammation (*white arrow*) with interposed mild effusion.

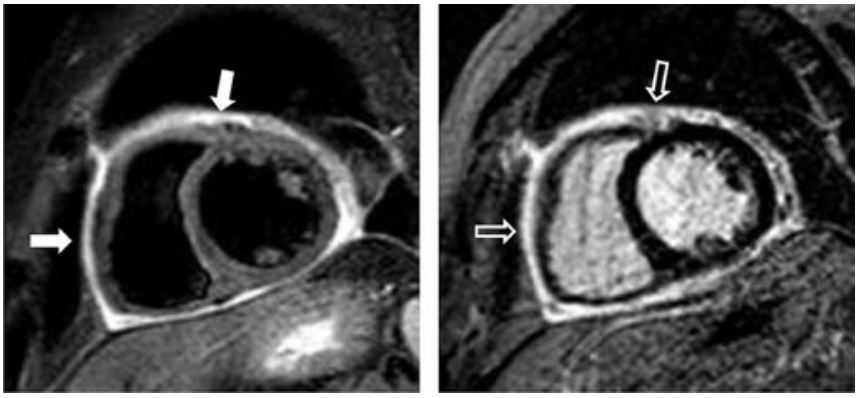

Figure 20 Pericardial enhancement due to inflammation on T2W and postcontrast CMR (short axis). The T2W STIR image (*left*) clearly demonstrates bright pericardial edema (*closed arrows*); a corresponding postgadolinium delayed enhancement CMR image (*right*) reveals prominent signal of the pericardium due to its inflammatory nature (*open arrows*).

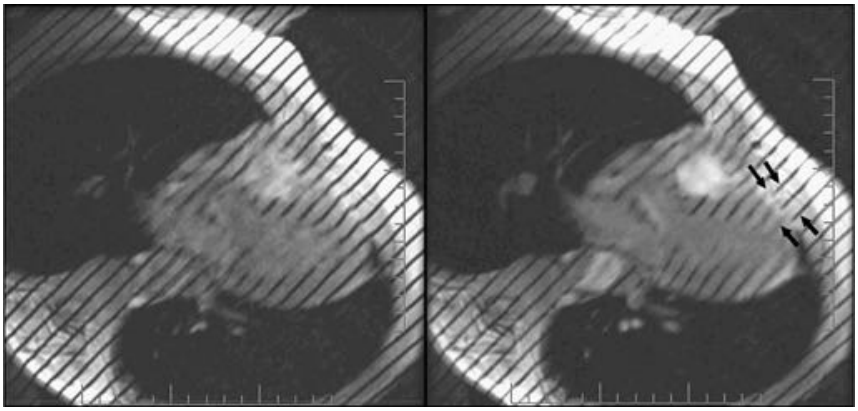

Figure 21 CMR tag line: gated cine CMR with tag lines placed orthogonal to the pericardium demonstrates breaking of the tag lines along the pericardium. Tag line breaking indicates the absence of adhesions and is against the presence of constrictive physiology. Reproduced with permission from Kojima.[56]

pericardial rather than pleural (Figure 25).[73] Clinically, 2D echocardiography followed by Doppler provides the easiest way to demonstrate and assess PEff.

Two-dimensional echocardiography allows the qualitative assessment of the size and distribution of a PEff as well as the detection of fluid that may be loculated or have density features consistent

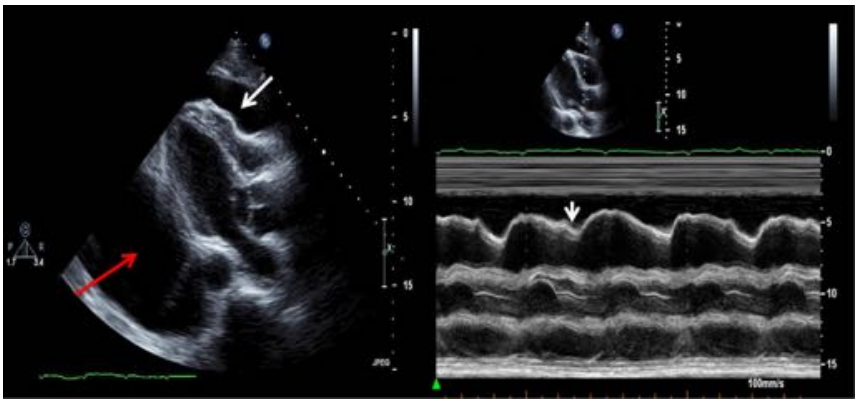

Figure 22 Two-dimensional echocardiogram shows a moderate anterior PEff (*white arrow*) and large pleural effusion (*red arrow*) (Video 3; available at www.onlinejase.com). There is early RV diastolic collapse combined with tamponade physiology, as noted on M-mode (*white arrowhead*).

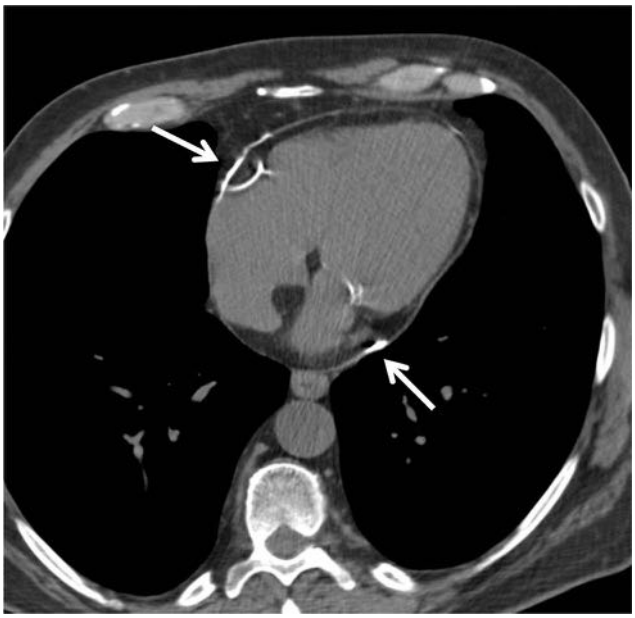

Figure 23 Nongated unenhanced cardiac CT demonstrates only minimal thickening of the pericardium up to 3 mm but presence of linear pericardial calcification (*white arrows*) over the right and left atrioventricular grooves suggestive of prior pericardial process.

with an exudate or clot rather than a transudative fluid. Anterior and posterior echo-free spaces are frequent findings that occur in ≥5% of patients.[70] In the early days of 2D echocardiography, it was frequently difficult to distinguish epicardial fat from PEff.[74] Improvements in image quality have made this less of a problem today. Epicardial fat is often brighter than the myocardium and tends to move in concert with the heart. These two characteristics help distinguish it from a simple transudative PEff, which is generally echolucent and motionless (Figure 26).

By 2D echocardiography, a PEff is semiquantitatively described on the basis of the size of the echo-free space seen between the parietal and visceral pericardium at end-diastole (Figure 27): trivial (seen only in systole), small (<10 mm), moderate (10–20 mm), large (>20 mm), or very large (>25 mm).[75] Seeing an evenly distributed PEff from multiple 2D transducer positions increases the predictive value of the estimated size of the effusion. Small and very large effusions are most likely to be unevenly distributed in the pericardial space and its recesses.[76] An exudative PEff may show features such as stranding, adhesions, or an uneven distribution reflecting its more inflammatory and complicated nature. Effusions that contain clots, such as those seen after cardiac surgery, remain diagnostically challenging by TTE[77] and are often better evaluated using TEE (Figure 28), CT, or CMR.

4. CT. PEff is often an incidental findings detected by a chest CT performed for other clinical indications.[78] In emergency room patients who underwent CT to exclude pulmonary embolus, the incidence of PEff was 5%.[79] In these patients, pulmonary embolus, pneumonia, pulmonary nodules, and mediastinal adenopathy were all seen more frequently and may have contributed to the effusions seen. Although clinically suspected cases of PEff are initially investigated by echocardiography, CT is an important adjunct study when localization and quantification of pericardial fluid are important (Figure 29) or when the effusion is complex or loculated or clot is present.[9] The latter may be especially difficult to appreciate by echocardiography but is better characterized by CT. Epicardial fat is reliably identified by CT, which can be diagnostically helpful when echocardiographic findings are equivocal or fibrin is adherent to the cardiac surface.[80-83] The most difficult pericardial areas for echocardiography to image are in the anterior or superior locations. These are readily demonstrated by the wider field of view provided by both cardiac CT and CMR.[48,83] Chest CT can also help resolve other pathologic conditions that simulate pericardial disease. Complex pleural effusions, lower lobe atelectasis, external masses abutting the pericardium, or other mediastinal abnormalities that may be difficult to diagnose by echocardiography are usually more definitively demonstrated by CT.[80]

A PEff may be characterized with CT by measuring its level of attenuation (Figure 30). Computed tomographic attenuation close to that of water (<10 Hounsfield units) suggests a simple, transudative effusion.[8,39,40] Low attenuation values with measurements close to that of fat (−60 to −80 Hounsfield units) have been reported in cases of chylopericardium.[40,57] If computed tomographic attenuation is in the range of 20 to 60 Hounsfield units, the PEff

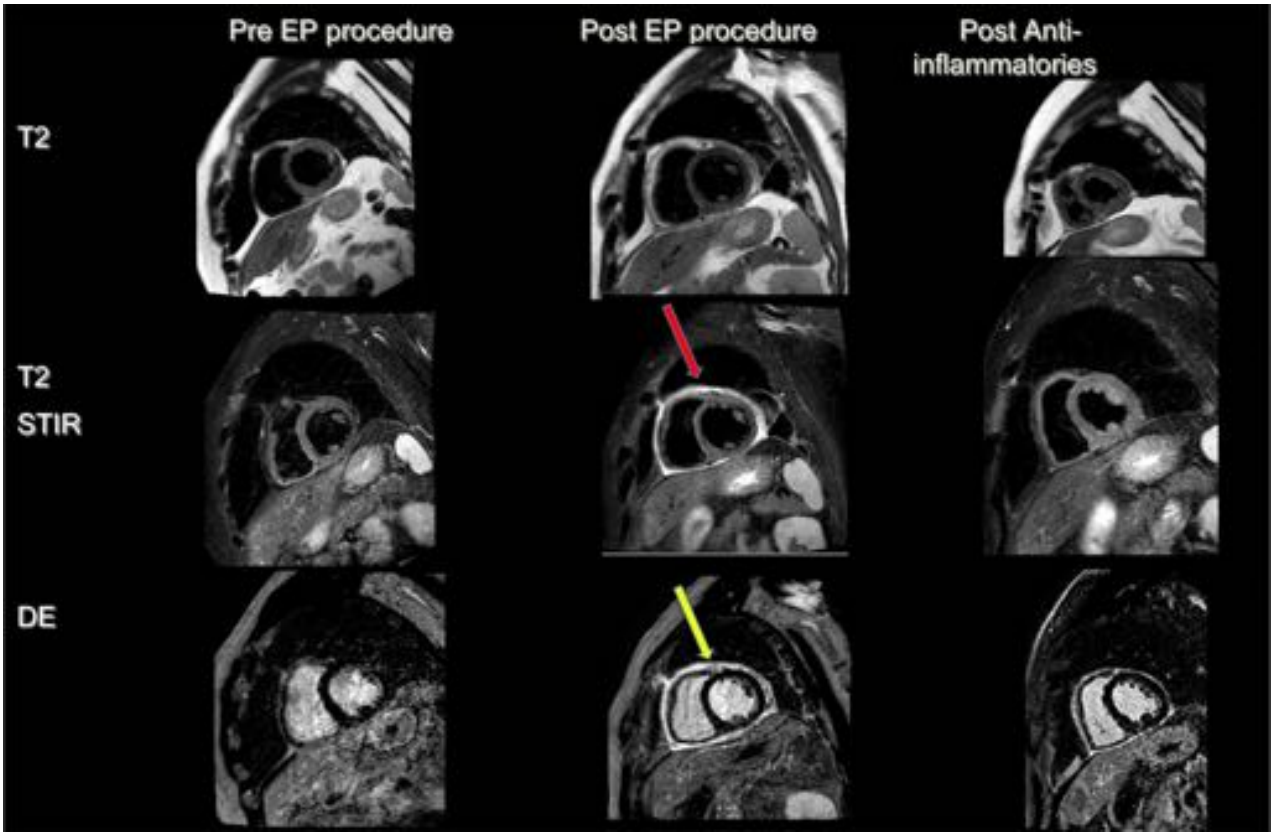

Figure 24 CMR findings in a 65-year-old man who developed recurrent pericarditis after an electrophysiologic study (ventricular tachycardia ablation). Preprocedural CMR images (*left*), 3 weeks after onset of symptoms after the procedure (*middle*), and 6 months after starting ''triple therapy'' anti-inflammatory treatment (*right*) are shown. The T2 STIR, ''edema-weighted'' images (*red arrow*) and the delayed-contrast enhanced (DE), images (*yellow arrow*) show a rim of increased pericardial signal after the procedure consistent with an inflammatory response. These findings show partial resolution after effective pharmacologic treatment. Courtesy of Dr. Arun Dahiya.

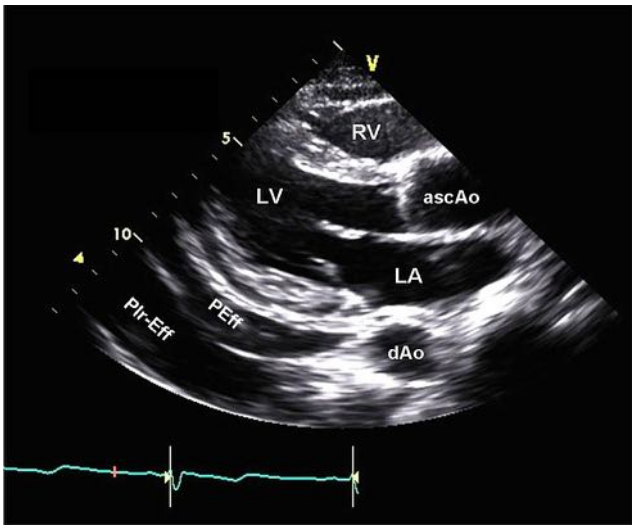

Figure 25 Two-dimensional parasternal long-axis view of a heart in a patient with both a pericardial effusion (PEff) and a left pleural effusion (Plr-Eff). The extension of fluid between the descending aorta (dAo) and heart establishes the fluid as pericardial, while the pleural effusion courses behind the descending aorta (dAo). *ascAo*, Ascending aorta; *LA*, left atrium; *LV*, left ventricle; *RV*, right ventricle.

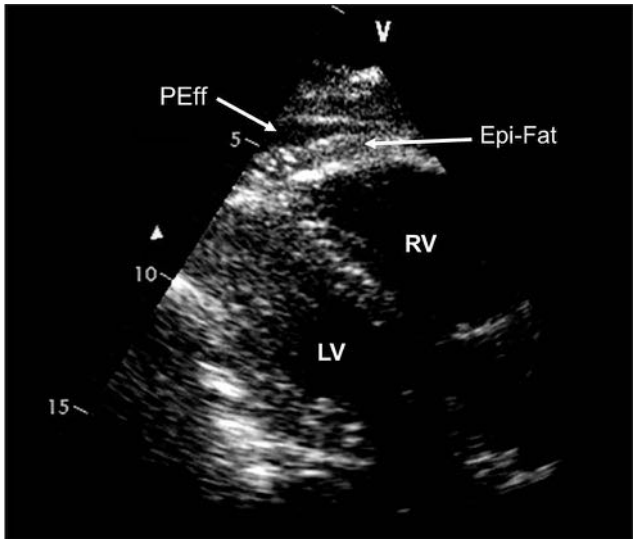

Figure 26 Two-dimensional subcostal view of a heart in a patient with both epicardial fat (Epi-Fat) and a pericardial effusion (PEff). Epicardial fat is often brighter than myocardium, tends to be of uniform thickness, and moves in concert with the heart. These characteristics help distinguish it from a transudative PEff, which is generally echolucent and motionless throughout the cardiac cycle.

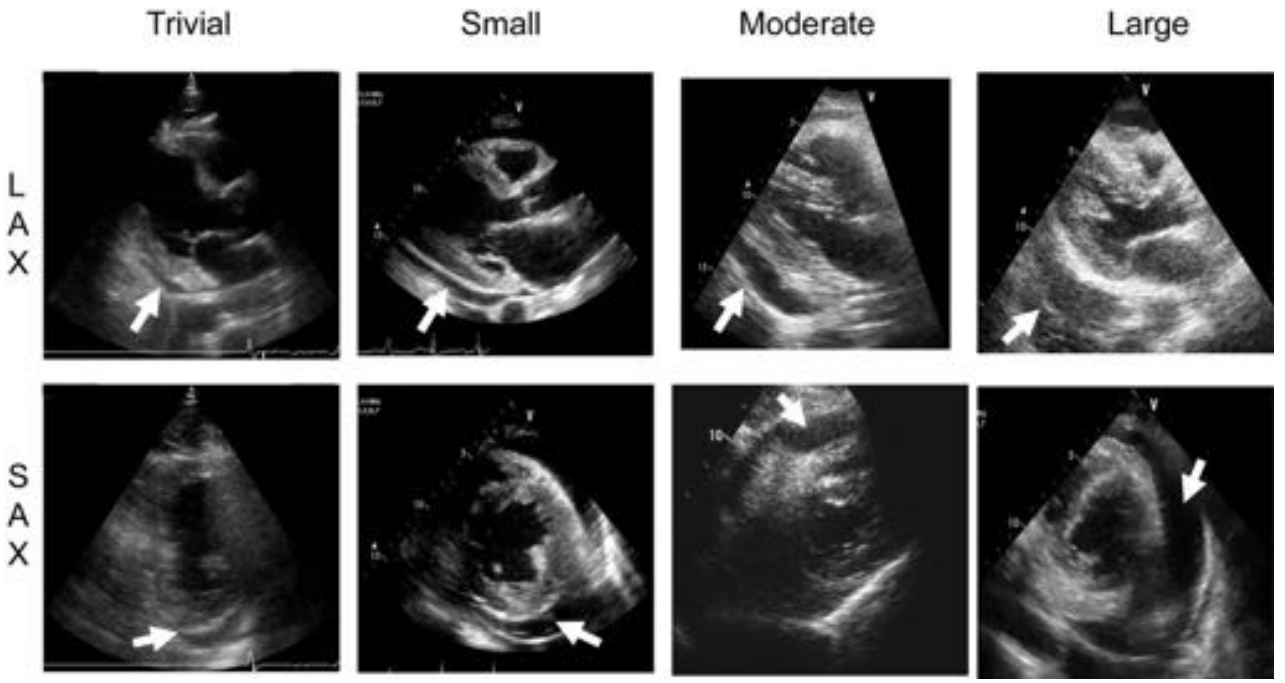

Figure 27 Representative trivial (Videos 4 and 5; available at www.onlinejase.com), small (Videos 6 and 7; available at www.onlinejase.com), moderate (Videos 8 and 9; available at www.onlinejase.com), and large (Videos 10 and 11; available at www.onlinejase.com) PEff sizes, parasternal long axis (*top*) and parasternal short axis (*bottom*).

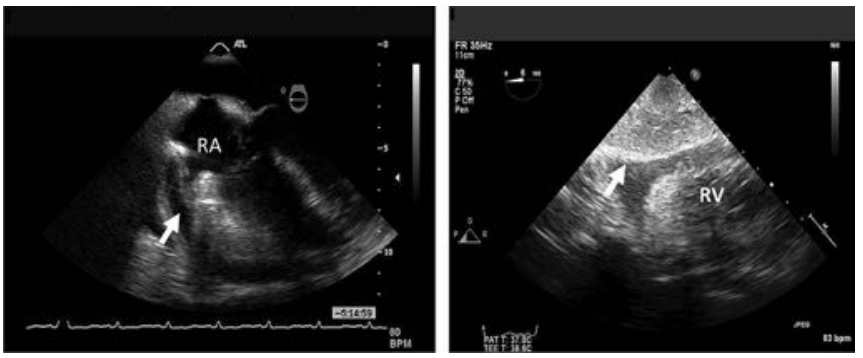

Figure 28 TEE in midesophageal view showing small localized PEff (*arrow*) adjacent to the right atrium in a postcardiac procedure (*left*) and organized moderate effusion adjacent to the right ventricle in a patient with Dressler's syndrome (*left*) (Videos 12 and 13; available at www.onlinejase.com).

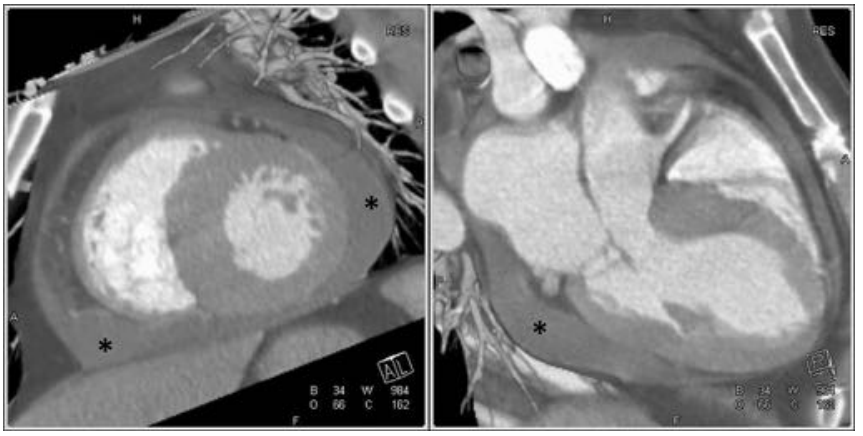

Figure 29 PEff distribution on CT. Dynamic computed tomographic images in the short-axis (*left*; Video 14; available at www.onlinejase.com) and LV outflow tract (*right*; Video 15; available at www.onlinejase.com) orientations demonstrate a small simple PEff with focal collections (*asterisks*) inferior to the right ventricle, lateral to the left ventricle, and inferior to the left atrioventricular groove.

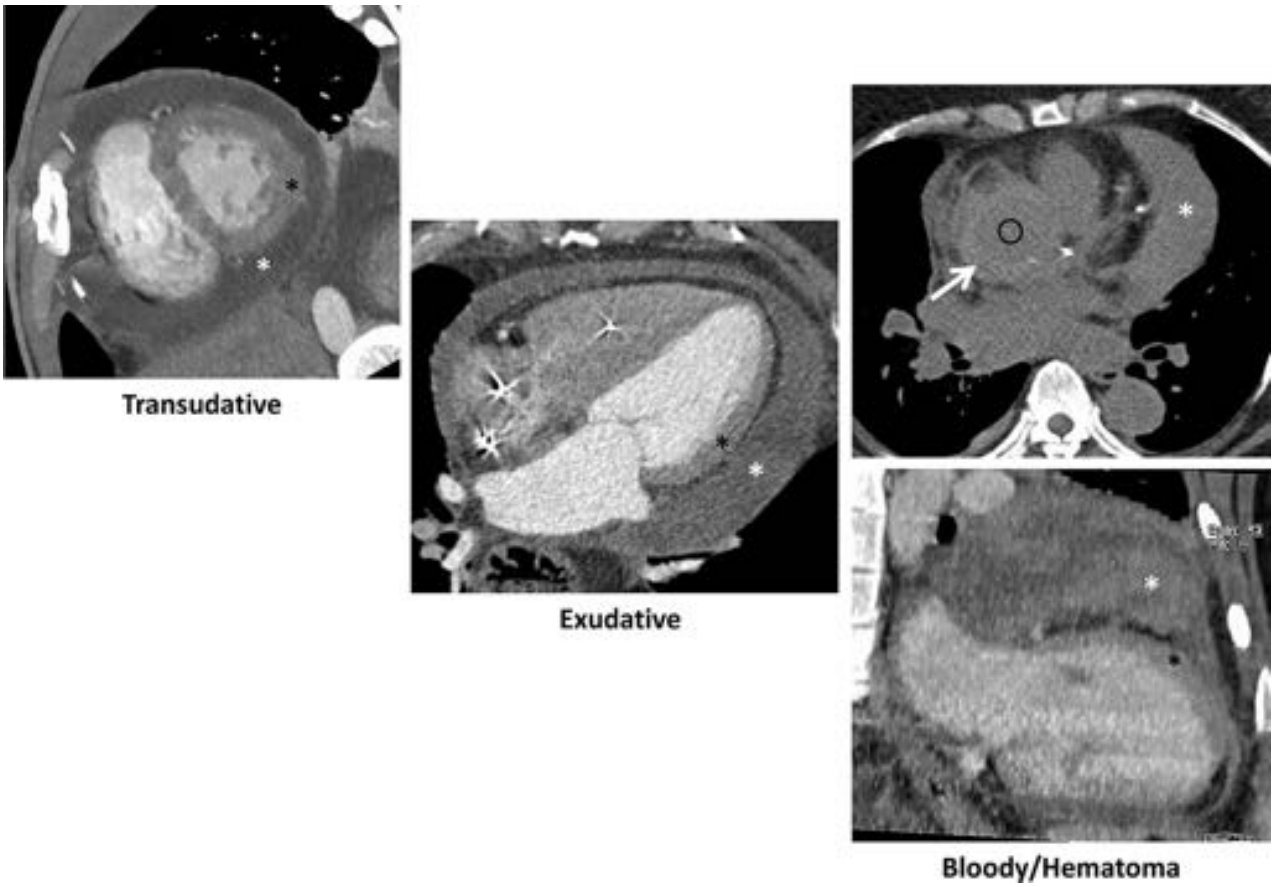

Figure 30 PEff characteristics on CT. Computed tomographic images demonstrate characteristic attenuation changes of PEffs (*white asterisks*) (relative to contrast-enhanced myocardium [*black asterisks*]) for transudative fluid (*lower*), exudative fluid (*slightly lower*), and bloody effusions/hematoma (*equal*), which are (like dissecting intramural hematoma [*arrow*]) inherently higher attenuating than non-contrast-enhanced blood (*open circle*). Intramural hematoma image courtesy of Dr. A. E. Stillman.

may be purulent, malignant, or myxedematous.[39,40,80] Effusions with attenuation values > 60 Hounsfield units suggest hemorrhage.[40,84] Features on CT that differentiate pericardial thickening from pericardial fluid include the presence of nodular areas of increased attenuation, the typical anterior location of the thickened pericardium, the lack of change with decubitus positioning, and pericardial enhancement with the administration of contrast material.[82]

5. CMR. CMR is rarely used as a primary imaging modality for evaluating a PEff; however, it can provide accurate information on PEff size and location and pericardial thickening. As on CT, pericardial abnormalities can be incidental or associated findings on CMR examinations performed for other indications. Because of similar attenuation coefficients, differentiating thickened pericardium from a small effusion can be occasionally challenging using CT.[8] In these cases, CMR easily makes this differentiation.[53] Like CT, CMR delineates the distribution and amount of pericardial fluid more precisely than echocardiography.[41,85] By CMR, a PEff usually demonstrates fluid mobility and changes in the regional dimension of the pericardial sac throughout the cardiac cycle that are not obvious on echocardiography, which help distinguish it from epicardial fat.[48] Additional sequences with fat suppression should be considered if distinguishing fat from surrounding nonfat tissue planes, specifically pericardial fluid, is difficult.

CMR can detect effusions as small as 30 mL.[80,81] However, as with echocardiography, a strong linear relationship between the width of a PEff at a fixed anatomic location and total fluid volume does not exist, because pericardial fluid distribution is usually not uniform. There is preferential accumulation of fluid posterolateral to the left ventricle, along the inferolateral wall of the right ventricle, and in the superior pericardial recess.[41] In general, if CMR shows a circumferential fluid-filled pericardial space width of <4 mm anterior to the right ventricle, the effusion is small, whereas >5 mm indicates a larger effusions.[42,86] The precise amount of pericardial fluid can be determined by multislice volumetric quantification, as is done for cardiac chamber volumes.[41,48]

Using gated images to limit cardiac motion of the beating heart, some CMR features help characterize the nature of PEff. Transudative effusions usually exhibit low signal intensity on standard dark-blood images (partly because of fluid motion and the slower acquisition) and very high signal intensity on bright-blood cine images with their high rate of acquisition (Figure 31).[36,41,54,85] The presence of loculations, septations, and debris on CMR suggests a complex PEff.[54] Proteinaceous, exudative, and hemorrhagic effusions generally exhibit high signal intensity on both T1 and T2 images because of their high protein content.[9,41] Acute hemorrhage into the pericardial space usually exhibits low signal intensity on gradient-echo images,[39] although both the composition of the fluid and time from hemorrhage affect the CMR appearance.[9,36,42,87,89]

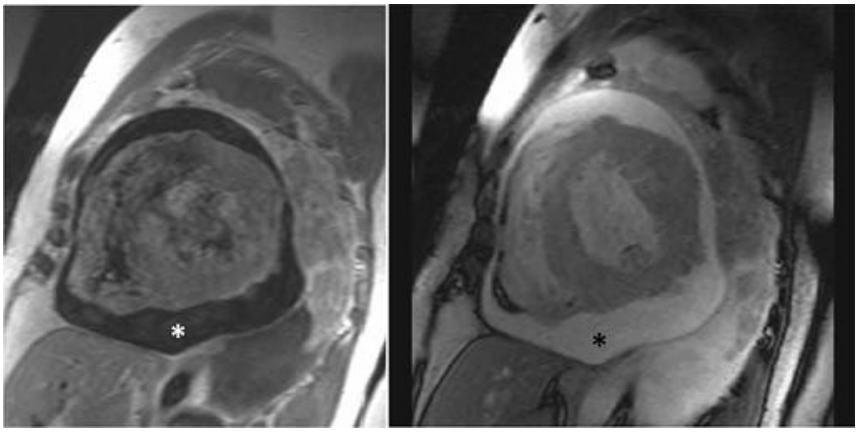

Figure 31 Simple PEff on CMR. A simple free-flowing PEff (*asterisks*) typically appears dark on SE images (*left*), while appearing bright on cine images (*right*; Video 16; available at www.onlinejase.com), which are acquired faster.

Table 6 Imaging findings in PEff and tamponade

Echocardiography	CT	CMR
Effusion		
Echolucent space between visceral and parietal pericardium	Localization and quantitation of pericardial fluid	Localization and quantitation of fluid
Qualitative size and distribution of effusion	Tissue characterization on the basis of computed tomographic attenuation	Tissue characterization on the basis of signal intensity
Stranding, adhesions, slow moving contrast (if blood present) with exudative effusions	Differentiation of pericardial thickening from fluid	Differentiation of pericardial thickening from fluid
Tamponade		
PEff	Feasibility of surgery vs percutaneous drainage of complex effusions	Same as CT
Reduced LV size, appearance of LV hypertrophy	"Flattened heart"; compressed coronary sinus; septal bowing ↑ SVC, IVC size using static CT	
Dilated IVC and hepatic veins	Information similar to echocardiography using dynamic CT	
Cardiac chamber collapses		
Respiratory variation in chamber size (↑ RV, ↓ LV with inspiration)		
Respiratory variation in transvalvular velocities (↑ tricuspid, pulmonic, ↓ mitral, aortic with inspiration) and ↑ isovolumic relaxation time with inspiration		
Low hepatic vein velocities, decreased expiratory diastolic hepatic vein velocities, with large reversals		

Similarly, the MR characteristics of a pericardial hematoma depend on its age because hemoglobin has different MR characteristics than its breakdown products: deoxyhemoglobin and methemoglobin.[36,48,54,88,90] Because of the loss of water and protons, chronic organized hematomas generally show low signal intensity with dark foci representing calcifications, fibrosis, or hemosiderin deposition, which is usually surrounded by a dark peripheral rim.[86]

6. When to Consider Added Imaging. Although echocardiography is the initial procedure of choice to detect a PEff, additional imaging may be warranted when the effusion is complex or loculated or a clot is present; in these instances, CMR or CT may be equally useful. Additional imaging may also be helpful for localization, characterization, and quantification of pericardial fluid; in these instances, CMR may be preferable to CT. Table 6 summarizes the imaging findings for PEff.

D. Cardiac Tamponade

1. Introduction. Cardiac tamponade is a life-threatening condition caused by fluid accumulation in the pericardial sac that compresses the cardiac chambers and inhibits normal filling.[63,91,92] In its

advanced stage, it is characterized by elevation and equalization of cardiac diastolic and pericardial pressures, reduced cardiac output, and an exaggerated inspiratory decrease in systolic blood pressure (>10 mm Hg) known as pulsus paradoxus. As fluid accumulates in the pericardial sac, pericardial pressure rises, and systemic and pulmonary venous pressures must increase to maintain cardiac filling. As cardiac tamponade becomes more severe, these venocardiac gradients continue to diminish, resulting in a progressive decrease in cardiac output. When compensatory mechanisms are exhausted, preload becomes insufficient to sustain cardiac filling and coronary and systemic perfusion. An abrupt drop in heart rate and blood pressure is the usual terminal event.

The pathophysiology of tamponade relates to the effect of the excessive pericardial fluid limiting cardiac filling. Cardiac tamponade markedly alters cardiac filling dynamics as the cardiac chambers compete with the pericardial fluid in the "fixed" and noncompliant space. The excessive pericardial fluid raises pressure in all chambers of the heart throughout the cardiac cycle, which diminishes cardiac filling and output. Atrial filling from the systemic and pulmonary veins predominates over diastolic filling because pericardial pressure falls mainly during early ventricular systole, when total cardiac volume is falling because of ventricular ejection. Ventricular diastolic filling is reduced because of reduced inflow pressure gradients. Inspiration continues to result in an increase in venous return to the right heart, albeit diminished compared with normal, with a simultaneous decrease in left heart filling. This ventricular interaction is observed in imaging studies as an inspiratory bulge of the interventricular septum from right to left (Figure 15), and is the principal mechanism responsible for pulsus paradoxus in cardiac tamponade. With expiration, opposite changes are observed (i.e., an increase in left heart filling and decrease in right heart filling). This explains the opposite respiratory variation of mitral and tricuspid inflow by Doppler echocardiography.

Cardiac tamponade may be acute or subacute to chronic and shows a hemodynamic spectrum ranging from mild to severe and life threatening. Mild cardiac tamponade (typically, PEff pressure <10 mm Hg) is frequently asymptomatic, whereas moderate tamponade, especially severe tamponade (typically, PEff pressure >15 mm Hg), usually results in tachycardia and marked dyspnea. Arterial hypotension is a late sign in tamponade as heightened sympathetic tone maintains systemic blood pressure as cardiac output is decreasing.[93] Eventually, the compensatory mechanisms of tachycardia, increased systemic venous pressures to maintain cardiac filling, and arterial vasoconstriction become exhausted, and a decrease in arterial pressure and coronary perfusion results in cardiac arrest and death.[63,91,92]

In addition to acute and subacute to chronic cardiac tamponade, tamponade may be either low pressure (occult) or regional, due to a loculated effusion or a compressive pericardial blood clot. Tamponade may also be caused by a large pleural effusion in the presence of an insignificant PEff.[94] Patients who are hypovolemic because of traumatic hemorrhage, hemodialysis or ultrafiltration, poor oral intake and vomiting (patients with cancer), or overdiuresis may have low-pressure tamponade in which cardiac filling is severely impaired, but the equalized pericardial and end-diastolic intracardiac pressures are normal at <10 mm Hg.[95,96] A loculated, eccentric effusion or localized hematoma can produce regional tamponade in which only selected (often left-sided) chambers are compressed.[97] As a result, the typical physical, hemodynamic, and echocardiographic signs of tamponade are often absent. Regional cardiac tamponade is most often seen after cardiac surgery, pericardiotomy, or myocardial infarction, and clinical suspicion should be heightened in these settings. Cardiac tamponade associated with cardiac surgery may occur early (<24 hours), or late (arbitrarily defined as >5–7 days). Early tamponade is usually related to surgical bleeding or cardiopulmonary bypass–induced coagulopathy and should be suspected whenever there is evidence of hemodynamic compromise. Late tamponade is multifactorial; excessive mediastinal drainage and postcardiotomy syndrome have been implicated. In contrast to cardiac tamponade with an intact pericardium, the cardiac compression is usually caused by a hematoma that compresses the cardiac chambers, especially on the right side. Because TTE may be difficult in these patients, TEE at the bedside is often helpful in identifying this condition. In one "modern-era" retrospective survey of >4,500 postoperative patients, only 48 were found to have moderate or large effusions by echocardiography, and of those, 36 met diagnostic criteria for tamponade.[98] Use of preoperative anticoagulants, valve surgery, and female gender were all associated with a higher incidence of tamponade. Of note, the echocardiographic criteria to diagnose tamponade on the basis of mitral inflow patterns are different during positive-pressure ventilation than during spontaneous breathing. In fact, there is only minimal respiratory variation when tamponade is present during positive-pressure ventilation.[99]

Postpericardiotomy syndrome usually presents days to weeks after cardiac surgery and is associated with a PEff or a mixed PEff and inflammatory "peel."[3,7,8,100] In these patients, the range of Doppler findings can vary from those seen in classic cardiac tamponade to those seen in effusive CP.

The symptoms and signs of cardiac tamponade depend on the etiology of the PEff and the rate of fluid accumulation, as discussed above. Ascending aortic dissection or invasive cardiac procedures that result in acute bleeding into the pericardium often cause tamponade, with volumes as small as 250 mL. For patients with viral, malignant, or hypothyroid etiologies of pericarditis, it is more usual that the tamponade develops over several days or weeks and a moderate-sized or large PEff is present.

The treatment of cardiac tamponade is the removal of the PEff. An echocardiography-guided approach to pericardiocentesis is recommended as first-line therapy and is usually approached from the para-apical region. In one large series, this approach was found to be relatively safe, with a 97% procedural success rate, a 4.7% complication rate, and one procedural death.[101]

2. General Indications for Imaging. Generally, echocardiography is used as the initial imaging in cases of suspected tamponade, whereas CT and CMR would be used for only complicated cases (i.e., postoperative or loculated effusions). Table 6 shows a summary of the imaging findings in PEff and cardiac tamponade.

3. Echocardiography. When cardiac tamponade is suspected, 2D echocardiography with Doppler should be obtained emergently. Regardless of effusion size, cardiac tamponade is potentially lethal. Therefore, the most important echocardiographic findings are the presence of a PEff, a dilated IVC, hepatic veins indicating that systemic venous pressures are elevated, and a left ventricle that has reduced end-diastolic and end-systolic dimensions, with Doppler evidence of reduced stroke volume and cardiac output. In most cases of cardiac tamponade, other "classic" Doppler echocardiographic findings are also present and confirmatory. These include right heart diastolic chamber collapse when pericardial pressures exceed intracardiac pressure, an inspiratory bulge or "bounce" of the interventricular septum into the left ventricle, and characteristic abnormal respiratory changes in Doppler flow velocity recordings.

a. M-Mode and 2D Echocardiography.–Two-dimensional echocardiographic imaging from standard transducer positions establishes the qualitative size of a PEff, whether it is circumferential or loculated, and whether it appears to be transudative or exudative or contains nonclotted blood, which characteristically shows the slowly swirling spontaneous contrast of clumped red blood cells. When cardiac tamponade is present with a moderate or large PEff, the parasternal short-axis view shows the effects of the cardiac compression and reduced filling. LV cavity dimensions in systole and diastole are reduced, while the myocardium, which retains the same mass, appears "hypertrophied."[102] RV diastolic diameter increases during inspiration, while LV diastolic diameter decreases, with the opposite changes seen during expiration (Figure 32).[103] An important 2D sign of tamponade expected in >90% of patients is IVC plethora. In one series, IVC plethora was present in 92% of effusions that were associated with pulsus paradoxus and that required pericardial drainage.[104] A dilated IVC (>2.1 cm) with <50% reduction in diameter during inspiration reflects the elevation in systemic venous pressure that occurs as pericardial pressure increases the intracardiac pressures (Figure 33). If the IVC is difficult to image or assess, dilatation of the hepatic veins is a reliable confirmatory sign of systemic venous pressure elevation. Although IVC dilation is highly sensitive for cardiac tamponade, it is a common finding in multiple other cardiac diseases in which PEff is absent.

Diastolic RA and RV chamber indentation or "collapse" on 2D echocardiography is usually seen in cardiac tamponade and is particularly important in the diagnosis of low-pressure tamponade, when IVC dilation is minimal or absent. Both chambers collapse during their relaxation phase, when intracavitary pressure reaches its lowest value and transiently falls below pericardial pressure.[105] For the atria, the indentation starts near the peak of the R wave; whereas for the ventricles, the indentation occurs in early diastole after the end of the T wave (Figure 34). The right atrium stays indented until filling during ventricular systole increases its pressure above that in the pericardial space. Because the right atrium is a thin-walled structure, a brief inversion of the RA wall may be seen in the absence of cardiac tamponade. It is important that the duration of the RA collapse be evaluated. Duration of RA collapse that exceeds one third of the cardiac cycle is nearly 100% sensitive and specific for clinical cardiac tamponade.[106] Early diastolic collapse of the right ventricle also signifies that pericardial pressure transiently exceeds RV pressure. RV diastolic collapse generally occurs with moderate elevations in pericardial pressures when cardiac output has decreased by about 20% but systemic blood pressure has not fallen.[107] Initially, RV diastolic collapse is seen only during inspiration; but as tamponade becomes more severe, it is observed throughout the respiratory cycle (Figure 35). The RV free wall also stays indented until chamber pressure with diastolic filling exceeds pericardial pressure; thus, the longer the duration of compression, the more severe the tamponade.[108] Experimental studies indicate that right heart chamber collapse occurs earlier than pulsus paradoxus and that the sensitivity and specificity of chamber collapse improve as the severity of tamponade increases. The same studies suggest that RA chamber collapse may have a higher predictive value than RV collapse.[109,110]

An M-mode cursor placed through the affected wall is an excellent method for judging the timing and duration of chamber indentation or collapse (Figure 35). Occasionally, left atrial chamber collapse is also observed during atrial relaxation, and its timing and duration is also best assessed using M-mode echocardiography.

The absence of any cardiac chamber collapse has a >90% negative predictive value for clinical cardiac tamponade.[111] However, right heart diastolic collapse may occur only at higher levels of pericardial pressure (or not at all) in conditions in which right heart chamber pressures were elevated before the effusion accumulated, as may be seen with RV hypertrophy, severe pulmonary hypertension, or coexisting severe LV dysfunction.[112,113] Conversely, collapse of the right heart chamber may occur earlier than normal when intracardiac pressures are low because of hypovolemia.[114] Posterior loculated effusions after cardiac surgery and severe pulmonary arterial hypertension may produce left atrial and LV diastolic collapse.[115] Establishing the diagnosis of regional tamponade is challenging and may require additional echocardiographic views, TEE (Figure 28), CT, or CMR, as previously discussed.

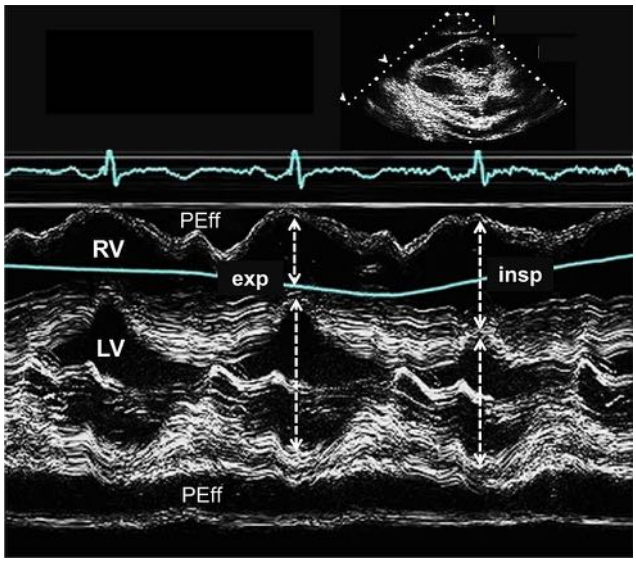

Figure 32 M-mode echocardiogram obtained from a patient with a pericardial effusion (PEff) and cardiac tamponade. When the right ventricle (RV) enlarges with inspiration (insp), the left ventricle (LV) becomes smaller (*dashed arrows*). The opposite changes are seen on expiration (exp).

An inspiratory bulge or "bounce" of the interventricular septum into the left ventricle during inspiration as seen by 2D echocardiography is another common finding seen in cardiac tamponade that is the equivalent of the reciprocating LV and RV dimensions seen by M-mode echocardiography in Figure 32. During inspiration, an increase in RV dimension and a decrease in LV dimension due to septal movement toward the LV free wall is characteristic. In cardiac tamponade, as in normal individuals, inspiration lowers right heart pressures and augments systemic venous return. Unlike the normal situation, in which left-sided filling changes minimally during normal inspiration (<5%), left heart filling decreases abnormally in cardiac tamponade, which results in reduced stroke volume and pulsus paradoxus. This phenomenon is due to ventricular interdependence, wherein an increase in filling on one side of the heart is associated with a decrease on the opposite side (Figure 15). Hemodynamic recordings show an exaggerated decrease in the pulmonary venous–to–left atrial pressure gradient on inspiration and an increased gradient on expiration compared with normal individuals.[91] It should be noted that an inspiratory septal bulge or "bounce" is not specific for cardiac tamponade, as it can also be seen in other conditions associated with pulsus paradoxus, such as marked dyspnea due to metabolic disorders, chronic obstructive pulmonary disease, and pulmonary embolism.[116] In these cases, the clinical history, absence of a PEff, and "overfilling" of the heart with inspiration on venous Doppler rule out cardiac tamponade as

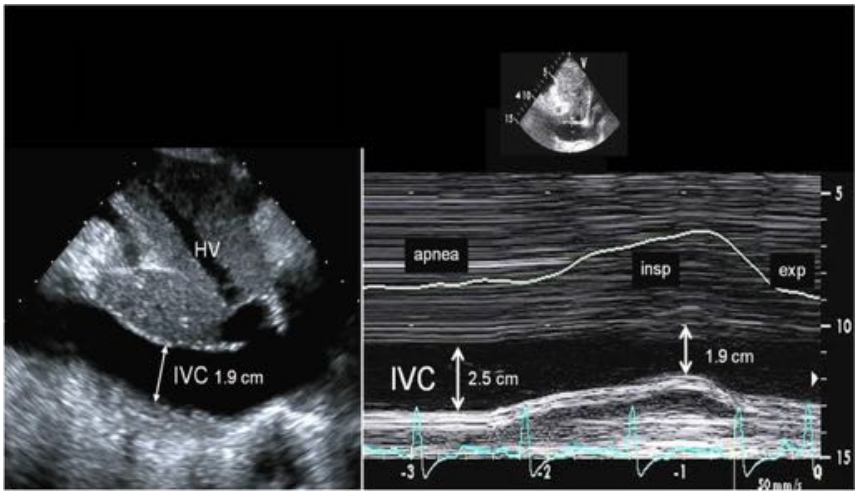

Figure 33 Two-dimensional subcostal view of the heart in a patient with cardiac tamponade showing a dilated IVC (2.5 cm) by 2D echocardiography and M-mode of the IVC throughout a respiratory cycle. The M-mode recording is used to calculate the inspiratory reduction in diameter as shown. With tamponade, the inspiratory decrease in IVC diameter is characteristically <50%, as seen in this case, and is often minimal. Note also the dilation of the hepatic veins (HV).

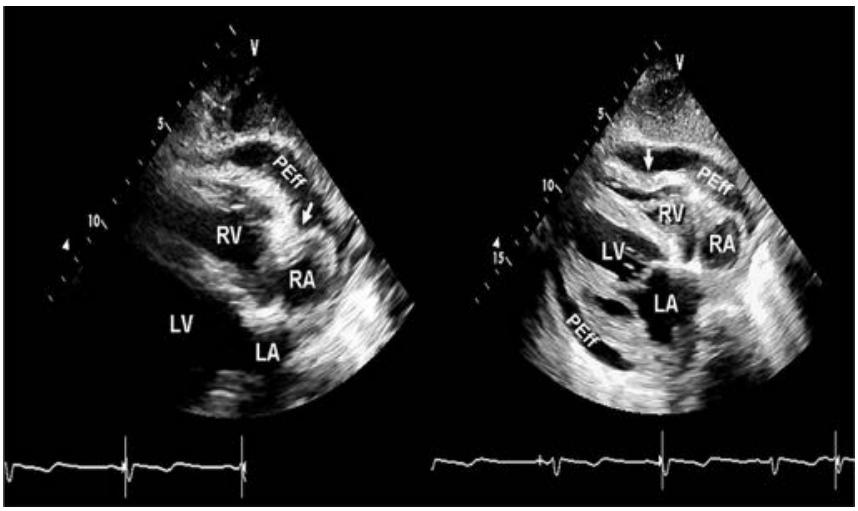

Figure 34 Two-dimensional subcostal view of the heart in a patient with cardiac tamponade showing right atrial and RV indentation or "collapse" (*small arrows*). In both the right atrial and RV chambers, the indentation occurs during their relaxation, when their pressure is lowest and transiently falls below pericardial pressure. As shown by the *arrows*, atrial relaxation and indentation occurs near the top of the QRS complex while RV indentation occurs in early diastole. *LA*, Left atrium; *LV*, left ventricle; *RA*, right atrium.

the cause. Conversely, an inspiratory septal bulge may be absent in cardiac tamponade when there is LV hypertrophy or preexisting markedly elevated LV filling pressures.

b. Doppler Flow Velocity Recordings.–For reasons previously described, characteristic abnormal respiratory changes in transvalvular velocities are present in cardiac tamponade.[117] Thus, tricuspid and pulmonary flow velocities by Doppler echocardiography increase with inspiration, while flow velocities in the mitral and aortic valves simultaneously decrease compared with normal controls and patients with asymptomatic effusions (Figures 36–39). Under normal circumstances, the change in peak E-wave mitral flow velocity is approximately 5%, and changes in the isovolumic relaxation time are minimal.[118] In cardiac tamponade, changes in mitral flow velocity are much larger and are accompanied by changes in the isovolumic relaxation time; similarly, increased respiratory variation in pulmonic and aortic velocities is accompanied by changes in ejection times. The changes in mitral and tricuspid flow velocity are the greatest on the first beats of inspiration and expiration, with intermediate beats having values between these extremes (Figure 36). In research studies, generally a 30% inspiratory reduction in mitral peak E-wave velocity is considered diagnostic.[111,112,117] The absolute velocity changes also vary with each respiratory cycle depending on where early diastolic filling occurs within the cycle (Figure 38). In patients who have ventricular filling only with atrial contraction, the typical reciprocal changes in tricuspid and mitral peak velocities are still seen. Although mitral and tricuspid inflow velocities are typically recorded with pulsed-wave (PW) Doppler, continuous-wave Doppler can be

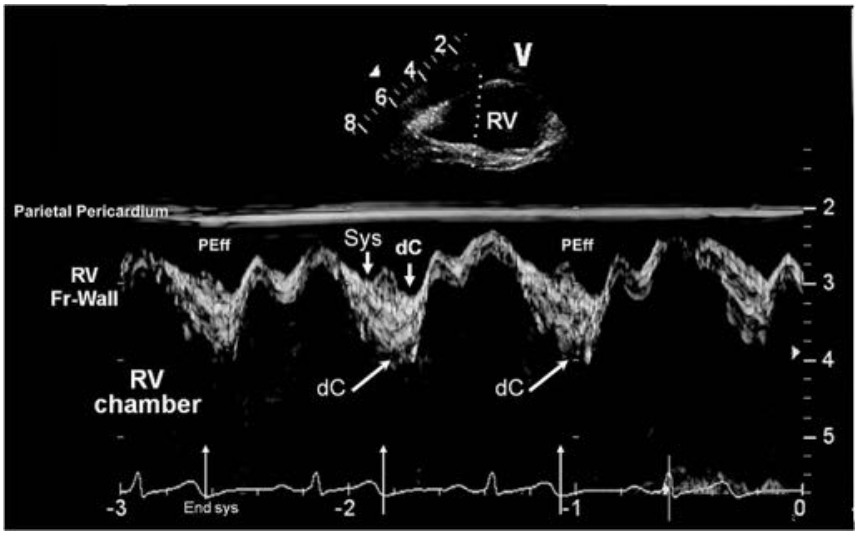

Figure 35 Two-dimensional subcostal view of the heart in a patient with a pericardial effusion (PEff) and cardiac tamponade. An M-mode cursor is placed across the RV free wall (Fr-Wall) to show the timing and duration of diastolic RV indentation or "collapse" (dC). During systole (Sys), the right ventricle contracts and moves inward, as expected. However, after the end of RV systole (*thin arrows* on the electrocardiogram) RV relaxation causes intracavitary pressure to fall below pericardial pressure, resulting in early diastolic RV collapse (dC). Subsequently, as RV filling occurs, the chamber pressure increases, and the myocardial wall moves back toward the parietal pericardium. Maximum RV chamber size occurs after atrial contraction.

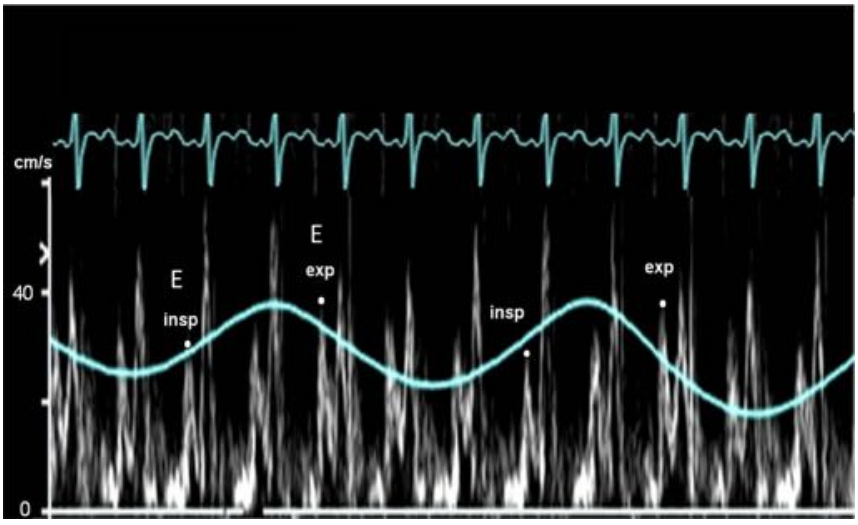

Figure 36 PW Doppler recording of mitral inflow with a respirometer in a patient with cardiac tamponade. Peak velocities and velocity-time integrals are low, reflecting the reduced cardiac output. There is increased respiratory variation in peak E-wave inflow (E) velocity compared with normal, with the lowest values on the first beat of inspiration (insp) and the highest values on the first beat of expiration (exp). The beats in between inspiration and expiration have intermediate values. From expiration to inspiration, the decrease in peak mitral E-wave velocity exceeds 30%, as is typical in significant tamponade. Note that percentage of respiratory variation for mitral inflow should be calculated as (expiration − inspiration)/expiration based on the consensus of the Writing Group.

used and shows the same findings in cases in which respiration or cardiac movement makes it difficult to keep the PW sample volume between the mitral and tricuspid leaflet tips.

Recording hepatic venous flow velocity with PW Doppler is important in assessing the effects of a PEff. Although high positive and negative predictive values for cardiac tamponade are reported using hepatic venous recordings (82% and 88%, respectively), they cannot be evaluated in about one third of patients.[111]

Normal hepatic venous flow is biphasic, with systolic velocity greater than diastolic velocity, and is punctuated by reduced forward velocity or small reversals at atrial contraction (atrial reversal) and end-systole (venous reversal).[119] With inspiration, both peak systolic and diastolic flow velocities increase. When a PEff inhibits cardiac filling, forward flow velocities decrease (typically from the normal 50 cm/sec to 20–40 cm/sec) and systolic venous flow predominates because intrapericardial pressure decreases significantly only during ventricular ejection (Figure 39). In moderate tamponade, diastolic flow velocity is often nearly absent but still exhibits some inspiratory augmentation. With marked tamponade, systolic forward flow is seen but diastolic forward flow disappears completely throughout

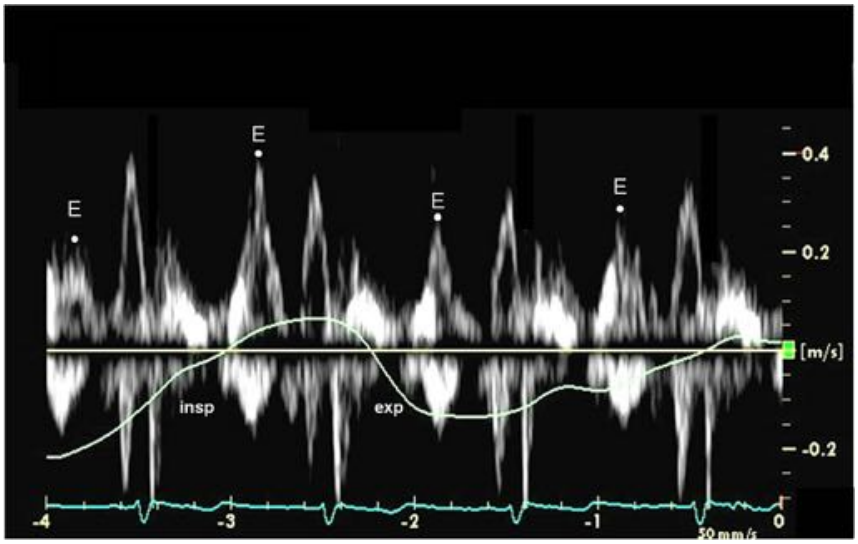

Figure 37 PW Doppler recording of tricuspid inflow in a patient with cardiac tamponade. Peak velocities and velocity-time integrals are low reflecting the reduced cardiac output. There is increased respiratory variation in peak E-wave inflow velocity compared with normal (*white dots*), with the highest value on the first beat of inspiration (insp) and the lowest values on the first beat of expiration (exp). These respiratory changes are opposite to those seen in mitral flow velocity (Figure 36). Note that percentage of respiratory variation for tricuspid inflow should be calculated as (expiration − inspiration)/expiration based on the consensus of the Writing Group.

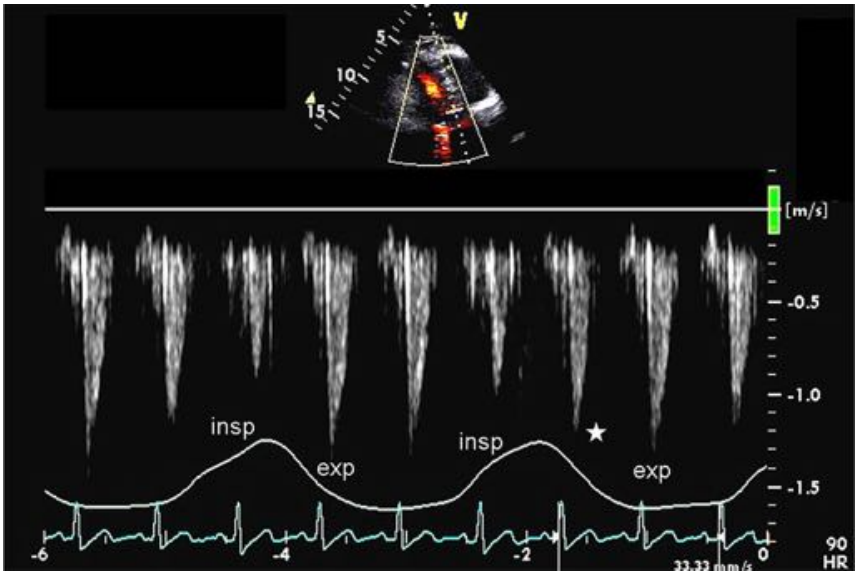

Figure 38 PW Doppler recording of LV outflow tract velocity in a patient with cardiac tamponade and pulsus paradoxus. On inspiration (insp), peak LV outflow tract velocity and ejection time decrease, with the opposite changes seen on expiration (exp). Note that there is a beat with an intermediate value during the second respiratory cycle (*star*) but not the first, reflecting that the dynamic relation between the cardiac heart rate and respiratory cycle. The LV outflow tract velocity changes occur as a result of respiratory changes in LV filling.

the cardiac cycle. When no hepatic forward flow is observed except during inspiration, systemic venous and intracardiac pressures are equalized, and cardiac arrest is imminent.

PW Doppler hepatic venous flows also exhibit characteristic changes in expiration in cardiac tamponade. On the first beat of expiration, either diastolic flow velocity decreases below all other diastolic beats or reversal of flow is seen (Figure 39). This corresponds to the time that tricuspid peak E-wave flow velocity is lowest and mitral peak E-wave flow velocity is highest. SVC flow is intrathoracic and appears less affected by respiration, suggesting preferential RA-RV filling from these systemic veins during expiration.

In summary, the key points in using echocardiography in tamponade are the following[118]:

- It is the combination of a PEff, reduced stroke volume and cardiac output, elevated central venous pressure, and corroborating features of chamber collapse and typical Doppler changes that makes the diagnosis.
- The consensus for the calculation of percentage respiratory variation in tamponade for mitral and tricuspid inflow is (expiration − inspiration)/expiration.

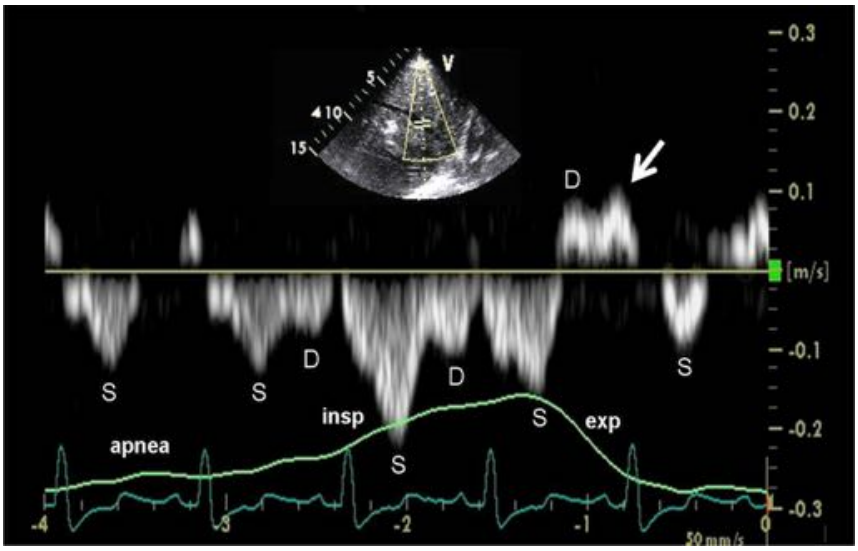

Figure 39 PW Doppler recording of hepatic venous flow velocity in a patient with cardiac tamponade. Flow below the zero baseline is toward the heart and above the baseline is reverse flow. Compared with normal forward flow, velocities in tamponade are markedly reduced, reflecting reduced cardiac filling. During apnea, forward flow is seen only during ventricular systole (S). With inspiration (insp), systolic flow predominates, but diastolic flow (D) also appears. On the first beat of expiration (exp), there is a diastolic flow reversal (*arrow*). This reversal is at the same time tricuspid inflow is lowest (Figure 34). SVC flow velocity (not shown) continues to show some diastolic forward flow on this first beat of expiration.

- For peak mitral E inflow, the maximal drop occurs with the first beat of inspiration and the first beat of expiration and usually exceeds >30% respiratory variation.
- For peak tricuspid E inflow, the maximal drop is on the first beat in expiration at the same time as the hepatic vein atrial reversal and usually exceeds >60% respiratory variation. The calculated % will be a negative value.
- Significant respiratory variation of the mitral and tricuspid inflows should not be used as a stand-alone criterion for tamponade without the presence of chamber collapse, IVC dilation, or abnormal hepatic vein flows (blunting or reversal of diastolic flows in expiration).
- It is important to distinguish between the timing in the respiratory variation of cardiac tamponade and chronic obstructive pulmonary disease. In tamponade, with the first beat of inspiration, the tricuspid shows the largest increase, with the second beat showing an intermediate value; the lowest is with expiration. In contrast, with chronic obstructive pulmonary disease, the largest beat is the second beat, not the first beat, and the expiratory beat is not the lowest.

4. CT and CMR. Neither cardiac CT nor CMR has a role in life-threatening acute cardiac tamponade requiring urgent pericardiocentesis. However, when subacute cardiac tamponade is due to a loculated or complex effusion, CT may help determine the feasibility of percutaneous versus surgical drainage. CMR is an excellent imaging technique for pericardial pathology but is limited in cardiac tamponade because of the relatively long duration of MR examinations in acutely ill patients, who are usually dyspneic, tachycardic, and restless.

Signs of cardiac tamponade on CT include a "flattened heart" from compression of the anterior surface secondary to the presence of fluid, air, or tissue compressing the cardiac chambers[120] and compression of the coronary sinus.[80,121] Another "static" CT finding that can sometimes be observed in cardiac tamponade is angulation or bowing of the interventricular septum, which correlates with the inspiratory septal bulge or "bounce" of the septum commonly seen on echocardiography.[81,122,123] Dynamic forms of CT can provide information similar to echocardiography with respect to abnormal interventricular septal motion and chamber collapse during the cardiac cycle.[9]

Indirect findings in cardiac tamponade detected by CT include enlargement of the SVC with a diameter similar to or greater than that of the adjacent thoracic aorta, enlargement of the IVC with a diameter greater than twice that of the adjacent abdominal aorta, periportal lymphedema, reflux of contrast material into the IVC or azygos vein, and enlargement of hepatic and renal veins.[80,124-127]

Imminent cardiac tamponade documented as an incidental finding during CMR has been reported,[128,129] including cine images that demonstrate diastolic chamber collapse (Figure 40).[48] Additional findings that have been reported with dynamic MR imaging include a "swinging heart"[128] and inspiratory septal bounce.[87]

5. When to Consider Added Imaging. Two-dimensional echocardiography with Doppler is the test of choice for suspected cardiac tamponade. As previously discussed, neither cardiac CT nor CMR has a role in life-threatening acute cardiac tamponade requiring urgent pericardiocentesis. However, CT may help determine the feasibility of percutaneous versus surgical drainage when subacute cardiac tamponade is due to a loculated or complex effusion. CMR has little role in the management of cardiac tamponade. TEE may be useful in the postoperative or postprocedural setting to assess regional tamponade (see Table 6).

E. CP

1. Introduction. CP is a condition in which a thickened, scarred, inelastic, and often calcified noncompliant pericardium limits diastolic filling of the ventricles.[6,7,130] The etiologies of CP are diverse, including viral pericarditis, cardiac surgery, collagen vascular disease, radiation, tuberculosis, and sometimes idiopathic.[131] The most frequent cause of constriction varies depending on the geographic region. In Europe and the United States, CP is now most frequently encountered after a cardiac operation as well as an idiopathic or

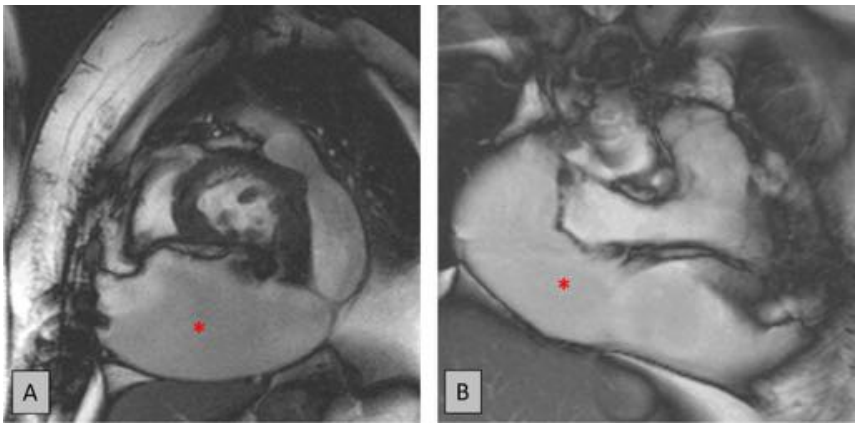

Figure 40 Pericardial tamponade on cine CMR. Dynamic cine CMR images in the short-axis (*left*; Video 17; available at www.onlinejase.com) and *right* two-chamber (*right*; Video 18; available at www.onlinejase.com) orientations demonstrate massive loculated pericardial fluid collection (*asterisks*), causing diastolic collapse to the ventricles inferiorly.

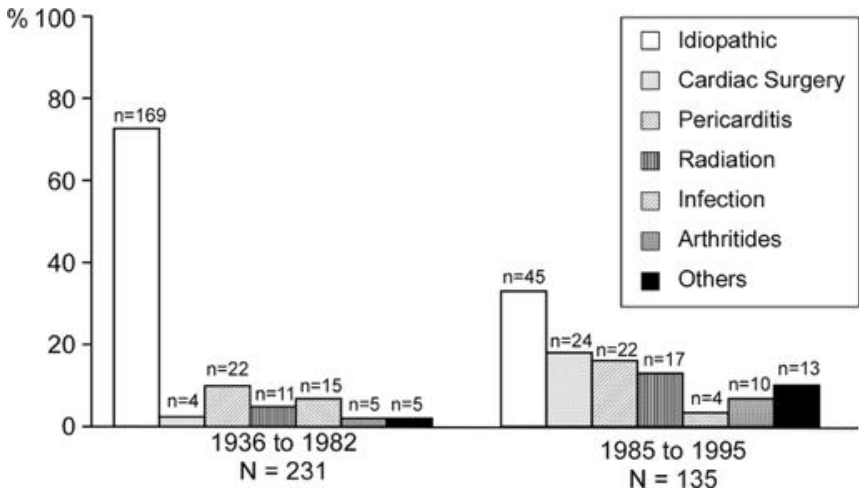

Figure 41 Etiologies of CP were compared between the period from 1936 to 1982 and the period from 1985 to 1995. The major change is that cardiac surgery is now the most common known cause of constriction in developed countries. Reproduced with permission from Ling.[132]

nonspecific viral insult[131,132] (Figure 41). In other parts of the world, tuberculosis is more common. Although CP is most often chronic, variants include subacute, transient, and occult CP. A good example of the long latency after pericardial damage is radiation therapy, in which constriction typically manifests itself >20 years after the initial treatment. The pericardium becomes thickened in most, but not all, cases of constriction. One study measured pericardial thickness in patients with surgically confirmed CP and found that the thickness was normal (≤2 mm) in 18% of cases.[133]

The pathophysiology of CP relates to the elevated and equalized cardiac pressures, because the total cardiac volume is determined by the scarred, fibrotic and inelastic pericardium. Like tamponade, this causes the heart chambers to operate in a "fixed" and noncompliant space and systemic and pulmonary venous pressures to rise in an attempt to maintain cardiac filling. Unlike cardiac tamponade, early diastolic filling in CP is more rapid than normal because the restraining effects of the pericardium do not occur until mid-diastole, after which little ventricular filling is seen even at atrial contraction. As CP becomes more severe and total cardiac volume is reduced further, cardiac output becomes lower and systemic venous pressures become high enough that ascites may occur.

Table 7 compares the pathophysiology of cardiac tamponade and CP. As in cardiac tamponade, ventricular interdependence is seen in CP, with an inspiratory shift in the interventricular septum to the left (Figure 15). The thickened, rigid pericardium also prevents the normal inspiratory decrease in intrathoracic pressure from being transmitted fully to the heart chambers. As the pressure in the extrapericardial pulmonary veins decreases normally with inspiration, a reduced pulmonary venous–to–left atrial gradient also contributes to the inspiratory decrease in LV filling. Opposite changes in the filling of the two ventricles are seen on expiration. Limited filling to the right ventricle during expiration results in substantial blood flow going back to the IVC and hepatic veins. These findings relate to the classic Doppler findings in CP.

Clinically, patients with CP usually present with fluid retention (ascites and leg edema), dyspnea, fatigue, abdominal discomfort, and sometimes persistent pleural effusion. Characteristic physical findings are increased jugular venous pressure with rapid "y" descent and Kussmaul's sign, peripheral edema, hepatomegaly, a diastolic gallop soon after the second heart sound (pericardial knock), and ascites. The entity is often not considered clinically, and patients may be referred to imaging laboratories without clinical suspicion of CP, with

Table 7 Comparison of the pathophysiology of cardiac tamponade and CP

Cardiac tamponade	CP
Fixed cardiac volume limiting cardiac filling ↑ respiratory variation of ventricular filling	Fixed cardiac volume limiting cardiac filling ↑ respiratory variation of ventricular filling
Ventricular interdependence (septal shift)	Ventricular interdependence (septal shift)
Elevated and equalized central venous, pulmonary venous and ventricular diastolic pressures	Elevated and equalized central venous, pulmonary venous and ventricular diastolic pressures
Prominent systolic filling (attenuated Y descent)	Prominent early diastolic filling (exaggerated Y descent)
Inspiratory ↓ in intrathoracic pressure not transmitted to heart (dissociation of intracardiac and intrathoracic pressures)	Inspiratory ↓ in intrathoracic pressure not transmitted to heart (dissociation of intracardiac and intrathoracic pressures)
Pulsus paradoxus common	Pulsus paradoxus uncommon
Kussmaul's sign not present	Kussmaul's sign

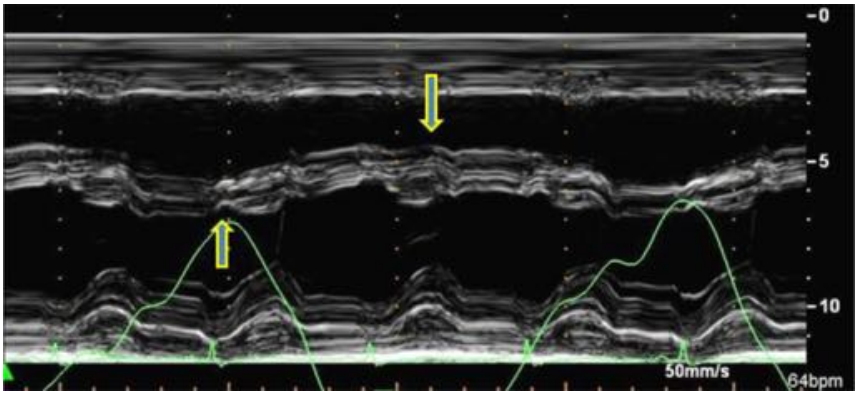

Figure 42 M-mode echocardiogram of a typical CP patient with the ventricular septum moving with respiration toward the left ventricle with inspiration (*upward arrow*) and toward the right ventricle with expiration (*downward arrow*). A simultaneous respirometric recording is shown at the *bottom* of the figure. Video 19 (available at www.onlinejase.com) shows the "septal bounce" on 2D echocardiography in the apical four-chamber view.

the diagnosis being established de novo after an imaging test. Pericardiectomy is usually advised in advanced cases, and outcomes are often related to the etiology of the pericarditis.[131]

2. General Indications for Imaging. The suspicion for CP is based on clinical history and examination, which require subsequent evaluation and confirmation by imaging and hemodynamic data. Because a substantial portion of patients with CP are referred without clinical consideration of CP, common referral reasons for imaging in these patients are heart failure, shortness of breath, evaluation of cardiac function, and peripheral edema. In clinically unsuspected cases, abnormal ventricular septal motion and/or increased pericardial thickness suggests the possibility of CP, which can be confirmed by diagnostic hemodynamic features. In patients with suspected constriction, imaging tests can focus on diagnostic information, including pericardial thickness, interventricular dependence, other associated abnormalities (valvular, myocardial, or coronary artery disease), and evidence of alternative pathologies, such as restrictive cardiomyopathy, RV dysfunction, or severe tricuspid regurgitation. On the basis of its ability for comprehensive morphologic assessment of the heart as well as the pericardium and hemodynamic characteristics, echocardiography remains the initial imaging test, and can provide a definite diagnosis of CP for most patients. The well-defined typical 2D and Doppler echocardiographic findings allow the correct diagnosis but also permit differentiation of CP from restrictive cardiomyopathy and other conditions mimicking constriction.

In those situations in which echocardiographic findings are equivocal, additional imaging testing (CT or CMR) is needed to make the diagnosis with more confidence. In some patients, hemodynamic cardiac catheterization may be necessary to establish the diagnosis. Even when the diagnosis of CP is certain after echocardiography, other imaging tests are often necessary to evaluate pericardial inflammation, coexisting myocardial disease, or comprehensive pericardial as well as cardiovascular anatomy for subsequent management decisions.

3. Echocardiography. *a. M-Mode and 2D Echocardiography.*– Echocardiography is usually the initial diagnostic procedure in patients with suspected CP. Pericardial thickening and calcification and abnormal ventricular filling produce characteristic changes on M-mode echocardiography (Figure 42). Increased pericardial thickness is suggested by parallel motion of the visceral and parietal pericardium, which is separated by a relatively echo-free space. Echocardiographic correlates of the hemodynamic abnormalities of CP include diastolic flattening of the LV posterior wall endocardium, abrupt posterior motion of the ventricular septum in early diastole with inspiration (septal shudder and bounce), and, occasionally, premature opening of the pulmonary valve.

Two-dimensional echocardiography reveals dilation and absent or diminished collapse of the IVC and hepatic veins (plethora, a sign of elevated RA pressure), moderate biatrial enlargement (restrictive cardiomyopathy is more often associated with severe atrial

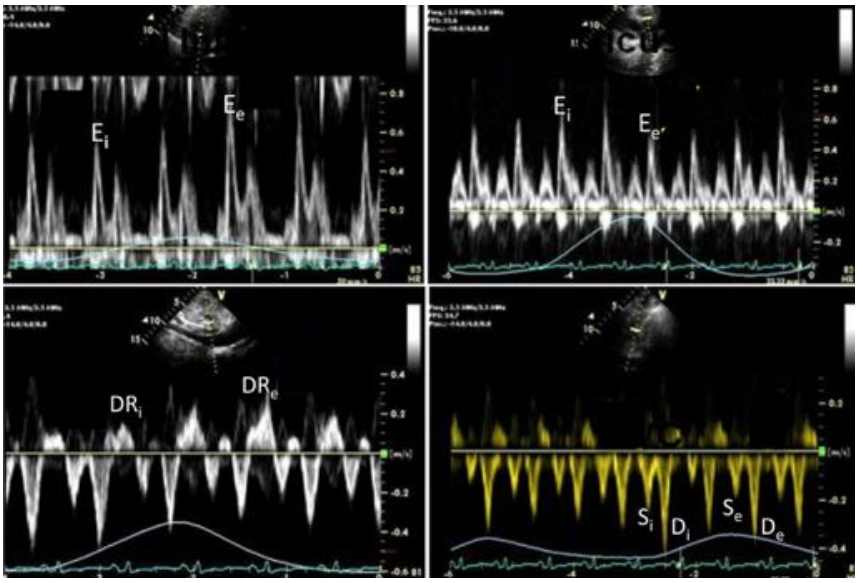

Figure 43 Characteristic PW Doppler echo findings of CP are shown with mitral inflow velocity (*top left*), tricuspid inflow velocity (*top right*), hepatic vein (*bottom left*), and SVC (*bottom right*), with simultaneous respirometric recording. E, DR_i, and S_i represent E velocity, diastolic reversal velocity, and systolic velocity, respectively, during inspiration. E_e, DR_e, and S_e represent E velocity, diastolic reversal velocity, and systolic velocity, respectively, during expiration.

enlargement), a sharp halt in ventricular diastolic filling, and abnormal ventricular septal motion that results from interventricular dependence (Figure 42). LV systolic function as judged by the ejection fraction is typically normal but may be impaired in mixed constrictive-restrictive disease, which may occur with radiation-induced disease or after cardiac surgery. Measurement of pericardial thickness by TEE correlates strongly with that obtained by CT and has deserved an American College of Cardiology, American Heart Association, and American Society of Echocardiography class Iib IIb recommendation.[19] However, it is important to remember that demonstration of the characteristic "constrictive" hemodynamics is required to establish a firm diagnosis.

b. Doppler Flow Velocity Recordings.–Doppler echocardiography is essential for establishing the diagnosis and usually shows a restrictive LV and RV diastolic filling pattern, characterized by a high early (E) velocity, a shortened deceleration time, and a reduced atrial (A) wave. Mitral inflow velocity usually, but not always, falls by as much as 25% to 40%, and tricuspid velocity greatly increases (>40%–60%) in the first beat after inspiration (Figure 43).[134,135]

In summary, the key points using Doppler echocardiography in CP are the following:

- The consensus for the calculation of percentage respiratory variation in CP for mitral and tricuspid inflow is (expiration − inspiration)/expiration.
- For peak mitral E inflow, the maximal drop occurs with the first beat of inspiration and the first beat of expiration and usually exceeds 25% respiratory variation.
- For peak tricuspid E inflow, the maximal drop is on the first beat in expiration at the same time as the hepatic vein atrial reversal and usually exceeds 40% respiratory variation. The calculated % will be a negative value.

These phenomena are manifestations of greatly enhanced ventricular interaction and are not present in either normal subjects or patients with restrictive cardiomyopathy. Increased respiratory variation of mitral inflow may be missing in patients with markedly elevated left atrial pressure but can sometimes be brought out in such patients by preload reduction with a head-up tilt or diuretic administration[136]; however, this maneuver is often not as necessary using the mitral annular velocity for the diagnosis of CP. Similarly, the respiratory variation in pulmonary venous (particularly diastolic) flow is often pronounced,[137,138] similar to mitral inflow, but not always necessary for the diagnosis of constriction. Hepatic vein diastolic flow reversal increases with expiration, reflecting the ventricular interaction and the dissociation of intracardiac and intrathoracic pressures (Figure 43), which is essential in the diagnosis of constriction; inspiratory hepatic vein diastolic flow reversals suggest restrictive cardiomyopathy. The propagation velocity of early diastolic transmitral flow on color M-mode is normal or increased and is often >100 cm/sec[139] (Figure 44).

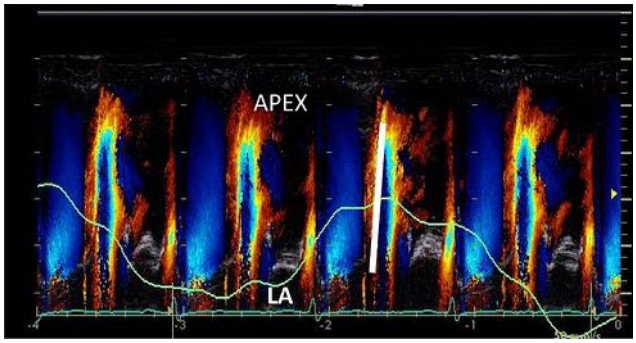

Figure 44 Characteristic color M-Mode echocardiographic findings in a patient with CP showing the rapid (100 cm/sec) flow propagation slope (line at the junction of the *red-yellow* aliasing velocity) from the left atrium (LA) to the apex of the left ventricle.

Doppler tissue imaging is particularly useful in differentiating between CP and restrictive cardiomyopathy.[140-143] Tissue Doppler shows a prominent early diastolic velocity (e′) from the medial mitral annulus, which is an important point of distinction from restrictive cardiomyopathy in which transmitral E is tall and narrow

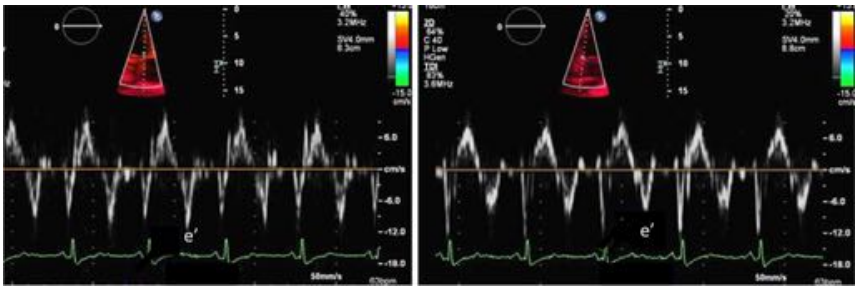

Figure 45 Doppler tissue imaging of medial (*left*) and lateral mitral annulus (*right*). The medial e′ velocity (*arrow*) is 12 cm/sec, and the lateral e′ velocity is lower at 8 cm/sec.

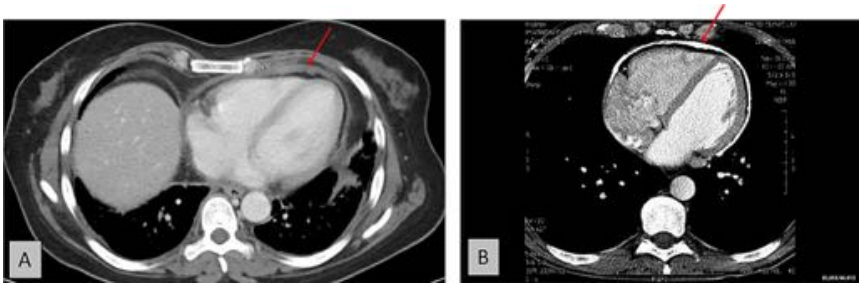

Figure 46 **(A)** CT of the chest showing increased pericardial thickness (*red arrow*). **(B)** CT of the chest showing circumferential calcification of the pericardium (*red arrow*) in a 40-year-old man who became short of breath and developed fluid retention. Video 20 (available at www.onlinejase.com) of cine CT shows septal bounce and severe calcification around the right side of the heart.

but tissue e′ is reduced (<7 cm/sec). The usually positive linear relation between E/e′ ratio and left atrial pressure, which is useful for assessing left atrial pressure in cardiomyopathy, is reversed ("annulus paradoxus") in most patients with CP[144] because medial e′ increases progressively as the severity of constriction becomes worse. Lateral mitral annular e′ is usually lower than e′ from the medial annulus ("annulus reversus") in patients with CP (Figure 45).[145,146] The finding of annulus reversus appears to be related to the tethering of the lateral mitral annulus to the thickened pericardium. The pericardial thickness at the left atrioventricular groove measured by CT is found to have an inverse relationship with lateral e′ velocity.[147] After pericardiectomy, the lateral and medial mitral annulus normalizes.[146]

c. Strain Imaging.–Differences in longitudinal and circumferential deformation may be useful to distinguish CP from restrictive cardiomyopathy. Usually, circumferential strain, torsion, and early diastolic untwisting are reduced, and global longitudinal strain, displacement, and early diastolic tissue velocities are unchanged in constriction, whereas circumferential strain and early diastolic untwisting are preserved and longitudinal strain is reduced in restrictive cardiomyopathy.[148] Recent work using speckle-tracking showed that there are significant differences in regional longitudinal systolic strain in constriction compared to restriction. The ratio of LV lateral wall strain to LV septal wave strain was more robust than regional annular velocity using tissue Doppler in differentiating constriction from restriction. Removal of the pericardial constraint by pericardiectomy led to improvement in longitudinal strain in the RV and LV free walls as well the circumferential strain.[149] From these two studies, it can be concluded that longitudinal strains may be attenuated regionally in the free wall of the right and left ventricles, but in general, the reductions in global strains are more pronounced in constriction in the circumferential directions, whereas in restriction, they are more profoundly attenuated in the longitudinal direction.[148,149]

Technically, a comprehensive "diastology" echocardiography exam is required for assessing CP, and the study needs to be performed with attention to detail with an accurate ECG recording as well as simultaneous recording of the patient's respiration. Most current state-of-the art echocardiographic machines have integrated respirometry recording capability, but the recordings from the machines can be unstable and depend on the patient's position. Thus, it is important to adjust the respirometer recordings to be able to assess the onset of inspiration and onset of expiration (as described above). It is also critical to place the sample volume (1–2 mm) at the correct location to record the highest mitral E velocities and to enlarge the sample volume size (3–4 cm) when hepatic vein flow velocities are obtained (see Appendix for technical details). The entire screen space should be used for recording flow velocities so that their respiratory variation can be easily recognized. M-mode recording of the ventricular septal motion is helpful in patients with a subtle abnormality related to ventricular interdependence.

4. CT. CT is a highly accurate method of evaluating pericardial thickness and therefore plays an important role in the diagnosis and management of CP.[150] The normal pericardium is identified as a 1-mm to 2-mm curvilinear line of soft-tissue density, whereas in CP, the parietal pericardium is usually 4 to 20 mm thick. Because of the close physiologic similarities of CP and restrictive cardiomyopathy, increased pericardial thickness detected by CT is a useful means of distinguishing between the two disorders (Figure 46A). However, as mentioned, 28% of 143 surgically confirmed cases had normal pericardial thickness on CT, and 18% had normal thickness on histopathologic examination.[133] CT is also the best diagnostic technique to detect pericardial calcification (Figure 46B). Irregular calcification may be found anywhere over the surface of the heart but is primarily found in regions where pericardial fat is abundant (i.e., the atrioventricular groove and base of the heart). About 50% of constriction cases show some degree of calcification.

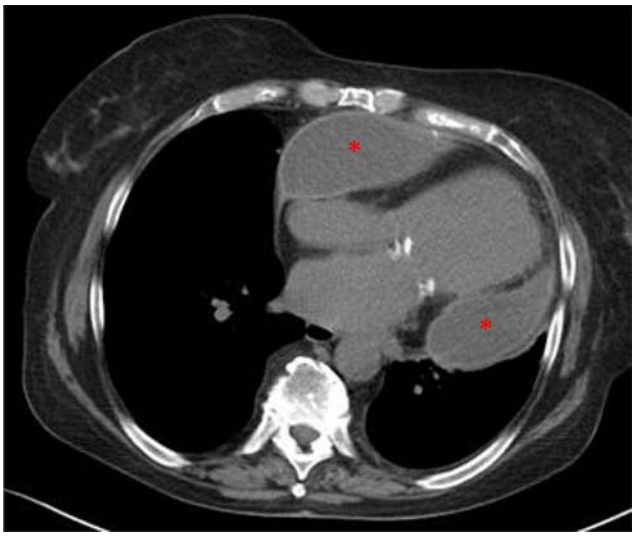

Figure 47 CT of the chest from a patient with rheumatoid arthritis and constriction, demonstrating deformed heart shape with a large pericardial mass (*asterisk*).

Indirect findings on CT that suggest CP include a narrowing and tubular deformation of the right or left ventricle, normal or small ventricular size, and straightening of the interventricular septum (Figure 47). Signs of impaired diastolic filling of the RV include dilatation of the IVC, hepatic veins, and right atrium; hepatosplenomegaly; ascites; and pleural effusions.

CT may assist in the preoperative planning of pericardiectomy by detailing the location and severity of pericardial thickening and calcification in patients with histories of cardiothoracic surgery, given its ability to identify critical vascular structures.[8,36] In addition, CT offers the ability to assess the extent of lung injury in patients with previous radiation exposure, evaluate the location and extent of pericardial calcification, and determine the need for invasive coronary angiography in those with normal results on computed tomographic coronary angiography.

Dedicated imaging of the pericardium with CT should use cardiac (electrocardiographically synchronized) protocols[150,151] and should be performed with low-dose, prospective triggering whenever possible (see Appendix). Additional dose sparing techniques (reduced tube voltage [100 kV], iterative reconstruction) should be used if possible.[151] CT may be used to examine the effect of cardiac motion transmitted to the surrounding pulmonary parenchyma. Failure of the immediately adjacent pulmonary structures to pulsate during the cardiac cycle, in the presence of a regionally or globally thickening pericardium, is virtually diagnostic of CP. Failure to visualize the posterolateral LV wall on dynamic CT suggests myocardial fibrosis or atrophy and is associated with a poor surgical outcome. However, retrospectively gated computed tomographic image acquisition and reconstructions, which allow four-dimensional dynamic display in cine loops, are associated with high radiation exposure and limited clinical value. They remain a niche indication for a few patients with limited echocardiograms and contraindications to CMR, such as pacemakers or implantable cardioverter-defibrillators.

Because of the natural contrast between the pericardium and the surrounding epicardial and pericardial fat rim, intravenous contrast is not absolutely necessary. However, intravenous contrast administration is preferred by many investigators because it provides clear delineation of the cardiac chambers and may occasionally demonstrate pericardial enhancement as a sign of inflammation (Figure 48).

5. CMR. Gated CMR provides direct visualization of the normal pericardium, which is composed of fibrous tissue and has a low CMR signal intensity. CMR is advocated by some as the diagnostic procedure of choice for the detection of certain pericardial diseases, including CP; however, echocardiography remains the first-line imaging modality. Characteristic CMR features in patients with CP include increased pericardial thickening and dilatation of the IVC, an indirect sign of impaired RV diastolic filling and elevated right-sided filling pressures.

Although CT is superior to CMR in detecting calcification, CMR better differentiates small effusions from pericardial thickening; in addition, focal, nodular fibrocalcific changes may be seen. CMR also has the potential to resolve hemodynamic events (such as septal bounce) and is able to better identify pericardial inflammation and pericardial-myocardial adherence.[43,45] Unlike cardiac CT, CMR does not involve exposure to ionizing radiation.

Gadolinium contrast–enhanced CMR of the pericardium commonly demonstrates LGE in patients with CP; however, this is not a universal finding. Patients with CP and pericardial LGE have greater fibroblast proliferation, chronic inflammation, neovascularization, and pericardial thickening compared with those without LGE.[26] Pericardial LGE might also be a predictor of reversibility of CP after treatment with anti-inflammatory agents (Figure 49).[152]

Comprehensive CMR examinations include morphologic imaging (T1W sequences) and functional imaging (cine sequences).[45] Additional T2 STIR morphologic sequences and delayed contrast imaging after gadolinium administration are used for the identification of pericardial edema and inflammation (see Appendix for sequences).

CMR allows reliable anatomic delineation of the pericardium from adjacent tissue and measurement of pericardial thickness. As described for CT, a thickened pericardium (>4 mm) in the proper clinical setting often supports the diagnosis, although absence of pericardial thickening does not necessarily rule out CP. Prior studies have demonstrated that CMR has an accuracy of 93% when differentiating between CP and restrictive cardiomyopathy, using pericardial thickening of >4 mm as the cutoff,[153] but it is important to emphasize that the diagnosis of CP is a clinical and hemodynamic one.

CMR, like echocardiography, is a functional modality with good (but inferior to echocardiography) temporal resolution, allowing the detection of hemodynamic features of constriction. These include abrupt cessation of diastolic filling, septal bounce,[154] or respirophasic variation in septal excursion, identified on real-time cine sequences[155] (Figure 50). CMR myocardial tagging sequences can demonstrate pericardial-myocardial adherence. Fibrotic pericardial adhesions are present when tag deformation is absent.[11]

Phase-encoding velocimetry provides information similar to that provided by Doppler echocardiography.[153,156] A recent study demonstrated that real-time phase-contrast CMR acquired over 10 sec of unrestricted breathing and without ECG gating could demonstrate the characteristic hemodynamic changes of constrictive physiology. Respiratory variation in transmitral valve flow velocities exceeding 25% was seen in all patients with CP, and a greater variation of 45% was seen across the tricuspid valve in patients with CP. Although theoretically appealing, this sequence is not easy to use in practice, because respiration changes the position of the imaging slice with regard to the mitral and tricuspid valves, potentially influencing inflow velocities or patterns. Real-time cine imaging of the ventricular septal motion to assess the septal flattening or inversion is far easier.

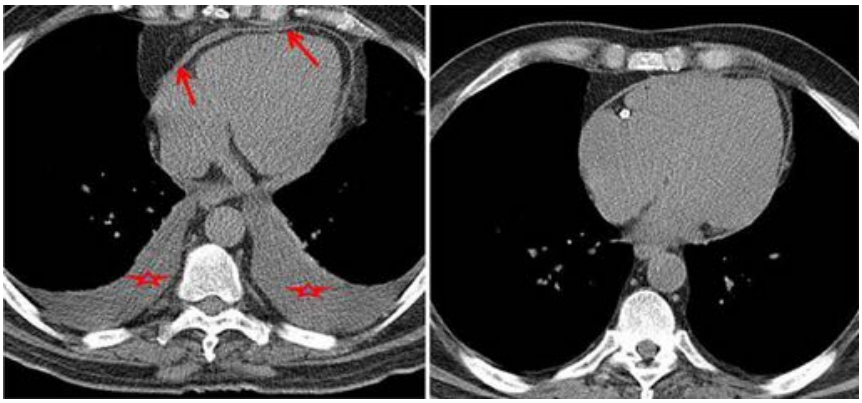

Figure 48 CT of the chest from a patient with transient CP, demonstrating thick pericardium (*arrows in left image*) and pleural effusion (*star*) at baseline when the patient was having symptoms of constriction, which was returned to normal thickness (*right*) after 1 month of steroid therapy.

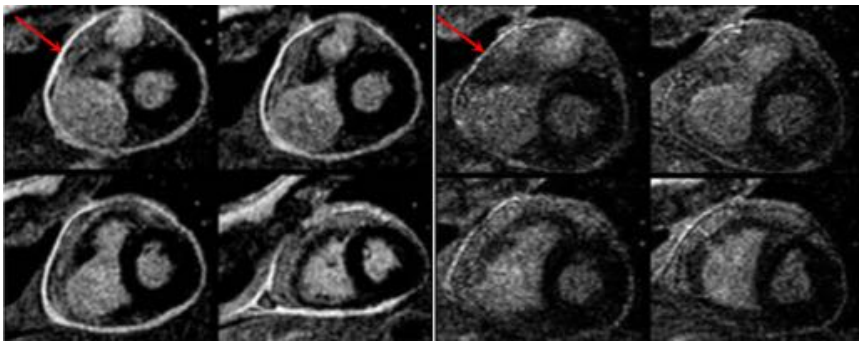

Figure 49 CMR with intense delayed enhancement (*red arrows*) of the pericardium (*left*). After 6 weeks of prednisone therapy, the delayed enhancement was reduced (*right*).

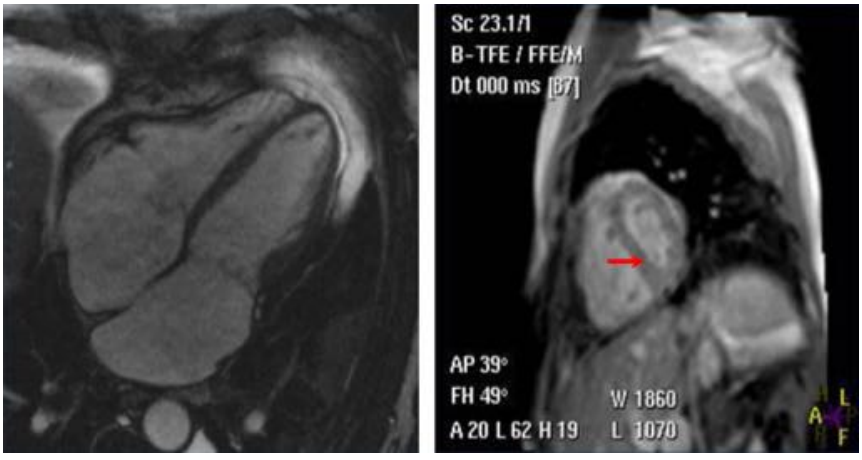

Figure 50 Cine CMR with septal bounce (*left*; Video 21; available at www.onlinejase.com) and free-breathing sequence showing the interventricular dependence with shift of septum toward left (*red arrow*) (*right*; Video 22; available at www.onlinejase.com). Courtesy of Dr. Teerapat Yingchoncharoen.

Calculation of the maximal septal shift is easily achieved providing useful information with regard to ventricular coupling.

6. When to Consider Added Imaging. The number of imaging studies needed for the diagnosis and management of patients with CP depends on the expertise of operators in each imaging modality and clinical needs. If a patient has a very likely diagnosis of constriction from initial history, physical examination, and blood work, any one of the imaging tests can be sufficient to confirm the diagnosis. However, in most patients, echocardiography is usually the initial imaging test, and it is able to identify the characteristic hemodynamic as well as structural features of constriction. Also important is to assess the severity of atrioventricular valve regurgitation, even when constriction is diagnosed by another test, because it may get worse after

Table 8 Imaging findings of CP

Summary of echocardiographic findings
• M-mode: diastolic flattening of the LV posterior wall endocardium with little or absent respiratory movement, abrupt inspiratory posterior motion of the ventricular septum in early diastole with reciprocal changes in LV/RV dimensions throughout the respiratory cycle; premature opening of the pulmonary valve
• 2D: abrupt early diastolic LV and RV diastolic filling halt "diastolic checking"; inspiratory ventricular septal motion toward right ventricle (septal bounce); marked dilation and absent or diminished collapse of the IVC and hepatic veins
• Doppler: restrictive filling pattern of RV and LV diastolic filling; >25% fall in mitral inflow velocity and >40% increase in tricuspid velocity in the first beat after inspiration; opposite changes in expiration; low hepatic vein velocities; decreased expiratory diastolic hepatic vein velocities with large reversals
• Tissue Doppler: normal or increased mitral annular velocity (>7 cm/sec); annulus paradoxus; annulus reversus
• Color M-mode: normal or increased propagation velocity of early diastolic transmitral flow
Summary of CT findings
• Pericardial thickness > 4 mm; definition of pericardial calcification
• Indirect findings: narrowing and tubular deformation of the right or left ventricle; normal or small ventricular size; straightening of the IVS; dilatation of the IVC, hepatic veins, and right atrium; hepatosplenomegaly, ascites, and pleural effusions
Summary of CMR findings
• Pericardial thickening; functional changes similar to echocardiography using cine sequences (abrupt cessation of diastolic filling, septal bounce, or respirophasic variation in septal excursion)
• Pericardial edema and inflammation using T2 STIR and LGE sequences
• CMR myocardial tagging sequences: pericardial-myocardial adherence
• Phase encoding velocimetry: information similar to Doppler echocardiography
• Real-time cine imaging:demonstration of respirophasic shift of the ventricular septum

IVS, Interventricular septum.

pericardiectomy because of enlargement of the atrioventricular valve annulus. If a patient has increased inflammatory biomarkers or a short duration of constrictive symptoms (<3 months, usually), CMR is valuable to assess the extent of pericardial inflammation. If the pericardial inflammation is intense, a trial of anti-inflammatory agents should be considered before pericardiectomy.[8,26,152]

In patients who develop (recurrent) constriction after pericardiectomy or cardiac surgery, CT is very helpful to delineate coronary, cardiac, and pericardial anatomy before consideration of redo pericardiectomy.

It is very possible that a surgeon may not feel comfortable proceeding with pericardiectomy solely on the basis of echocardiographic findings, because pericardiectomy is not a common procedure. In this situation, another imaging test or cardiac catheterization is reasonable to confirm the diagnosis. When echocardiography is not diagnostic for CP in patients suspected for the diagnosis, hemodynamic cardiac catheterization is almost always necessary to demonstrate the characteristic hemodynamics, which are different from those of myocardial diseases. Table 8 shows a summary of the imaging findings in CP.

F. Effusive CP

1. Introduction. Effusive CP is the most uncommon of the pericardial constraint syndromes. It is a distinct entity with transitional and concomitant pathophysiologic features of acute effusive pericarditis with cardiac tamponade and chronic CP. Effusive CP occurs when pericardial fluid accumulates between a thickened, edematous, or fibrotic parietal and visceral pericardium.[157] The hallmark of this condition is the hemodynamic occurrence of an elevated RA pressure, elevated RV and LV end-diastolic pressures with associated "dip and plateau" ventricular waveforms, and respiratory interventricular dependence occurring after pericardiocentesis.[158] The prevalence of effusive CP was reported to be 1.3% in a prospective series of patients evaluated from 1986 to 2001 presenting with pericarditis and 6.9% of those with cardiac tamponade.[158] In a surgical series of 95 patients undergoing surgery for CP, effusive-constrictive etiology accounted for 24% of patients.[159] Similar to other pericardial diseases in which broad spectra of etiologies are reported, idiopathic conditions are the most common. However, in contrast to chronic noneffusive CP, radiation-related and malignancy-related diseases appear more frequent than a postsurgical etiology.[158] The distinguishing histopathologic feature of effusive CP is the involvement of the visceral pericardium along with a tense PEff contributing to constrictive physiology. Otherwise known as "epicarditis," there is involvement of both the visceral and parietal pericardium with inflammation, fibrotic thickening, and variable myocardial adherence (Figure 51).[160]

The clinical features of effusive CP are similar to those of chronic noneffusive CP. The clinical course may be variable depending on the underlying etiology, with many patients dying of comorbidities related to malignancy, radiation, or infection. Patients with idiopathic-related effusive CP undergoing pericardiectomy generally have favorable outcomes, with improved hemodynamics, quality of life, and survival.[159]

2. General Indications for Imaging. The approach to the diagnosis of effusive CP mirrors that of CP. Because this is generally a chronic condition, the clinical presentation is more consistent with constrictive pericardial physiology than cardiac tamponade. Patients tend to present with three clinical scenarios: (1) active pericarditis with a PEff composed of echogenic material; (2) a chronic PEff with right heart failure symptoms or signs; and (3) cardiac tamponade that fails to improve after pericardiocentesis, as reflected by ongoing right heart failure, persistent elevation of right and left heart filling pressures, or clinical and/or echocardiographic findings that suggest CP. Therefore, imaging is indicated in the evaluation and management of pericardial disease in the settings described above or in the workup of CP.

3. Echocardiography. The echocardiographic findings of effusive CP depend on the stage of the disease, although most often,

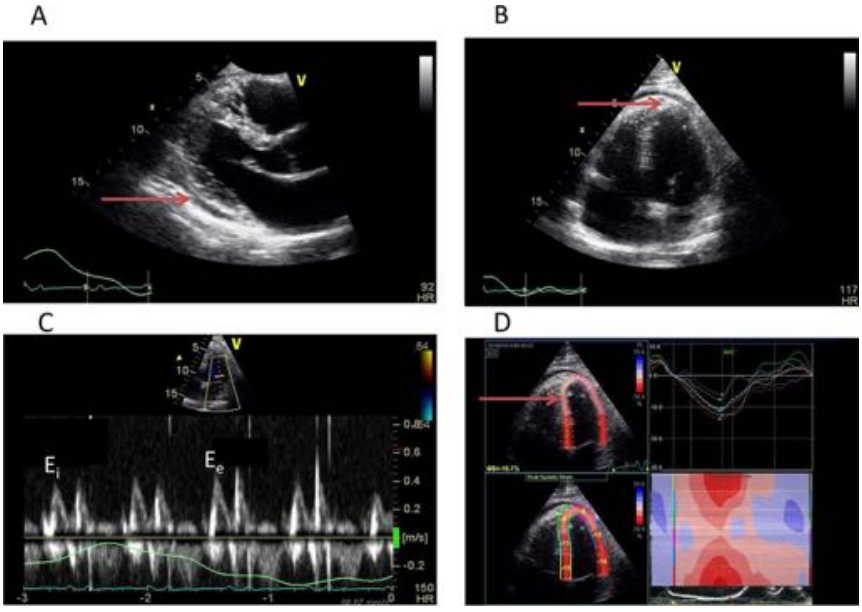

Figure 51 Characteristic two-dimensional echocardiographic findings in the parasternal long-axis view (**A**; Video 23; available at www.onlinejase.com) and apical four-chamber view (**B**; Video 24; available at www.onlinejase.com), Doppler findings from the mitral inflow with the E velocity in inspiration (E_i) and expiration (E_e) noted **(C)**, and speckle-tracking **(D)** in a patient with effusive constriction. Note the thickened pericardium (*arrow*), respiratory variation in the mitral inflow, and decreased regional longitudinal strain. Reprinted with permission from Dahiya.[160]

the M-mode, 2D, and Doppler features are consistent with a sizable PEff and cardiac tamponade. Later stages of effusive pericarditis may have features more suggestive of CP. Most reports describe either a transition to or the presence of organized intrapericardial material or echogenic PEff.[161-163] Within the effusion, there may be bandlike fibrinous strands that traverse the pericardial cavity from visceral to parietal surfaces, resulting in regions of loculation.[163] Because of the regions of loculation, there may be no alteration in the location of pericardial fluid with change in position. Visceral pericardial thickening and irregularities may sometimes be appreciated. Recently, speckle-tracking was used to evaluate regional strain in a patient with effusive CP before and after pericardiectomy (Figure 51).[160]

4. CT. CT can evaluate the degree of pericardial thickening in effusive CP, similar to pure CP. A thickness >3 mm is considered pathologic. Although increased pericardial thickening along with a PEff supports the diagnosis of effusive CP, the clinical diagnosis also requires demonstration of concomitant constrictive physiology. However, effusive CP can also occur with only minimal pericardial thickening.

5. CMR. Like CT, CMR can evaluate the degree of pericardial thickening similar to pure CP. In addition, the ability of CMR to distinguish pericardial fluid from the pericardium and to detect inflammation makes it useful in atypical forms of the effusive CP.[41] Increased ventricular interdependence results in flattening or inversion of the septum.

6. When to Consider Added Imaging. In addition to clinical information, echocardiography, preferably with a dedicated comprehensive diastologic evaluation, is performed in all patients with suspected effusive CP. CT and CMR are complementary to echocardiography. In the past, the diagnosis of effusive CP required hemodynamic demonstration of constrictive physiology after pericardiocentesis or direct surgical inspection, but it is now often detected earlier with imaging techniques.[164] Table 9 summarizes the imaging findings in effusive constriction.

G. Pericardial Masses (Tumors, Cysts, and Diverticulum)

1. Pericardial Tumors. *a. Introduction.*–Tumors of the pericardium can be divided into primary (benign and malignant) and metastatic. Primary pericardial tumors are very rare and, when found, are more often benign. Benign pericardial primary tumors include teratoma, lipoma, fibroma, hemangioma, and lymphangioma. Most of these benign tumors are found in children and adults, while teratomas can be detected even in utero by fetal echocardiography. In children and adults, these tumors may be found incidentally or patients may present with palpitations and arrhythmias. Benign pericardial masses may grow to sizable lesions before they produce compression of cardiac chambers or displacement of mediastinal structures. Benign tumors can be found in both the parietal pericardium and epicardium as discrete pedunculated or sessile masses. Complete surgical excision is the treatment of choice for both histopathologic diagnosis and relief of symptoms.

Malignant mesothelioma is the most common malignant primary tumor of the pericardium, followed by angiosarcoma. Symptoms are nonspecific and include chest pain, dyspnea, and dry cough. Presenting signs are usually due to recurrent PEff or the presence of invasion into the myocardium. Obliteration of the pericardial cavity can cause constriction. The yield of malignant cells in pericardiocentesis fluid has been poor in primary malignant pericardial tumors; therefore, antemortem diagnosis often requires open pericardial tissue biopsy. Most cases of primary malignant tumors are nonresectable at the time of diagnosis. Chemotherapy and radiotherapy offer little benefit.

Table 9 Imaging findings of effusive CP

Summary of Echo findings
• PEff
• Echogenic/organized material in PEff
• Bandlike fibrinous strands that traverse the pericardium from visceral to parietal surface
• Irregularities/thickening of pericardial surface
• Loculated PEff
• Associated findings consistent with cardiac tamponade
• Postpericardiocentesis findings consistent with CP
Summary of CT findings
• PEff
• High-attenuation material in PEff
• Enhancing pericardial layers ± bandlike strands/synechiae
• Nodular thickening of pericardial surface
• Pericardial calcification
• Loculations
• Chamber morphology and volumes ± ventricular function, if gated acquisition used
Summary of CMR findings
• PEff
• Abnormal signal intensity structures within effusion ± synechiae
• Early postgadolinium T1 shortening or LGE of pericardial layers
• Nodular thickening of pericardial surface
• Loculations
• Ventricular filling patterns on phase-contrast imaging
• Slow phase-contrast flow (using very low velocity encoding) differentiates pericardial fluid from pericardial thickening
• Chamber morphology and volumes and function, including respirophasic physiology (ventricular interdependence)
• Tagged cine may demonstrate adhesions in areas without pericardial fluid (in cases with loculation)

Secondary tumors from either local invasion or metastases are by far more common in the pericardium and most frequently occur from lymphoma, melanoma, as well as lung and breast carcinoma.[165,166]

Patients with known malignancies often present with signs and symptoms of pericarditis or PEff. The diagnostic yield of pericardial cytology is high in secondary malignancies from solid tumor metastases but can be quite low in cases of hematologic malignancies. Metastatic lesions to the pericardium often are associated with serosanguinous-appearing effusions. Pathologic examination of the pericardium with metastatic disease can show a thickened pericardium with regions of nodularity related to tumor deposition. Pericardial tumors generally do not invade into the myocardium. An exception to this is melanoma, which classically involves the myocardium as well.[165,167] Clinical status and prognosis will generally guide patient selection for surgical palliative therapy, including intrapericardial instillation of chemotherapeutic or sclerosing agents. Pericardial window may be indicated for symptomatic relief of a rapidly recurrent malignant PEff.

Clinical manifestations of pericardial tumors range from incidental findings during imaging to PEff with tamponade physiology, and rarely, CP can also occur. Atrial fibrillation, presumably due to irritation of the atria from a pericardial tumor, can also develop. Patients may develop palpitations, cough, pleuritic chest pain, or dyspnea. The treatment of patients with pericardial tumors depends on the type and extent of involvement and should be tailored to the individual situation. Tumors can be resected if they cause hemodynamic compromise or symptoms due to a mass effect. Chemotherapy or radiation treatment can be offered for malignant tumors.

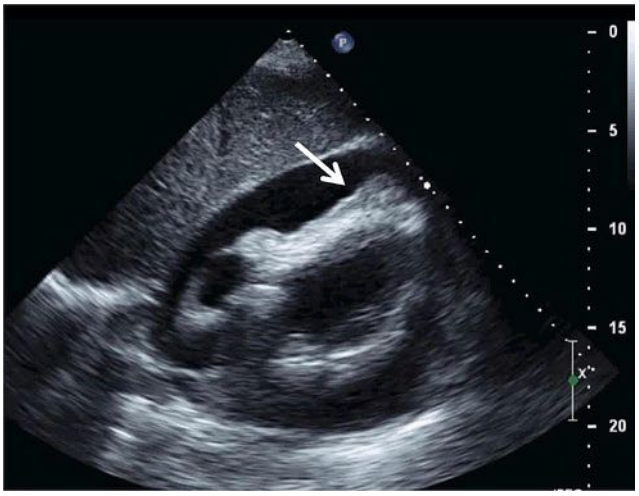

Figure 52 Pericardium is diffusely thickened with nodular regions (*arrow*) consistent with tumor mass (Video 25; available at www.onlinejase.com). Associated PEff is also present.

b. General Indications for Imaging.–Pericardial masses can readily be identified by echocardiography; however, tissue characterization and infiltration of the adjacent structures by the mass are not well defined by echocardiography. CT and CMR are often the imaging modalities of choice for further assessment of pericardial masses.

c. Echocardiography.–Pericardial tumors are seen as echodense masses on the pericardium. Masses can be nodular, or the pericardium can be diffusely thickened; and depending on the tumor, characteristics can appear homogeneous or heterogeneous. Typically, the masses are nonmobile, although there may be mobile elements on the surfaces. Pericardial thickening and PEff with or without constrictive physiology may be detected on echocardiography. A mass lesion may not be evident in malignant tumors, because these tend to exhibit a diffuse growth pattern rather than discrete mass lesions. Benign lesions, including teratomas, hemangiomas, and lymphangiomas, can appear as cystic masses with septations. Figure 52 shows an echocardiographic example of a pericardial tumor mass.

d. CT.–Although TTE is useful in the initial evaluation of pericardial tumors, CT or CMR can provide additional information about the morphology, location, and extent of a pericardial neoplasm. CT is complementary to MR but is more robust in identifying other thoracic lesions, including primary lung cancer, pulmonary metastases, and mediastinal nodes.[59]

CT offers excellent contrast resolution, which facilitates identification of PEff and pericardial masses.[8,168] Features of pericardial malignancy apparent on CT include an irregular, thickened, nodular pericardium; a complex PEff; pericardial enhancement with contrast[169]; and the presence of a mass in the pericardium.[37] Disruption of the pericardial sac; presence of hemorrhagic effusion; invasion into the epicardial fat tissue, myocardium, or a cardiac chamber; and mediastinal adenopathy are characteristics of a malignancy with an aggressive nature.[8]

A malignant pericardial mesothelioma may present as a PEff with pericardial nodules or plaques on CT.[170,171] Benign tumors of the pericardium include lipomas, which demonstrate low-attenuation fat (i.e., negative Hounsfield units) on CT, and teratomas, which present as masses containing both fat and high-attenuating calcium on CT.

Table 10 Imaging findings in pericardial tumors

	Imaging findings	Advantages
Echocardiography	Nodules or diffuse thickening on pericardium	Detection of hemodynamic effects of tumor or effusion
CT	Contrast-enhancing masses on pericardium	Accurate localization and sizing, detection of calcification, blood, or fat
CMR	High–signal intensity T2W images	Accurate localization and sizing; tissue characterization

e. CMR.–Tissue characterization in pericardial tumor evaluation by MR is superior to that of echocardiography and CT.[8] Most malignant soft-tissue tumors of the pericardium have signal-intensity characteristics similar to myocardium on T1W SE imaging, with the exception of melanoma, which has high intensity because of short T1 effects from paramagnetic metals bound by melanin,[9,48,172] and liposarcoma, which has high signal intensity because of a largely fatty content responding to fat suppression techniques.[8,48,59] Increased tissue edema in malignant pericardial tumors is typically manifested by increased signal on either T2W SE images or STIR images.[8,36,48,173,174]

In contrast, a benign pericardial fibroma usually demonstrates low signal intensity on T2W imaging because of its fibrous content.[48,169] Well-defined or encapsulated pericardial lesions without pericardial irregularity or effusions are more likely to be benign.[59] On the other hand, a malignant pericardial mesothelioma shows diffuse irregular cardiac encasement, as well as associated PEff or evidence of CP.[175-177]

The infiltration of the pericardium by a tumor arising outside the heart can be identified by the absence of the low-intensity pericardial line.[54,86,177]

Hemorrhagic PEffs, which are disproportionately large to the size of the tumor mass, are common in pericardial metastases and usually demonstrate high signal intensity on T1W SE images.[41,85]

When administered as a rapid bolus during first-pass imaging, both primary and secondary pericardial tumors typically show some degree of enhancement with gadolinium-based contrast media, helping confirm the presence and extent of tumor and differentiate it from hematoma or complex effusion.[59] Postcontrast T1W SE images and delayed enhancement images can also facilitate this differentiation.[59,178] Because of their increased vascularity, pericardial malignancies usually enhance heterogeneously after contrast administration.[9,36] On the other hand, benign fibromas have poor vascularization and demonstrate little to no postcontrast enhancement.[169,173]

Dynamic imaging is also a potentially useful adjunct in the assessment of pericardial tumors. Standard cine images, such as with balanced SSFP, will clearly identify PEff and show areas of pericardial thickening or mass. In addition, cine images will also provide information about physiologic consequences of the tumor on cardiac function. Pericardial tethering and/or direct extension to adjacent structures are generally indications of malignancy, and dynamic tagging may help identify such physical connections.[59]

The aforementioned capabilities allow CMR to be a useful modality for the identification of pericardial disease suggesting tumor, differentiation between benign and malignant pericardial tumor, and differentiation at times among specific types of pericardial malignancy. However, it is a combination of characteristics that provides the greatest yields.

On CMR, neoplasms exhibit medium signal intensity on T1W SE images and high signal intensity on T2W SE images.[179] Melanoma is an exception, with characteristic high intensity on T1W images. A pericardial hemorrhagic effusion, caused by a malignant primary or secondary tumor of the heart or pericardium, can be easily recognized by CMR or CT. Because of their vascularity, pericardial metastases usually enhance after contrast administration.

f. When to Consider Added Imaging.–Echocardiography is an appropriate initial imaging modality to detect tumor involvement of the pericardium and is best suited to assess hemodynamic consequences of tumor infiltration as well as for serial assessment. However, CMR or CT is superior for tumor localization and site and extent of invasion into surrounding tissue. CMR is best suited for tissue characterization, including differentiation from thrombus, fatty content, and tumor vascularity. Table 10 summarizes the imaging findings in pericardial masses.

2. Pericardial Cysts and Diverticula. *a. Introduction.*–Pericardial cysts are uncommon and generally benign lesions.[7-9] Most are congenital malformations, while some, such as hydatid cysts, are infectious in nature. Congenital pericardial cysts are fluid-filled, unilocular sacs lined by mesothelial cells. Cysts are enclosed spaces and do not communicate with the pericardial space. The majority are detected between the third and fourth decades as incidental findings on chest x-ray, echocardiography, or CT. Although most are asymptomatic, approximately 25% of patients with pericardial cysts present with nonspecific symptoms, such as chest pain, cough, dyspnea, and palpitations. Pericardial cysts are rarely of clinical significance unless they are associated with compression symptoms. Rupture of pericardial cysts with hemorrhage has been reported to cause cardiac tamponade. Asymptomatic patients are managed conservatively with close follow-up. Treatment of symptomatic patients includes percutaneous aspiration or surgical excision of the cyst. Monitoring is generally performed by serial CT or CMR (especially if there is a concern about radiation) every 1 to 2 years. Indications for resection or drainage are symptoms, large size, and potential for rupture or malignancy.

Pericardial diverticula are very rare and can be congenital or acquired malformations.[7-9] They form as out-pouchings or herniations through a defect in the parietal pericardium and occur most often at the costophrenic angles. Unlike pericardial cysts, pericardial diverticula can change in size (often decreasing), even within a short period of time. Differentiation of a diverticulum from a cyst is based on the presence of a communication with the pericardial space, identified by changes in contour and size related to body position and respiration. Cysts do not communicate with the pericardial space, whereas diverticula do. Asymptomatic lesions can be observed with serial CT or CMR. Surgical resection of pericardial diverticula is performed for diagnostic and therapeutic purposes in symptomatic cases.

b. General Indications for Imaging.–Echocardiography is usually the first-line test that incidentally detects a pericardial cyst or diverticulum, but CT and CMR offer better tissue characterization.

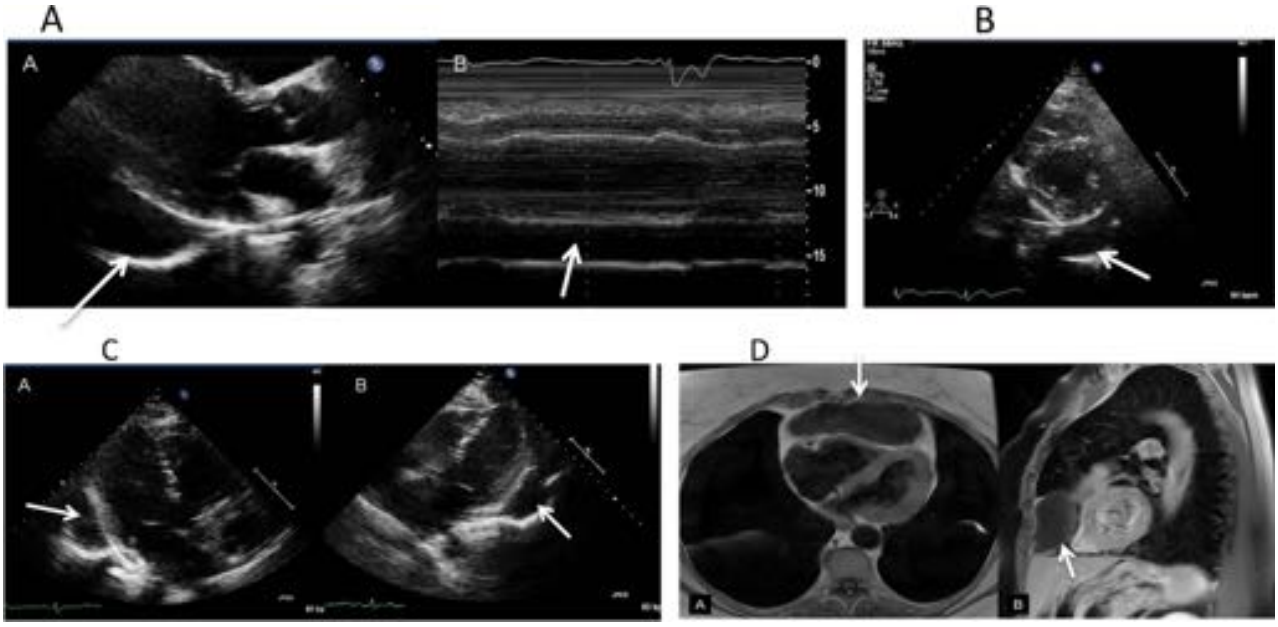

Figure 53 **(A)** Parasternal long-axis view (*left*) and M-mode (*right*) and short-axis view **(B)** (Videos 26 and 27; available at www.onlinejase.com) A large echo-free cystic structure posterior to the left ventricle. In the apical views **(C)**, the lucent structure could be visualized by echocardiography only when the probe was rotated slightly and the ultrasound beam directed posterior from a standard apical four-chamber (*left*) and three-chamber view (*right*) (Video 28; available at www.onlinejase.com). On CMR **(D)**, the pericardial cyst is well visualized. The T1W axial image (*left*) showing hypointensity in the loculated fluid in the anterior mediastinum, suggestive of cyst containing of simple fluid. The T1W sagittal view (*right*) after administration of gadolinium shows that the anterior mediastinal lesion is nonenhancing. The *white arrow* points to the pericardial cyst in all views.

c. Echocardiography.–A pericardial cyst appears as a circumscribed, echo-free space adjacent to the cardiac border. Common locations for cysts are adjacent to the right atrium and frequently extrinsically compressing the atrium. The lack of flow by color or PW Doppler supports the diagnosis of a cyst. Pericardial diverticula appear similar on echocardiography to cysts. Distinction from a cyst, when possible, is based on identifying a defect in the pericardial lining in the case of a diverticulum.

d. CT.–The typical appearance of a pericardial cyst on CT is one of a well-circumscribed, thin-walled, unilocular, ovoid fluid collection located adjacent to the pericardium in one of the cardiophrenic angles.[39] Pericardial cysts are most often found in the right cardiophrenic angle but may be found elsewhere in the mediastinum on CT.[57,180,181] A pointed contour is an unusual feature of a pericardial cyst that has been described on chest x-ray and CT.[182] The fluid content of pericardial cysts almost always has near-water attenuation and is nonenhancing with iodinated contrast media administration.[8,36,37,183] The appearance of a pericardial diverticulum is similar to a cyst on CT, although an open communication with the pericardial sac is identified.

e. CMR.–On MR, pericardial cysts are well-defined, smooth-bordered, encapsulated lesions abutting the pericardium that almost always demonstrate the characteristics of water.[41,42] As mentioned, they have no communication with the pericardial space and typically reside in the right cardiophrenic angle.[36,54] Pericardial cysts in unusual locations may be difficult to distinguish from bronchogenic or thymic cysts.[86] A pericardial cyst on echocardiography and CMR is shown in Figure 53.

Because of their typically transudative and simple-cystic nature, pericardial cysts almost always appear as low and homogeneous intensities on T1W SE images and as high and homogeneous intensities on either T2W SE images or STIR images.[48,86] They typically do not enhance with gadolinium-based contrast media administration.[48,184]

Very uncommonly, a pericardial cyst may contain highly proteinaceous fluid, leading to high signal intensity on T1W images.[36,48,54]

CMR is helpful in reaching a preoperative diagnosis of pericardial diverticulum. Although it resembles a pericardial cyst, the diagnosis of a diverticulum on CMR should be suspected when a complete wall cannot be identified along the circumference of the mass facing the pericardium.[185]

f. When to Consider Added Imaging.–Pericardial cysts are often detected on chest x-ray or echocardiography. However, CT or CMR provides better anatomic detail, including location, size, and involvement of contiguous structures. In addition, CT and CMR can better distinguish between a pericardial cyst and a diverticulum. In general, when a pericardial cyst is detected by chest x-ray or echocardiography, either CT or CMR can be done to confirm the diagnosis and guide management if needed. Table 11 summarizes the imaging findings in pericardial cysts and diverticulum.

H. Congenital Absence of the Pericardium

1. Introduction. Congenital absence of the pericardium is described predominantly in case reports and small series.[186-189] It is characterized as either isolated (65%) or associated with other congenital disorders.[186] A classification of congenital absence of the pericardium defines five types: complete absence of the entire pericardium, complete absence (left or right sided), and partial (left or right sided). Defect size may vary from small foraminal types to extensive. The most common type is complete absence of the left

Table 11 Imaging findings of pericardial diverticulum and pericardial cysts

	Pericardial Cyst	Pericardial Diverticulum
Echo	Echo-free space adjacent to cardiac border	Echo-free space adjacent to cardiac border with defect in pericardial lining
CT	Well-circumscribed fluid sac with signal attenuation of water; location typically at costophrenic angle; no communication to pericardial sac detected	Similar to cyst but with communication to pericardial sac
CMR	Smooth-bordered, encapsulated lesions abutting the pericardium with characteristics of water; high–signal intensity T2W images and low-intensity T1W images	Defect in pericardial lining or communication to pericardial sac

pericardium, the prevalence of which is widely estimated between 0.0001% and 0.044%.[190,191]

Identification of congenital absence of the pericardium is most often unexpectedly detected during surgery or as an incidental finding seen during thoracic or cardiac imaging for unrelated reasons. However, symptomatic presentations may occur, and some suggestive features should be recognized. Most often, patients are young, with a median age of 21 years.[189] In most reports, male patients account for approximately 70% of patients.[187] Patients may present with nonspecific symptoms of chest pain, dyspnea, or palpitations, although chest pain is the predominant symptom.

On physical examination, the apical impulse is laterally displaced past the midaxillary line with migratory apical pulsations. A systolic ejection murmur related to excessive motion of the heart may be present.[188,189]

Patients with complete absence of the pericardium are usually asymptomatic and do not generally require intervention. Patients with partial left-sided defects present with the greatest risk. Compression, herniation, or strangulation of cardiac chambers (most often the left atrial appendage), great vessels, or coronary arteries may occur. Indications for surgical repair include the presence of disabling symptoms or risk or occurrence of complications.[192]

2. General Indications for Imaging. Congenital absence of the pericardium is typically asymptomatic, or the presenting symptoms are nonspecific. Therefore, it is most often suggested or diagnosed by incidental findings on chest x-ray, echocardiography, CT, or CMR. The need for additional imaging modalities should be considered in the clinical context. For an asymptomatic person with suspicion on initial imaging modalities, further evaluation may not be necessary because it will not have therapeutic consequences.

3. Image Appearance of the Pericardium. As discussed, the normal pericardium consists of two adjacent layers, which are separated by a normally invisible trace amount of fluid. On either side, the pericardium is surrounded by a rim of epicardial or pericardial fat, respectively. The amount of fat varies with body habitus. The normal thickness of the pericardium is <2 mm (this combines both layers in segments in which no fluid is visible). The spatial resolution of CT and CMR is maximally 0.5 mm, which would theoretically allow reliable identification of a structure with 1-mm thickness. However, for both modalities, spatial resolution depends on details of the acquisition technique. Image quality depends on heart rate and body habitus. Therefore, identification of the pericardium can be limited in persons with minimal epicardial and pericardial fat. In this context, it is important to consider that the distribution of epicardial and pericardial fat varies in different segments of the heart. In persons with a normal pericardium, the epicardial and pericardial fat rim is often minimal in areas associated with the most frequent location of absence of the pericardium, creating the possibility of false-positive imaging results.

4. Echocardiography. Several nonspecific and few specific M-mode, 2D, and Doppler features of congenital absence of the pericardium are described in Table 12. These features are generally associated with absence of the left pericardium. Most commonly, this condition is suspected when there are (1) unusual imaging windows, (2) the appearance of an enlarged right ventricle, (3) excessive cardiac motion, and (4) abnormal interventricular septal motion.[193] Among these findings, an enlarged right ventricle is the finding that most often leads to additional testing because of suspicion for cardiac shunts or a myocardial disorder, such as RV cardiomyopathy. The right ventricle may be enlarged because of reduced compliance with an absent left-sided pericardium. Additionally, a normal-sized right ventricle may appear enlarged because of levoposition of the heart, resulting in a tangential image through the chamber (Figure 54).

In the parasternal long-axis view, the apex is pointed posteriorly, leading to an unusual imaging plane. M-mode imaging demonstrates paradoxical septal motion in systole and diastole and excessive posterior systolic wall anterior motion.[194,195] There is an absence of the normal epicardial-pericardial space seen on M-mode imaging. The ability to detect an absent pericardium by grayscale imaging is poor. Excessive motion of the heart may be evident in all views.

The apical views are typically laterally displaced. The appearance of a "teardrop" cardiac shape with elongation of the atrium and widening of the ventricles has been described. Additional findings that have been described in isolated reports include a sharp angle between the atrium and ventricles and an outward bulging motion of the inferior wall in diastole.[196]

Some relatively specific Doppler findings have been reported. These include a reductions in the systolic flow in the SVC flow and the systolic/diastolic flow ratio in the pulmonary veins.[197,198] These findings relate to a reduction in the negative intrapericardial pressure generated by the pericardium during systole with an absent pericardium. Severe tricuspid regurgitation may occur in some patients and is related to the abnormal geometry of the tricuspid annulus or chordal rupture.

5. CT and CMR. *a. Technique.*–Dedicated imaging of the pericardium with CMR and CT should use cardiac (electrocardiographically synchronized) protocols. Comprehensive CMR examinations include morphologic imaging (T1W sequences) and functional imaging (cine sequences).[36,199] Additional T2 morphologic sequences and delayed contrast imaging after gadolinium administration, used for identification of pericardial inflammation,[26,43,152] are not essential in the context of suspected pericardial absence.

Table 12 Imaging findings of congenital absence of the pericardium

Summary of Echo findings
• M-mode—paradoxical septal motion, accentuated movement of the posterior wall, absent separation of epicardium-pericardium
• 2D—RV dilation, exaggerated mobility of the heart "pendulum heart", posterior orientation of the apex and unusual acoustic windows (parasternal long axis view), lateral probe position, elongated atrium with widened ventricles "tear-drop" shape of the heart, abnormal atrial-ventricular angle, bulging outward of the inferior-posterior wall (apical view)
• Doppler—tricuspid regurgitation due to annular dilation or chordal rupture, ↓ pulmonary vein and SVC systolic flow
Summary of CT and CMR findings
• Absence of the pericardial layer
• Levorotation of the heart
• Interposition of lung tissue in the anterior space between aorta and pulmonary artery or between the diaphragm and the base of the heart

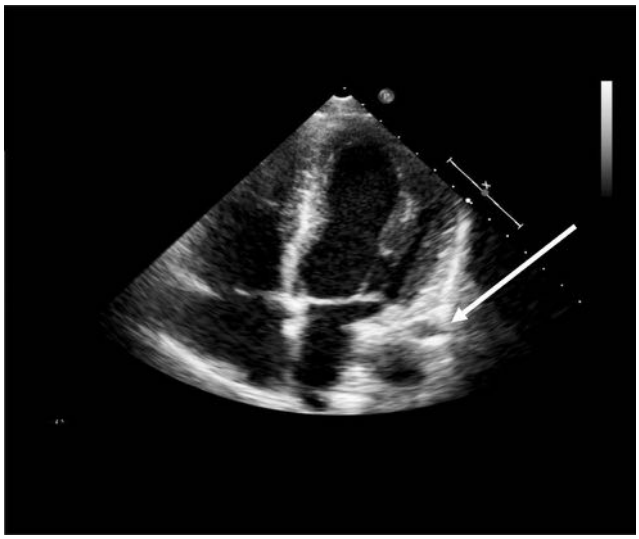

Figure 54 TTE in an apical four-chamber view. *Arrow* points to the left atrial appendage, which is herniated through a defect in a partial absence of the left pericardium. Video 29 (available at www.onlinejase.com) shows the same, along with excessive septal motion and angulation of the ventricular and atrial septum.

Dedicated cardiac CT should be performed with low-dose, prospective triggering whenever possible. Additional dose-sparing techniques (reduced tube voltage [100 kV], iterative reconstruction) should be used if possible.[151] Because of the natural contrast between the pericardium and the surrounding epicardial and pericardial fat rim, intravenous contrast is not absolutely necessary. Intravenous contrast administration is preferred by many investigators because it provides clear delineation of the cardiac chambers and may occasionally demonstrate pericardial enhancement as a sign of inflammation.

b. Image Appearance.–In good-quality, dedicated (electrocardiographically synchronized) CT and CMR studies, the pericardium can be identified because it is differentiated from the adjacent myocardium by the adjacent epicardial and pericardial fat layers. However, in patients with minimal epicardial and pericardial fat, the pericardium lies almost immediately on the myocardium, and differentiation becomes difficult. This creates a challenge in younger, lean, athletic patients, because pericardial visualization at the most common site of pericardial defects (the lateral, posterior, and inferior LV walls) can be impossible.[200] In these situations, overdiagnosis of pericardial absence should be avoided (Figure 55).

In addition to the direct visualization of the pericardium, there are important indirect morphologic and functional signs consistent with pericardial defects. Indirect morphologic findings include leftward cardiac displacement. Excessive levorotation usually accompanies complete left pericardial absence[201] and is visible on chest x-ray. A relatively specific sign is the interposition of lung tissue in spaces typically covered by the pericardium, including the anterior space between the aorta and pulmonary artery (Figure 56) or between the diaphragm and the base of the heart.[202] Patients with pericardial defects may have associated congenital abnormalities.

6. When to Consider Added Imaging. Absence of the pericardium is an exceedingly rare, incidental finding, typically in an asymptomatic and often young person. The diagnosis can be confirmed with clinical imaging modalities, but pitfalls and overdiagnoses need to be avoided. The need for dedicated cardiac imaging should be carefully considered in asymptomatic persons, because the diagnosis typically has no clinical consequences. Confirmatory testing should be reserved for symptomatic patients or those at risk for complications and only when patients are considered candidates for surgical options. It must be recognized that surgical management is based on small, uncontrolled observations, limiting any definitive recommendations.

V. FUTURE TECHNIQUES AND APPLICATIONS

The discussion of future techniques and applications in a guidelines report intended to provide a consensus of current imaging approaches to pericardial disease can only serve to make the reader aware of emerging trends, which may find their place in future recommendations.

A. Centers of Excellence in Pericardial Diseases

In comparison with other structural parts of the cardiovascular system, knowledge regarding the pericardium, its pathologic conditions, and therapeutic interventions has been relatively stable in the past decade. However, there is a growing interest in pericardial diseases, with the formation of centers of excellence in diagnosing and treating pericardial diseases in the United States as well as the development of an international pericardial registry, suggesting a new "renaissance" for these diseases.

B. Current Applications

Doppler echocardiography remains the most useful noninvasive modality to characterize the abnormal hemodynamics seen in pericardial disease because of its superior temporal resolution. However, recent studies have shown that real-time cine CMR sequences may be used

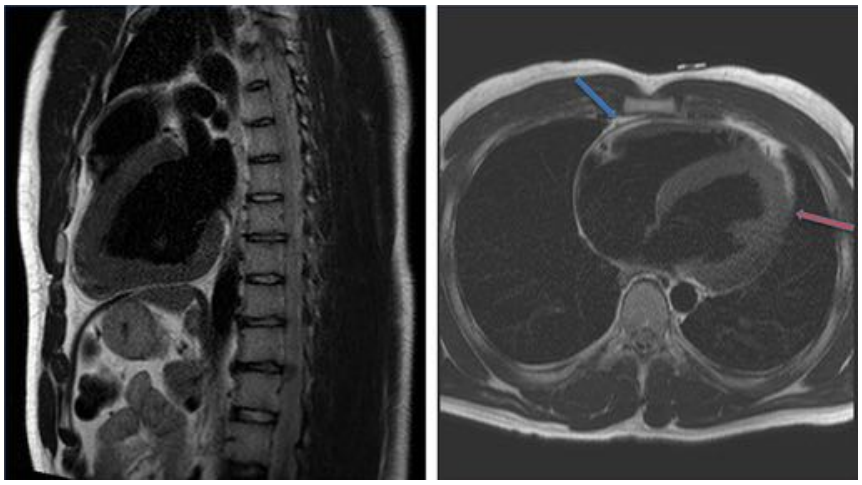

Figure 55 CMR in sagittal (*left*) and axial view (*right*) in an athlete showing the difficulty in determining absence of the pericardium over the lateral wall when there is minimal epicardial and pericardial fat. The *blue anterior arrow* clearly shows the normal pericardium anterior to the right ventricle layered between the epicardial and pericardial fat. In contrast, in the lateral LV wall, the pericardium is not well defined.

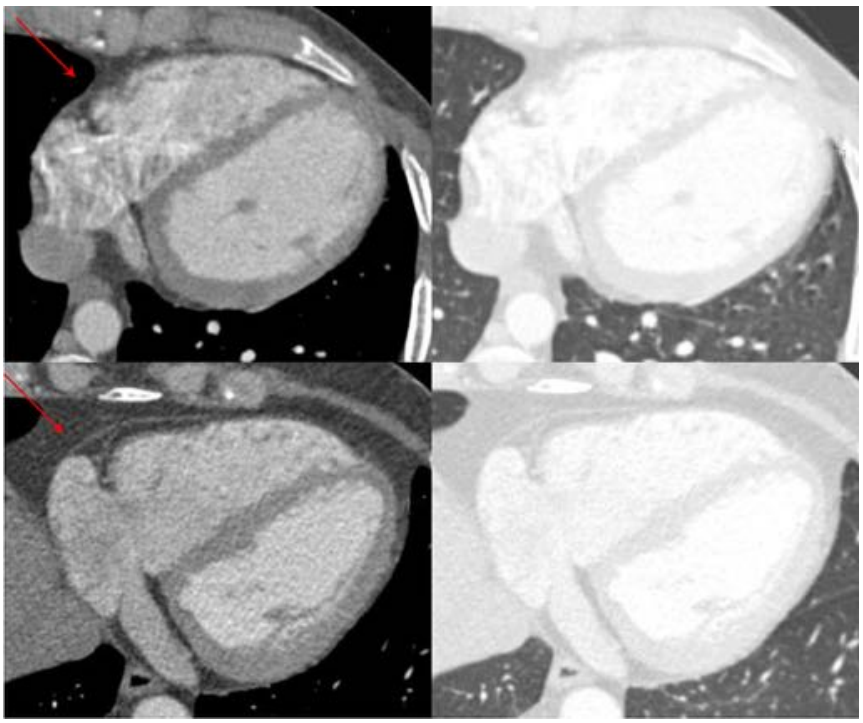

Figure 56 Axial computed tomographic images. The *right* and *left top* panels are from a patient with congenital absence of the pericardium. Characteristic interposition of lung tissue at the right (*red arrow*) and left atrioventricular groove is seen. (*Bottom*) A patient with an intact pericardium with the absence of this finding.

to evaluate the relative changes in LV and RV volumes during free-breathing, thus establishing the presence of exaggerated ventricular interaction in patients with CP (Figure 57). Analysis of tagged CMR cine sequences can also demonstrate areas of increased pericardial rigidity, supporting the diagnosis of this condition.[8,9] Advanced three-dimensional visualization of the pericardium may be helpful in providing a road map before pericardiectomy and to evaluate patients with residual symptoms after surgery. The high spatial and rapidly improving temporal resolution of CT as well as its ability to quantify the extent and location of calcification makes this an ideal imaging modality for this purposes.

C. Technological Advances

In the future, there will be some rapid technological advances in imaging that could influence the characterization of pericardial diseases:

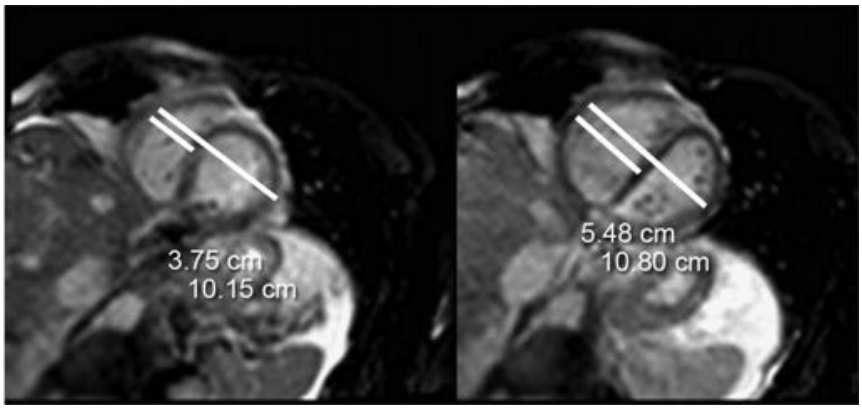

Figure 57 Real-time cine CMR sequences may be used to evaluate the relative changes in the right ventricle (3.75 cm in expiration, 5.48 cm in inspiration) and the left ventricle (10.15 cm in expiration, 10.80 cm in inspiration) during free breathing, thus establishing the presence of exaggerated ventricular interaction in patients with CP (Video 30; available at www.onlinejase.com). Courtesy of Dr. Michael Bolen.

- Improved spatial resolution and improved signal-to-noise ratios with modern systems have allowed and will continue to allow more reliable morphologic definition of the thin normal pericardium and structural abnormalities of the diseased pericardium.
- Improved temporal resolution of these systems has allowed and will allow better definition of the functional aspect of pericardial disease.
- Specifically for CT, improved systems and acquisition techniques (prospective triggering, reduced tube voltage [100 kV], iterative reconstruction) have decreased and will further decrease the associated radiation exposure.[151,203,204]

D. Novel Applications

In the future, the pericardial inflammatory response will play a central role in the diagnosis and management of acute and recurrent pericarditis and constriction.[205] Recent evolving data suggest that early forms of constriction can be reversible, which emphasizes the need for early diagnosis and therapeutic intervention.[152] With the use of anti-inflammatory therapy for transient CP, it is estimated that 20% to 30% of patients with acute or subacute CP can avoid pericardiectomy or alternatively be primed for subsequent surgery by treating the inflammation and thus avoiding adhesions around the heart.

There is ongoing research on whether a CMR-guided approach to the pericardial diseases, in particular acute or recurrent pericarditis and transient CP, may be beneficial in the management of these patients[62] and can be considered a first-line imaging test. Early observations suggest that CMR can be used to stage the severity of disease and subsequently modulate the number of anti-inflammatory drugs, including steroids, as well as the duration and tapering of these medications. The correlation and time course between the inflammatory response, serum markers, and imaging are incompletely understood. Further large-scale prospective studies are needed to elaborate on these observations.

CMR may also be useful in assessing the extent of the myopathic process in myopericarditis (predominantly pericarditis) or in perimyocarditis (predominantly myocarditis)[4] (Figure 58). In the latter, LGE may extend from the subepicardial lateral wall into the pericardial space and can be associated with PEff.[206]

PET with ^{18}F-fluorodeoxyglucose appears to have a promising role in the evaluation of certain patients with pericardial disease.[207] Focal intense activity is most commonly associated with malignancy and thus may be useful to evaluate the etiology of pericardial masses.[208-212] Mild to moderate activity is often seen in the presence of active infection or noninfective inflammatory processes.[212,213] Whether activity on ^{18}F-fluorodeoxyglucose PET may have potential incremental utility over serum inflammatory biomarkers or LGE by CMR for guiding therapy in patients with active pericarditis or acute or subacute constrictive disease remains to be determined. Recently, a hybrid of PET and CMR has been developed and may have a future role in pericardial diseases.

VI. RECOMMENDATIONS AND KEY POINTS FOR PERICARDIAL DISEASES

A. Acute Pericarditis Key Points

1. All patients with acute pericarditis should undergo TTE to assess for a PEff, tamponade physiology, and myocardial involvement.
   a. In addition to echocardiography, CT and CMR should be considered when there are complexities associated with the clinical presentation of acute pericarditis, including
      i. inconclusive echocardiographic findings and ongoing clinical concern;
      ii. failure to respond promptly to anti-inflammatory therapy;
      iii. atypical clinical presentation;
      iv. suspicion of CP on the basis of clinical examination;
      v. associated trauma (penetrating injury, chest injury)
      vi. in setting of acute myocardial infarction, neoplasm, lung or chest infection, pancreatitis.

B. Recurrent Pericarditis Key Points

1. Key points are similar to those for acute pericarditis (see above).

C. PEff and Tamponade Key Points

1. All patients with PEff or tamponade should undergo TTE to assess for the extent of effusion and hemodynamic compromise.

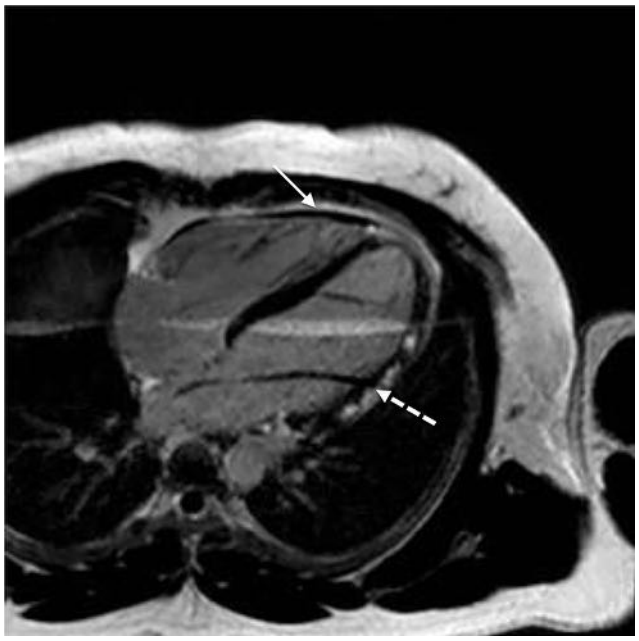

Figure 58 Delayed enhancement imaging in the four-chamber view in a 21-year-old patient with perimyocarditis. The *dashed arrow* shows subepicardial and midwall myocardial enhancement affecting the inferolateral and lateral wall. The *arrow* shows pericardial enhancement (Video 31; available at www.onlinejase.com). Courtesy of Dr.Teerapat Yingchoncharoen.

2. CT and/or CMR should be done for those patients with complex PEff with subacute tamponade with the need for drainage.
3. CT and/or CMR should be done for those with suspected hemopericardium or pericardial clot and to assess the source of PEff as in malignancy or inflammation.
4. TEE, CT, or CMR can be used to assess regional tamponade, which occurs in the postoperative or postprocedural setting.

D. CP Key Points

1. All patients with clinically suspected CP should undergo TTE with Doppler echocardiography as the initial imaging test, which can provide a definite diagnosis in most patients.
2. CMR and/or CT should be used as a complementary technique to confirm CP and in selected patients with poor echocardiographic windows or unclear findings. CT and/or CMR can additionally provide more accurate pericardial thickness measurements as well as tissue characterization, including T2 STIR (edema) and LGE (inflammation).
3. CT can be used in the preoperative planning of patients with known CP to assess for the degree of calcification and proximity to critical vascular structures in patients who previously had cardiac surgery.

E. Effusive Constriction Key Points

1. Key points are similar to those for CP (see above).

F. Pericardial Masses, Cysts and Diverticulum Key Points

1. Echocardiography is the initial imaging test to assess pericardial masses, cysts, and diverticulum.
2. CT and/or CMR should be done for better tissue characterization of the mass and detection of metastasis (if malignancy suspected).
3. CT and/or CMR should be done to evaluate for a pericardial diverticulum and cyst.

G. Congenital Absence of the Pericardium Key Points

1. Echocardiography is the initial imaging test to identify functional aspects (e.g., bulging of cardiac chambers and excessive motion) for those patients with suspected absence of pericardium and symptoms.
2. CT and CMR can be used for morphologic identification of a pericardial defect.

VII. CONCLUSIONS

In the modern era, multimodality imaging is essential in the diagnosis and management of pericardial syndromes. Echocardiography is the initial test for most pericardial syndromes, including acute pericarditis, recurrent pericarditis, and CP. CMR and CT can usually be added when there is complexity not handled by echocardiography or technically limited windows or when tissue characterization is needed, such as with edema and inflammation. In the future era of cost containment, clinical trials should be done to assess the role of multimodality imaging in the diagnosis and management of pericardial diseases.

ACKNOWLEDGMENTS

We acknowledge the editorial assistance of Marie D. Campbell, the library assistance of Jodith Janes, and administrative assistance of Rhonda A. Price.

Notice and Disclaimer

This report is made available by the ASE, the Society for Cardiovascular Magnetic Resonance (SCMR), and the Society of Cardiovascular Computed Tomography (SCCT) as a courtesy reference source for their members. This report contains recommendations only and should not be used as the sole basis to make medical practice decisions or for disciplinary action against any employee. The statements and recommendations contained in this report are based primarily on the opinions of experts rather than on scientifically verified data. The ASE, SCMR, and SCCT make no express or implied warranties regarding the completeness or accuracy of the information in this report, including the warranty of merchantability or fitness for a particular purpose. In no event shall the ASE, SCMR, or SCCT be liable to you, your patients, or any other third parties for any decision made or action taken by you or such other parties in reliance on this information. Nor does your use of this information constitute the offering of medical advice by the ASE, SCMR, or SCCT or create any physician-patient relationship between the ASE, SCMR, or SCCT and your patients or anyone else.

REFERENCES

1. Imazio M, Bobbio M, Cecchi E, Demarie D, Demichelis B, Pomari F, et al. Colchicine in addition to conventional therapy for acute pericarditis: results of the Colchicine for Acute Pericarditis (COPE) trial. Circulation 2005;112:2012-6.

2. Imazio M, Brucato A, Cemin R, Ferrua S, Belli R, Maestroni S, et al. Colchicine for Recurrent Pericarditis (CORP): a randomized trial. Ann Intern Med 2011;155:409-14.
3. Imazio M, Trinchero R, Brucato A, Rovere ME, Gandino A, Cemin R, et al. Colchicine for the Prevention of the Post-Pericardiotomy Syndrome (COPPS): a multicentre, randomized, double-blind, placebo-controlled trial. Eur Heart J 2010;31:2749-54.
4. Imazio M, Spodick DH, Brucato A, Trinchero R, Adler Y. Controversial issues in the management of pericardial diseases. Circulation 2010;121: 916-28.
5. Khandaker MH, Espinosa RE, Nishimura RA, Sinak LJ, Hayes SN, Melduni RM, et al. Pericardial disease: diagnosis and management. Mayo Clin Proc 2010;85:572-93.
6. Troughton RW, Asher CR, Klein AL. Pericarditis. Lancet 2004;363: 717-27.
7. Maisch B, Seferovic PM, Ristic AD, Erbel R, Rienmuller R, Adler Y, et al. Guidelines on the diagnosis and management of pericardial diseases executive summary; the Task Force on the Diagnosis and Management of Pericardial Diseases of the European Society of Cardiology. Eur Heart J 2004;25:587-610.
8. Verhaert D, Gabriel RS, Johnston D, Lytle BW, Desai MY, Klein AL. The role of multimodality imaging in the management of pericardial disease. Circ Cardiovasc Imaging 2010;3:333-43.
9. Yared K, Baggish AL, Picard MH, Hoffmann U, Hung J. Multimodality imaging of pericardial diseases. JACC Cardiovasc Imaging 2010;3:650-60.
10. Bogaert J, Francone M. Pericardial disease: value of CT and MR imaging. Radiology 2013;267:340-56.
11. American College of Cardiology Foundation Task Force on Expert Consensus Documents, Hundley WG, Bluemke DA, Finn JP, Flamm SD, Fogel MA, et al. ACCF/ACR/AHA/NASCI/SCMR 2010 expert consensus document on cardiovascular magnetic resonance: a report of the American College of Cardiology Foundation Task Force on Expert Consensus Documents. J Am Coll Cardiol 2010;55:2614-62.
12. Hendel RC, Patel MR, Kramer CM, Poon M, Hendel RC, Carr JC, et al. ACCF/ACR/SCCT/SCMR/ASNC/NASCI/SCAI/SIR 2006 appropriateness criteria for cardiac computed tomography and cardiac magnetic resonance imaging: a report of the American College of Cardiology Foundation Quality Strategic Directions Committee Appropriateness Criteria Working Group, American College of Radiology, Society of Cardiovascular Computed Tomography, Society for Cardiovascular Magnetic Resonance, American Society of Nuclear Cardiology, North American Society for Cardiac Imaging, Society for Cardiovascular Angiography and Interventions, and Society of Interventional Radiology. J Am Coll Cardiol 2006;48:1475-97.
13. Taylor AJ, Cerqueira M, Hodgson JM, Mark D, Min J, O'Gara P, et al. ACCF/SCCT/ACR/AHA/ASE/ASNC/NASCI/SCAI/SCMR 2010 appropriate use criteria for cardiac computed tomography. A report of the American College of Cardiology Foundation Appropriate Use Criteria Task Force, the Society of Cardiovascular Computed Tomography, the American College of Radiology, the American Heart Association, the American Society of Echocardiography, the American Society of Nuclear Cardiology, the North American Society for Cardiovascular Imaging, the Society for Cardiovascular Angiography and Interventions, and the Society for Cardiovascular Magnetic Resonance. J Cardiovasc Comput Tomogr 2010;4:407.e1-407.e33.
14. Mocumbi AO, Ferreira MB. Neglected cardiovascular diseases in Africa: challenges and opportunities. J Am Coll Cardiol 2010;55:680-7.
15. Ishihara T, Ferrans VJ, Jones M, Boyce SW, Kawanami O, Roberts WC. Histologic and ultrastructural features of normal human parietal pericardium. Am J Cardiol 1980;46:744-53.
16. Ferrans VJ, Ishihara T, Roberts WC. Anatomy of the pericardium. In: Reddy PS, Leon DF, Shaver JA, editors. Pericardial disease. New York: Raven; 1982. pp. 77-92.
17. Bull RK, Edwards PD, Dixon AK. CT dimensions of the normal pericardium. Br J Radiol 1998;71:923-5.
18. Sechtem U, Tscholakoff D, Higgins CB. MRI of the normal pericardium. AJR Am J Roentgenol 1986;147:239-44.
19. Ling LH, Oh JK, Tei C, Click RL, Breen JF, Seward JB, et al. Pericardial thickness measured with transesophageal echocardiography: feasibility and potential clinical usefulness. J Am Coll Cardiol 1997;29:1317-23.
20. Vesely TM, Cahill DR. Cross-sectional anatomy of the pericardial sinuses, recesses, and adjacent structures. Surg Radiol Anat 1986;8:221-7.
21. Levy-Ravetch M, Auh YH, Rubenstein WA, Whalen JP, Kazam E. CT of the pericardial recesses. AJR Am J Roentgenol 1985;144:707-14.
22. Miyazaki T, Pride HP, Zipes DP. Prostaglandins in the pericardial fluid modulate neural regulation of cardiac electrophysiological properties. Circ Res 1990;66:163-75.
23. Mebazaa A, Wetzel RC, Dodd-o JM, Redmond EM, Shah AM, Maeda K, et al. Potential paracrine role of the pericardium in the regulation of cardiac function. Cardiovasc Res 1998;40:332-42.
24. Yune HY, Klatte EC. Mediastinal venography. Subselective transfemoral catheterization technique. Radiology 1972;105:285-91.
25. Holt JP. The normal pericardium. Am J Cardiol 1970;26:455-65.
26. Zurick AO, Bolen MA, Kwon DH, Tan CD, Popovic ZB, Rajeswaran J, et al. Pericardial delayed hyperenhancement with CMR imaging in patients with constrictive pericarditis undergoing surgical pericardiectomy: a case series with histopathological correlation. JACC Cardiovasc Imaging 2011;4:1180-91.
27. Hoit BD, Dalton N, Bhargava V, Shabetai R. Pericardial influences on right and left ventricular filling dynamics. Circ Res 1991;68:197-208.
28. Spodick DH. Acute cardiac tamponade. N Engl J Med 2003;349:684-90.
29. Caforio AL, Brucato A, Doria A, Brambilla G, Angelini A, Ghirardello A, et al. Anti-heart and anti-intercalated disk autoantibodies: evidence for autoimmunity in idiopathic recurrent acute pericarditis. Heart 2010; 96:779-84.
30. Dudzinski DM, Mak GS, Hung JW. Pericardial diseases. Curr Probl Cardiol 2012;37:75-118.
31. Spodick DH. Acute pericarditis: current concepts and practice. JAMA 2003;289:1150-3.
32. Lange RA, Hillis LD. Clinical practice. Acute pericarditis. N Engl J Med 2004;351:2195-202.
33. Imazio M, Cecchi E, Demichelis B, Ierna S, Demarie D, Ghisio A, et al. Indicators of poor prognosis of acute pericarditis. Circulation 2007; 115:2739-44.
34. Salisbury AC, Olalla-Gomez C, Rihal CS, Bell MR, Ting HH, Casaclang-Verzosa G, et al. Frequency and predictors of urgent coronary angiography in patients with acute pericarditis. Mayo Clin Proc 2009;84:11-5.
35. Ordovas KG, Higgins CB. Pericardial disease. In: Higgins CB, de Roos A, editors. MRI and CT of the cardiovascular system. Philadelphia: Lippincott Williams & Wilkins; 2006. pp. 137-53.
36. Wang ZJ, Reddy GP, Gotway MB, Yeh BM, Hetts SW, Higgins CB. CT and MR imaging of pericardial disease. Radiographics 2003;23:S167-80.
37. O'Leary SM, Williams PL, Williams MP, Edwards AJ, Roobottom CA, Morgan-Hughes GJ, et al. Imaging the pericardium: appearances on ECG-gated 64-detector row cardiac computed tomography. Br J Radiol 2010;83:194-205.
38. Moncada R, Demos TC, Posniak HV. Computed tomography of pericardial heart diseases. In: Taveras JM, Ferrucci JT, editors. Radiology. Philadelphia: Lippincott; 1986.
39. Oyama N, Oyama N, Komuro K, Nambu T, Manning WJ, Miyasaka K. Computed tomography and magnetic resonance imaging of the pericardium: anatomy and pathology. Magn Reson Med Sci 2004;3: 145-52.
40. Tomoda H, Hoshiai M, Furuya H, Oeda Y, Matsumoto S, Tanabe T, et al. Evaluation of pericardial effusion with computed tomography. Am Heart J 1980;99:701-6.
41. Bogaert J, Francone M. Cardiovascular magnetic resonance in pericardial diseases. J Cardiovasc Magn Reson 2009;11:1-14.
42. Sechtem U, Tscholakoff D, Higgins CB. MRI of the abnormal pericardium. AJR Am J Roentgenol 1986;147:245-52.
43. Young PM, Glockner JF, Williamson EE, Morris MF, Araoz PA, Julsrud PR, et al. MR imaging findings in 76 consecutive surgically proven cases of pericardial disease with CT and pathologic correlation. Int J Cardiovasc Imaging 2012;28:1099-109.

44. Francone M, Carbone I, Agati L, Bucciarelli Ducci C, Mangia M, Iacucci I, et al. Utility of T2-weighted short-tau inversion recovery (STIR) sequences in cardiac MRI: an overview of clinical applications in ischaemic and non-ischaemic heart disease. Radiol Med 2011;116:32-46.
45. Taylor AM, Dymarkowski S, Verbeken EK, Bogaert J. Detection of pericardial inflammation with late-enhancement cardiac magnetic resonance imaging: initial results. Eur Radiol 2006;16:569-74.
46. Klein C, Graf K, Fleck E, Nagel E. Images in cardiovascular medicine. Acute fibrinous pericarditis assessed with magnetic resonance imaging. Circulation 2003;107:e82.
47. Sa MI, Kiesewetter CH, Jagathesan R, Prasad SK. Acute pericarditis assessed with magnetic resonance imaging: a new approach. Circulation 2009;119:e183-6.
48. Al-Mallah M, Kwong RY. Assessing pericardial disease by CMR. In: Kwong RY, editor. Contemporary cardiology: cardiovascular magnetic resonance imaging. Totowa, NJ: Humana; 2008. pp. 467-89.
49. Hayashi H, Kawamata H, Machida M, Kumazaki T. Tuberculous pericarditis: MRI features with contrast enhancement. Br J Radiol 1998;71:680-2.
50. Watanabe A, Hara Y, Hamada M, Kodama K, Shigematsu Y, Sakuragi S, et al. A case of effusive-constructive pericarditis: an efficacy of GD-DTPA enhanced magnetic resonance imaging to detect a pericardial thickening. Magn Reson Imaging 1998;16:347-50.
51. Koos R, Schroder J, Kuhl HP. Acute viral pericarditis without typical electrocardiographic changes assessed by cardiac magnetic resonance imaging. Eur Heart J 2009;30:2844.
52. Doulaptsis C, Goetschalckx K, Masci PG, Florian A, Janssens S, Bogaert J. Assessment of early post-infarction pericardial injury by CMR. JACC Cardiovasc Imaging 2013;6:411-3.
53. Breen JF. Imaging of the pericardium. J Thorac Imaging 2001;16:47-54.
54. Maksimovic R, Dill T, Seferovic PM, Ristic AD, Alter P, Simeunovic DS, et al. Magnetic resonance imaging in pericardial diseases. Indications and diagnostic value. Herz 2006;31:708-14.
55. Misselt AJ, Harris SR, Glockner J, Feng D, Syed IS, Araoz PA. MR imaging of the pericardium. Magn Reson Imaging Clin N Am 2008;16:185-99.
56. Kojima S, Yamada N, Goto Y. Diagnosis of constrictive pericarditis by tagged cine magnetic resonance imaging. N Engl J Med 1999;341:373-4.
57. Olson MC, Posniak HV, McDonald V, Wisniewski R, Moncada R. Computed tomography and magnetic resonance imaging of the pericardium. Radiographics 1989;9:633-49.
58. Kovanlikaya A, Burke LP, Nelson MD, Wood J. Characterizing chronic pericarditis using steady-state free-precession cine MR imaging. AJR Am J Roentgenol 2002;179:475-6.
59. Peebles C. Pericardial diseases. In: Plein S, Greenwood JP, Ridgway JP, editors. Cardiovascular MR manual. London: Springer-Verlag; 2011. pp. 333-60.
60. Shabetai R. Recurrent pericarditis: recent advances and remaining questions. Circulation 2005;112:1921-3.
61. Imazio M, Trinchero R, Shabetai R. Pathogenesis, management, and prevention of recurrent pericarditis. J Cardiovasc Med (Hagerstown) 2007;8:404-10.
62. Monvadi B, Srichai MB. CMR imaging in constrictive pericarditis: is seeing believing? J Am Coll Cardiol Img 2011;4:1192-4.
63. Spodick DH. The pericardium: a comprehensive textbook. New York: Marcel Dekker; 1997.
64. Spodick DH. Pericarditis in systemic diseases. Cardiol Clin 1990;8:709-16.
65. Permanyer-Miralda G, Sagrista-Sauleda J, Soler-Soler J. Primary acute pericardial disease: a prospective series of 231 consecutive patients. Am J Cardiol 1985;56:623-30.
66. Corey GR, Campbell PT, Van Trigt P, Kenney RT, O'Connor CM, Sheikh KH, et al. Etiology of large pericardial effusions. Am J Med 1993;95:209-13.
67. Sagrista-Sauleda J, Merce J, Permanyer-Miralda G, Soler-Soler J. Clinical clues to the causes of large pericardial effusions. Am J Med 2000;109:95-101.
68. Levy PY, Corey R, Berger P, Habib G, Bonnet JL, Levy S, et al. Etiologic diagnosis of 204 pericardial effusions. Medicine (Baltimore) 2003;82:385-91.
69. Seferovic PM, Ristic AD, Imazio M, Maksimovic R, Simeunovic D, Trinchero R, et al. Management strategies in pericardial emergencies. Herz 2006;31:891-900.
70. Savage DD, Garrison RJ, Brand F, Anderson SJ, Castelli WP, Kannel WB, et al. Prevalence and correlates of posterior extra echocardiographic spaces in a free-living population based sample (the Framingham study). Am J Cardiol 1983;51:1207-12.
71. Soler-Soler J, Sagrista-Sauleda J, Permanyer-Miralda G. Management of pericardial effusion. Heart 2001;86:235-40.
72. Galve E, Garcia-Del-Castillo H, Evangelista A, Batlle J, Permanyer-Miralda G, Soler-Soler J. Pericardial effusion in the course of myocardial infarction: incidence, natural history, and clinical relevance. Circulation 1986;73:294-9.
73. Haaz WS, Mintz GS, Kotler MN, Parry W, Segal BL. Two dimensional echocardiographic recognition of the descending thoracic aorta: value in differentiating pericardial from pleural effusions. Am J Cardiol 1980;46:739-43.
74. Rifkin RD, Isner JM, Carter BL, Bankoff MS. Combined posteroanterior subepicardial fat simulating the echocardiographic diagnosis of pericardial effusion. J Am Coll Cardiol 1984;3:1333-9.
75. Weitzman LB, Tinker WP, Kronzon I, Cohen ML, Glassman E, Spencer FC. The incidence and natural history of pericardial effusion after cardiac surgery—an echocardiographic study. Circulation 1984;69:506-11.
76. Martin RP, Rakowski H, French J, Popp RL. Localization of pericardial effusion with wide angle phased array echocardiography. Am J Cardiol 1978;42:904-12.
77. Kerber R, Payvandi M. Echocardiography in acute hemopericardium—production of false-negative echocardiograms by pericardial clots. Circulation 1977;56:24.
78. Bogaert J, Centonze M, Vanneste R, Francone M. Cardiac and pericardial abnormalities on chest computed tomography: what can we see? Radiol Med (Torino) 2010;115:175-90.
79. Hall WB, Truitt SG, Scheunemann LP, Shah SA, Rivera MP, Parker LA, et al. The prevalence of clinically relevant incidental findings on chest computed tomographic angiograms ordered to diagnose pulmonary embolism. Arch Intern Med 2009;169:1961-5.
80. Restrepo CS, Lemos DF, Lemos JA, Velasquez E, Diethelm L, Ovella TA, et al. Imaging findings in cardiac tamponade with emphasis on CT. Radiographics 2007;27:1595-610.
81. Chong HH, Plotnick GD. Pericardial effusion and tamponade: evaluation, imaging modalities, and management. Compr Ther 1995;21:378-85.
82. D'Cruz IA, Constantine A. Problems and pitfalls in the echocardiographic assessment of pericardial effusion. Echocardiography 1993;10:151-66.
83. Yousem D, Traill TT, Wheeler PS, Fishman EK. Illustrative cases in pericardial effusion misdetection: correlation of echocardiography and CT. Cardiovasc Intervent Radiol 1987;10:162-7.
84. Silverman PM, Harell GS, Korobkin M. Computed tomography of the abnormal pericardium. AJR Am J Roentgenol 1983;140:1125-9.
85. Mulvagh SL, Rokey R, Vick GW III, Johnston DL. Usefulness of nuclear magnetic resonance imaging for evaluation of pericardial effusions, and comparison with two-dimensional echocardiography. Am J Cardiol 1989;64:1002-9.
86. Frank H, Globits S. Magnetic resonance imaging evaluation of myocardial and pericardial disease. J Magn Reson Imaging 1999;10:617-26.
87. Glockner JF. Imaging of pericardial disease. Magn Reson Imaging Clin N Am 2003;11:149-62.
88. Seelos KC, Funari M, Chang JM, Higgins CB. Magnetic resonance imaging in acute and subacute mediastinal bleeding. Am Heart J 1992;123:1269-72.
89. Meleca MJ, Hoit BD. Previously unrecognized intrapericardial hematoma leading to refractory abdominal ascites. Chest 1995;108:1747-8.

90. Vilacosta I, Gomez J, Dominguez J, Dominguez L, Banuelos C, Ferreiros J, et al. Massive pericardiac hematoma with severe constrictive pathophysiologic complications after insertion of an epicardial pacemaker. Am Heart J 1995;130:1298-300.
91. Reddy PS, Curtiss EI, O'Toole JD, Shaver JA. Cardiac tamponade: hemodynamic observations in man. Circulation 1978;58:265-72.
92. Fowler NO. Cardiac tamponade. In: Fowler NO, editor. The pericardium in health and disease. Mount Kisco, NY: Futura; 1985. pp. 247-80.
93. Cogswell TL, Bernath GA, Raff H, Hoffmann RG, Klopfenstein HS. Total peripheral resistance during cardiac tamponade: adrenergic and angiotensin roles. Am J Physiol 1986;251:R916-22.
94. Vaska K, Wann LS, Sagar K, Klopfenstein HS. Pleural effusion as a cause of right ventricular diastolic collapse. Circulation 1992;86:609-17.
95. Antman EM, Cargill V, Grossman W. Low-pressure cardiac tamponade. Ann Intern Med 1979;91:403-6.
96. Sagrista-Sauleda J, Angel J, Sambola A, Alguersuari J, Permanyer-Miralda G, Soler-Soler J. Low-pressure cardiac tamponade: clinical and hemodynamic profile. Circulation 2006;114:945-52.
97. D'Cruz IA, Kensey K, Campbell C, Replogle R, Jain M. Two-dimensional echocardiography in cardiac tamponade occurring after cardiac surgery. J Am Coll Cardiol 1985;5:1250-2.
98. Kuvin JT, Harati NA, Pandian NG, Bojar RM, Khabbaz KR. Postoperative cardiac tamponade in the modern surgical era. Ann Thorac Surg 2002;74:1148-53.
99. Faehnrich JA, Noone RB Jr., White WD, Leone BJ, Hilton AK, Sreeram GM, et al. Effects of positive-pressure ventilation, pericardial effusion, and cardiac tamponade on respiratory variation in transmitral flow velocities. J Cardiothorac Vasc Anesth 2003;17:45-50.
100. Seferovic PM, Ristic AD, Maksimovic R, Simeunovic DS, Milinkovic I, Seferovic Mitrovic JP, et al. Pericardial syndromes: an update after the ESC guidelines 2004. Heart Fail Rev 2013;18:255-66.
101. Tsang TS, Enriquez-Sarano M, Freeman WK, Barnes ME, Sinak LJ, Gersh BJ, et al. Consecutive 1127 therapeutic echocardiographically guided pericardiocenteses: clinical profile, practice patterns, and outcomes spanning 21 years. Mayo Clin Proc 2002;77:429-36.
102. Di Segni E, Feinberg MS, Sheinowitz M, Motro M, Battler A, Kaplinsky E, et al. Left ventricular pseudohypertrophy in cardiac tamponade: an echocardiographic study in a canine model. J Am Coll Cardiol 1993;21:1286-94.
103. Settle HP, Adolph RJ, Fowler NO, Engel P, Agruss NS, Levenson NI. Echocardiographic study of cardiac tamponade. Circulation 1977;56:951-9.
104. Himelman RB, Kircher B, Rockey DC, Schiller NB. Inferior vena cava plethora with blunted respiratory response: a sensitive echocardiographic sign of cardiac tamponade. J Am Coll Cardiol 1988;12:1470-7.
105. Singh S, Wann LS, Klopfenstein HS, Hartz A, Brooks HL. Usefulness of right ventricular diastolic collapse in diagnosing cardiac tamponade and comparison to pulsus paradoxus. Am J Cardiol 1986;57:652-6.
106. Gillam LD, Guyer DE, Gibson TC, King ME, Marshall JE, Weyman AE. Hydrodynamic compression of the right atrium: a new echocardiographic sign of cardiac tamponade. Circulation 1983;68:294-301.
107. Schiller NB, Botvinick EH. Right ventricular compression as a sign of cardiac tamponade: an analysis of echocardiographic ventricular dimensions and their clinical implications. Circulation 1977;56:774-9.
108. Leimgruber PP, Klopfenstein HS, Wann LS, Brooks HL. The hemodynamic derangement associated with right ventricular diastolic collapse in cardiac tamponade: an experimental echocardiographic study. Circulation 1983;68:612-20.
109. Rifkin RD, Pandian NG, Funai JT. Sensitivity of right atrial collapse and right ventricular diastolic collapse in the diagnosis of graded cardiac tamponade. AM J Noninvasive Cardiol 1987;1:73-80.
110. Lopez-Sendon J, Garcia-Fernandez MA, Coma-Canella I, Sotillo J, Silvestre J. Mechanism of right atrial wall compression in pericardial-effusion—an experimental echocardiographic study in dogs. J Cardiovasc Ultrasonogr 1988;7:127-34.
111. Merce J, Sagrista-Sauleda J, Permanyer-Miralda G, Evangelista A, Soler-Soler J. Correlation between clinical and Doppler echocardiographic findings in patients with moderate and large pericardial effusion: implications for the diagnosis of cardiac tamponade. Am Heart J 1999;138:759-64.
112. Hoit BD, Gabel M, Fowler NO. Cardiac tamponade in left ventricular dysfunction. Circulation 1990;82:1370-6.
113. Hoit BD, Fowler NO. Influence of acute right ventricular dysfunction on cardiac tamponade. J Am Coll Cardiol 1991;18:1787-93.
114. Klopfenstein HS, Cogswell TL, Bernath GA, Wann LS, Tipton RK, Hoffmann RG, et al. Alterations in intravascular volume affect the relation between right ventricular diastolic collapse and the hemodynamic severity of cardiac tamponade. J Am Coll Cardiol 1985;6:1057-63.
115. Aqel RA, Aljaroudi W, Hage FG, Tallaj J, Rayburn B, Nanda NC. Left ventricular collapse secondary to pericardial effusion treated with pericardicentesis and percutaneous pericardiotomy in severe pulmonary hypertension. Echocardiography 2008;25:658-61.
116. Hoit BD, Shaw D. The paradoxical pulse in tamponade: mechanisms and echocardiographic correlates. Echocardiography 1994;11:477-87.
117. Leeman DE, Levine MJ, Come PC. Doppler echocardiography in cardiac tamponade: exaggerated respiratory variation in transvalvular blood flow velocity integrals. J Am Coll Cardiol 1988;11:572-8.
118. Appleton CP, Hatle LK, Popp RL. Cardiac tamponade and pericardial effusion: respiratory variation in transvalvular flow velocities studied by Doppler echocardiography. J Am Coll Cardiol 1988;11:1020-30.
119. Appleton CP, Hatle LK, Popp RL. Superior vena cava and hepatic vein Doppler echocardiography in healthy adults. J Am Coll Cardiol 1987;10:1032-9.
120. Hernandez-Luyando L, Calvo J, Gonzalez de las Heras E, de la Puente H, Lopez C. Tension pericardial collections: sign of "flattened heart" in CT. Eur J Radiol 1996;23:250-2.
121. Steiner MA, Marshall JJ. Coronary sinus compression as a sign of cardiac tamponade. Catheter Cardiovasc Interv 2000;49:455-8.
122. Doppman JL, Rienmuller R, Lissner J, Cyran J, Bolte HD, Strauer BE, et al. Computed tomography in constrictive pericardial disease. J Comput Assist Tomogr 1981;5:1-11.
123. Frantz KM, Fishman EK. Hemopericardium leading to cardiac tamponade in the traumatized pediatric patient: discovery by CT. Clin Imaging 1992;16:180-2.
124. Goldstein L, Mirvis SE, Kostrubiak IS, Turney SZ. CT diagnosis of acute pericardial tamponade after blunt chest trauma. AJR Am J Roentgenol 1989;152:739-41.
125. Killeen KL, Poletti PA, Shanmuganathan K, Mirvis SE. CT diagnosis of cardiac and pericardial injuries. Emerg Radiol 1999;6:339-44.
126. Krejci CS, Blackmore CC, Nathens A. Hemopericardium: an emergent finding in a case of blunt cardiac injury. AJR Am J Roentgenol 2000;175:250.
127. Rotondo A, Scialpi M, Catalano O, Strada A, Grassi R, Angelelli G, et al. Periportal lymphatic distension resulting from cardiac tamponade: CT findings and clinical-pathologic correlation. Emerg Radiol 1999;6:85-93.
128. Sievers B, Brandts B, Moon JC, Pennell DJ, Trappe HJ. Cardiovascular magnetic resonance of imminent cardiac tamponade due to postpericardiotomy syndrome. Int J Cardiol 2003;91:241-4.
129. Chatelain P, Didier D. Detection of myocardial rupture by cine-magnetic resonance imaging. Am J Cardiol 1994;73:1033-5.
130. Little WC, Freeman GL. Pericardial disease. Circulation 2006;113:1622-32.
131. Bertog SC, Thambidorai SK, Parakh K, Schoenhagen P, Ozduran V, Houghtaling PL, et al. Constrictive pericarditis: etiology and cause-specific survival after pericardiectomy. J Am Coll Cardiol 2004;43:1445-52.
132. Ling LH, Oh JK, Schaff HV, Danielson GK, Mahoney DW, Seward JB, et al. Constrictive pericarditis in the modern era: evolving clinical spectrum and impact on outcome after pericardiectomy. Circulation 1999;100:1380-6.
133. Talreja DR, Edwards WD, Danielson GK, Schaff HV, Tajik AJ, Tazelaar HD, et al. Constrictive pericarditis in 26 patients with histologically normal pericardial thickness. Circulation 2003;108:1852-7.

134. Hatle LK, Appleton CP, Popp RL. Differentiation of constrictive pericarditis and restrictive cardiomyopathy by Doppler echocardiography. Circulation 1989;79:357-70.
135. Oh JK, Hatle LK, Seward JB, Danielson GK, Schaff HV, Reeder GS, et al. Diagnostic role of Doppler echocardiography in constrictive pericarditis. J Am Coll Cardiol 1994;23:154-62.
136. Oh JK, Tajik AJ, Appleton CP, Hatle LK, Nishimura RA, Seward JB. Preload reduction to unmask the characteristic Doppler features of constrictive pericarditis. A new observation. Circulation 1997;95:796-9.
137. Klein AL, Cohen GI, Pietrolungo JF, White RD, Bailey A, Pearce GL, et al. Differentiation of constrictive pericarditis from restrictive cardiomyopathy by Doppler transesophageal echocardiographic measurements of respiratory variations in pulmonary venous flow. J Am Coll Cardiol 1993; 22:1935-43.
138. Sun JP, Abdalla IA, Yang XS, Rajagopalan N, Stewart WJ, Garcia MJ, et al. Respiratory variation of mitral and pulmonary venous Doppler flow velocities in constrictive pericarditis before and after pericardiectomy. J Am Soc Echocardiogr 2001;14:1119-26.
139. Rajagopalan N, Garcia MJ, Rodriguez L, Murray RD, Apperson-Hansen C, Stugaard M, et al. Comparison of new Doppler echocardiographic methods to differentiate constrictive pericardial heart disease and restrictive cardiomyopathy. Am J Cardiol 2001;87:86-94.
140. Garcia MJ, Rodriguez L, Ares M, Griffin BP, Thomas JD, Klein AL. Differentiation of constrictive pericarditis from restrictive cardiomyopathy: assessment of left ventricular diastolic velocities in longitudinal axis by Doppler tissue imaging. J Am Coll Cardiol 1996;27:108-14.
141. Ha JW, Ommen SR, Tajik AJ, Barnes ME, Ammash NM, Gertz MA, et al. Differentiation of constrictive pericarditis from restrictive cardiomyopathy using mitral annular velocity by tissue Doppler echocardiography. Am J Cardiol 2004;94:316-9.
142. Sohn DW, Kim YJ, Kim HS, Kim KB, Park YB, Choi YS. Unique features of early diastolic mitral annulus velocity in constrictive pericarditis. J Am Soc Echocardiogr 2004;17:222-6.
143. Ha JW, Oh JK, Ommen SR, Ling LH, Tajik AJ. Diagnostic value of mitral annular velocity for constrictive pericarditis in the absence of respiratory variation in mitral inflow velocity. J Am Soc Echocardiogr 2002;15: 1468-71.
144. Ha JW, Oh JK, Ling LH, Nishimura RA, Seward JB, Tajik AJ. Annulus paradoxus: transmitral flow velocity to mitral annular velocity ratio is inversely proportional to pulmonary capillary wedge pressure in patients with constrictive pericarditis. Circulation 2001;104:976-8.
145. Reuss CS, Wilansky SM, Lester SJ, Lusk JL, Grill DE, Oh JK, et al. Using mitral "annulus reversus" to diagnose constrictive pericarditis. Eur J Echocardiogr 2009;10:372-5.
146. Veress G, Ling LH, Kim KH, Dal-Bianco JP, Schaff HV, Espinosa RE, et al. Mitral and tricuspid annular velocities before and after pericardiectomy in patients with constrictive pericarditis. Circ Cardiovasc Imaging 2011; 4:399-407.
147. Choi JH, Choi JO, Ryu DR, Lee SC, Park SW, Choe YH, et al. Mitral and tricuspid annular velocities in constrictive pericarditis and restrictive cardiomyopathy: correlation with pericardial thickness on computed tomography. JACC Cardiovasc Imaging 2011;4:567-75.
148. Sengupta PP, Krishnamoorthy VK, Abhayaratna WP, Korinek J, Belohlavek M, Sundt TM III, et al. Disparate patterns of left ventricular mechanics differentiate constrictive pericarditis from restrictive cardiomyopathy. JACC Cardiovasc Imaging 2008;1:29-38.
149. Kusunose K, Dahiya A, Popovic ZB, Motoki H, Alraies MC, Zurick AO, et al. Biventricular mechanics in constrictive pericarditis comparison with restrictive cardiomyopathy and impact of pericardiectomy. Circ Cardiovasc Imaging 2013;6:399-406.
150. Rajiah P, Kanne JP. Computed tomography of the pericardium and pericardial disease. J Cardiovasc Comput Tomogr 2010;4:3-18.
151. Schoenhagen P, Thompson CM, Halliburton SS. Low-dose cardiovascular computed tomography: where are the limits? Curr Cardiol Rep 2012; 14:17-23.
152. Feng D, Glockner J, Kim K, Martinez M, Syed IS, Araoz P, et al. Cardiac magnetic resonance imaging pericardial late gadolinium enhancement and elevated inflammatory markers can predict the reversibility of constrictive pericarditis after antiinflammatory medical therapy: a pilot study. Circulation 2011;124:1830-7.
153. Thavendiranathan P, Verhaert D, Walls MC, Bender JA, Rajagopalan S, Chung YC, et al. Simultaneous right and left heart real-time, free-breathing CMR flow quantification identifies constrictive physiology. JACC Cardiovasc Imaging 2012;5:15-24.
154. Giorgi B, Mollet NR, Dymarkowski S, Rademakers FE, Bogaert J. Clinically suspected constrictive pericarditis: MR imaging assessment of ventricular septal motion and configuration in patients and healthy subjects. Radiology 2003;228:417-24.
155. Francone M, Dymarkowski S, Kalantzi M, Rademakers FE, Bogaert J. Assessment of ventricular coupling with real-time cine MRI and its value to differentiate constrictive pericarditis from restrictive cardiomyopathy. Eur Radiol 2006;16:944-51.
156. Oh JK, Chang SA, Choe YH, Young PM. CMR imaging for diastolic hemodynamic assessment fantasy or reality? JACC Cardiovasc Imaging 2012;5:25-7.
157. Hancock EW. A clearer view of effusive-constrictive pericarditis. N Engl J Med 2004;350:435-7.
158. Sagrista-Sauleda J, Angel J, Sanchez A, Permanyer-Miralda G, Soler-Soler J. Effusive-constrictive pericarditis. N Engl J Med 2004;350:469-75.
159. Cameron J, Oesterle SN, Baldwin JC, Hancock EW. The etiologic spectrum of constrictive pericarditis. Am Heart J 1987;113:354-60.
160. Dahiya A, Lytle BW, Klein AL. Constrictive epicarditis. J Am Coll Cardiol 2011;58:e11.
161. Choi HO, Song JM, Shim TS, Kim SH, Jung IH, Kang DH, et al. Prognostic value of initial echocardiographic features in patients with tuberculous pericarditis. Korean Circ J 2010;40:377-86.
162. Martin RP, Bowden R, Filly K, Popp RL. Intrapericardial abnormalities in patients with pericardial effusion. Findings by two-dimensional echocardiography. Circulation 1980;61:568-72.
163. Baker CM, Orsinelli DA. Subacute effusive-constrictive pericarditis: diagnosis by serial echocardiography. J Am Soc Echocardiogr 2004;17:1204-6.
164. Zurick AO III, Klein AL. Effusive-constrictive pericarditis. J Am Coll Cardiol 2010;56:86.
165. Luk A, Ahn E, Vaideeswar P, Butany JW. Pericardial tumors. Semin Diagn Pathol 2008;25:47-53.
166. Klatt EC, Heitz DR. Cardiac metastases. Cancer 1990;65:1456-9.
167. Wilkes JD, Fidias P, Vaickus L, Perez RP. Malignancy-related pericardial effusion. 127 cases from the Roswell Park Cancer Institute. Cancer 1995;76:1377-87.
168. Wolverson MK, Grider RD, Sundaram M, Heiberg E, Johnson F. Demonstration of unsuspected malignant disease of the pericardium by computed tomography. J Comput Tomogr 1980;4:330-3.
169. Funari M, Fujita N, Peck WW, Higgins CB. Cardiac tumors: assessment with Gd-DTPA enhanced MR imaging. J Comput Assist Tomogr 1991; 15:953-8.
170. Yilling FP, Schlant RC, Hertzler GL, Krzyaniak R. Pericardial mesothelioma. Chest 1982;81:520-3.
171. Grebenc ML, Rosado de Christenson ML, Burke AP, Green CE, Galvin JR. Primary cardiac and pericardial neoplasms: radiologic-pathologic correlation. Radiographics 2000;20:1073-103.
172. Enochs WS, Petherick P, Bogdanova A, Mohr U, Weissleder R. Paramagnetic metal scavenging by melanin: MR imaging. Radiology 1997;204: 417-23.
173. Hoffmann U, Globits S, Frank H. Cardiac and paracardiac masses. Current opinion on diagnostic evaluation by magnetic resonance imaging. Eur Heart J 1998;19:553-63.
174. Kalra MK, Abbara S. Imaging cardiac tumors. Cancer Treat Res 2008; 143:177-96.
175. Gossinger HD, Siostrzonek P, Zangeneh M, Neuhold A, Herold C, Schmoliner R, et al. Magnetic resonance imaging findings in a patient with pericardial mesothelioma. Am Heart J 1988;115:1321-2.
176. Khin MM, Kwong RY. Cardiac and pericardial tumors. In: Kwong RY, editor. Contemporary cardiology: cardiovascular magnetic resonance imaging. Totowa, NJ: Humana; 2008. pp. 429-65.

177. Kaminaga T, Takeshita T, Kimura I. Role of magnetic resonance imaging for evaluation of tumors in the cardiac region. Eur Radiol 2003; 13(suppl):L1-10.
178. Sparrow PJ, Kurian JB, Jones TR, Sivananthan MU. MR imaging of cardiac tumors. Radiographics 2005;25:1255-76.
179. van Beek EJ, Stolpen AH, Khanna G, Thompson BH. CT and MRI of pericardial and cardiac neoplastic disease. Cancer Imaging 2007;7: 19-26.
180. Rogers CI, Seymour EQ, Brock JG. Atypical pericardial cyst location: the value of computed tomography. J Comput Assist Tomogr 1980; 4:683-4.
181. Stoller JK, Shaw C, Matthay RA. Enlarging, atypically located pericardial cyst. Recent experience and literature review. Chest 1986;89: 402-6.
182. Demos TC, Budorick NE, Posniak HV. Benign mediastinal cysts: pointed appearance on CT. J Comput Assist Tomogr 1989;13:132-3.
183. Brunner DR, Whitley NO. A pericardial cyst with high CT numbers. AJR Am J Roentgenol 1984;142:279-80.
184. Vinee P, Stover B, Sigmund G, Laubenberger J, Hauenstein KH, Weyrich G, et al. MR imaging of the pericardial cyst. J Magn Reson Imaging 1992;2:593-6.
185. Bogaert J, Duerinckx AJ. Appearance of the normal pericardium on coronary MR angiograms. J Magn Reson Imaging 1995;5:579-87.
186. Ellis K, Leeds NE, Himmelstein A. Congenital deficiencies in the parietal pericardium: a review with 2 new cases including successful diagnosis by plain roentgenography. Am J Roentgenol Radium Ther Nucl Med 1959; 82:125-37.
187. Broadbent JC, Callahan JA, Kincaid OW, Ellis FH Jr. Congenital deficiency of the pericardium. Dis Chest 1966;50:237-44.
188. Nasser WK, Helmen C, Tavel ME, Feigenbaum H, Fisch C. Congenital absence of the left pericardium. Clinical, electrocardiographic, radiographic, hemodynamic, and angiographic findings in six cases. Circulation 1970;41:469-78.
189. Gatzoulis MA, Munk MD, Merchant N, Van Arsdell GS, McCrindle BW, Webb GD. Isolated congenital absence of the pericardium: clinical presentation, diagnosis, and management. Ann Thorac Surg 2000;69:1209-15.
190. Southworth H, Stevenson CS. Congenital defects of the pericardium. Arch Intern Med 1993;61:223-40.
191. Van Son JA, Danielson GK, Schaff HV, Mullany CJ, Julsrud PR, Breen JF. Congenital partial and complete absence of the pericardium. Mayo Clin Proc 1993;68:743-7.
192. Brulotte S, Roy L, Larose E. Congenital absence of the pericardium presenting as acute myocardial necrosis. Can J Cardiol 2007;23: 909-12.
193. Connolly HM, Click RL, Schattenberg TT, Seward JB, Tajik AJ. Congenital absence of the pericardium: echocardiography as a diagnostic tool. J Am Soc Echocardiogr 1995;8:87-92.
194. Nicolosi GL, Borgioni L, Alberti E, Burelli C, Maffesanti M, Marino P, et al. M-mode and two-dimensional echocardiography in congenital absence of the pericardium. Chest 1982;81:610-3.
195. Oki T, Tabata T, Yamada H, Manabe K, Fukuda K, Abe M, et al. Cross sectional echocardiographic demonstration of the mechanisms of abnormal interventricular septal motion in congenital total absence of the left pericardium. Heart 1997;77:247-51.
196. Candan I, Erol C, Sonel A. Cross sectional echocardiographic appearance in presumed congenital absence of the left pericardium. Br Heart J 1986;55:405-7.
197. Topilsky Y, Tabatabaei N, Freeman WK, Saleh HK, Villarraga HR, Mulvagh SL. Images in cardiovascular medicine. Pendulum heart in congenital absence of the pericardium. Circulation 2010;121:1272-4.
198. Fukuda N, Oki T, Iuchi A, Tabata T, Manabe K, Kageji Y, et al. Pulmonary and systemic venous flow patterns assessed by transesophageal Doppler echocardiography in congenital absence of the pericardium. Am J Cardiol 1995;75:1286-8.
199. Smith WH, Beacock DJ, Goddard AJ, Bloomer TN, Ridgway JP, Sivananthan UM. Magnetic resonance evaluation of the pericardium. Br J Radiol 2001;74:384-92.
200. Baim RS, MacDonald IL, Wise DJ, Lenkei SC. Computed tomography of absent left pericardium. Radiology 1980;135:127-8.
201. Gassner I, Judmaier W, Fink C, Lener M, Waldenberger F, Scharfetter H, et al. Diagnosis of congenital pericardial defects, including a pathognomic sign for dangerous apical ventricular herniation, on magnetic resonance imaging. Br Heart J 1995;74:60-6.
202. Tanaka H, Oishi Y, Mizuguchi Y, Miyoshi H, Ishimoto T, Nagase N, et al. Contribution of the pericardium to left ventricular torsion and regional myocardial function in patients with total absence of the left pericardium. J Am Soc Echocardiogr 2008;21:268-74.
203. Halliburton SS, Abbara S, Chen MY, Gentry R, Mahesh M, Raff GL, et al. SCCT guidelines on radiation dose and dose-optimization strategies in cardiovascular CT. J Cardiovasc Comput Tomogr 2011;5: 198-224.
204. Truong QA, Siegel E, Cannon CP. Cardiac CT angiography–radiation dose-how effective are we in reducing radiation dose from cardiac CT angiography? Rev Cardiovasc Med 2009;10:236-9.
205. Imazio M, Brucato A, Maestroni S, Cumetti D, Dominelli A, Natale G, et al. Prevalence of C-reactive protein elevation and time course of normalization in acute pericarditis: implications for the diagnosis, therapy, and prognosis of pericarditis. Circulation 2011;123:1092-7.
206. Yelgec NS, Dymarkowski S, Ganame J, Bogaert J. Value of MRI in patients with a clinical suspicion of acute myocarditis. Eur Radiol 2007; 17:2211-7.
207. Alter P, Figiel JH, Rupp TP, Bachmann GF, Maisch B, Rominger MB. MR, CT, and PET imaging in pericardial disease. Heart Fail Rev 2013;18: 289-306.
208. Derlin T, Clauditz TS, Habermann CR. Adrenal epithelioid angiosarcoma metastatic to the epicardium: diagnosis by 18F-FDG PET/CT. Clin Nucl Med 2012;37:914-5.
209. Douroukas A, Arena V, Pelosi E. Detection of metastatic involvement of the pericardium on F-18 FDG-PET/CT imaging. Clin Nucl Med 2009; 34:40-1.
210. Ghesani NV, Sun X, Zhuang H, Sam JW, Alavi A. Fluorodeoxyglucose positron emission tomography excludes pericardial metastasis by recurrent lung cancer. Clin Nucl Med 2003;28:666-7.
211. Lobert P, Brown RK, Dvorak RA, Corbett JR, Kazerooni EA, Wong KK. Spectrum of physiological and pathological cardiac and pericardial uptake of FDG in oncology PET-CT. Clin Radiol 2013; 68:e59-71.
212. Shao D, Wang SX, Liang CH, Gao Q. Differentiation of malignant from benign heart and pericardial lesions using positron emission tomography and computed tomography. J Nucl Cardiol 2011;18:668-77.
213. Testempassi E, Kubota K, Morooka M, Ito K, Masuda-Miyata Y, Yamashita H, et al. Constrictive tuberculous pericarditis diagnosed using 18F-fluorodeoxyglucose positron emission tomography: a report of two cases. Ann Nucl Med 2010;24:421-5.
214. Hoit BD. Pericardial disease. In: Fuster V, Walsh RA, Harrington RA, editors. Hurst's the heart. 13th ed. New York: McGraw-Hill; 2011. pp. 1917-39.
215. Atherton JJ, Moore TD, Thomson HL, Frenneaux MP. Restrictive left ventricular filling patterns are predictive of diastolic ventricular interaction in chronic heart failure. J Am Coll Cardiol 1998;31:413-8.

APPENDIX

Technical Approach to Pericardial Disease

A-1. Echocardiographic Approach to the Evaluation of PEff and Tamponade

The following systematic approach is recommended:

I. Parasternal long-axis view (PLAX; Figures A1 and A2): 2D and M-mode
   A. Increase depth to assess PEff (anterior to aorta) versus pleural effusion
   B. Modify view to evaluate location, size, and extent of PEff
   C. Assess if free flowing or loculated PEff
   D. Evaluate for RV diastolic collapse in the most perpendicular orientation to transducer
   E. Evaluate for RV diastolic collapse by M-mode echocardiography

II. Parasternal short-axis view (PSAX; Figure A3): 2D and M-mode
   A. Serial sweeping scans
   B. Modify view to evaluate location, size, and extent of PEff
   C. Assess if free flowing or loculated

III. Apical views (Figures A4–A6): 2D and PW Doppler
   A. Evaluate location size and extent of PEff
   B. Assess if free flowing or loculated PEff
   C. Evaluate for RA collapse (diastole and systole) in apical four-chamber view
   D. Assess PW Doppler mitral and tricuspid inflow for respiratory variation
   E. Use sample volume between 1 and 2 mm (slow sweep speed, 25 or 50 mm/sec) with simultaneous respirometry

IV. Subcostal view (Figures A7–A10): 2D, M-mode, and PW Doppler
   A. Assess location, size, and extent of PEff
   B. Assess if free flowing or loculated PEff
   C. Assess for RV and RA free wall collapse with M-mode perpendicular to wall
   D. Evaluate PW Doppler of hepatic veins for marked decrease in diastolic forward flow with large reversals of flow in expiration
   E. 1. Assess IVC size and collapse with sniff test by 2D and M-mode
      2. Sniff test to evaluate IVC collapse (plethoric – dilated [>2.1 cm] and does not collapse >50%)

*Note imaging should be done with patient in a supine position when evaluating before pericardiocentesis

III. Apical views (Figures A15–A25): 2D and PW Doppler
   A. Evaluate LV and RV conical compression, tubular narrowing, and septal bounce (signs of interventricular dependence) with serial sweeping scans
   B. Increase depth to assess for left atrial and RA tethering and annular motion
   C. 1. Use PW Doppler mitral and tricuspid inflow for respiratory variation (slow sweep speed, 25/50 mm/sec) with sample volume between 1 and 2 mm
      2. Consider to assess mitral valve inflow with patient sitting upright to bring out respiratory variation (preload reduction)
   D. Obtain PW tissue Doppler of medial and lateral mitral annular walls, sample volume size between 5 and 6 mm placed on annulus in the apical four-chamber and two-chamber views; obtain PW tissue Doppler of the tricuspid annulus in the apical four-chamber view
   E. Obtain PW Doppler of pulmonary veins, sample volume 3 to 4 mm
   F. Obtain isovolumic relaxation time continuous-wave or PW Doppler to delineate aortic valve closure to mitral valve opening
   G. Obtain color M-mode of diastolic transmitral inflow, baseline shift upward between 30 and 40 cm
   H. Obtain 2D strain from apical four-chamber, two-chamber, and three-chamber views (40 to 90 frames/sec)
   I. Obtain 3D echocardiography/triplane echocardiography for assessment of volumes/ejection fraction and septal bounce
   J. Use contrast agents for assessment of volumes/ejection fraction and septal bounce in technically difficult studies (i.e., obesity)

IV. Subcostal view (Figure A26): 2D, M-mode, and PW Doppler
   A. Assess for septal bounce
   B. Perform sniff test to evaluate for IVC size and plethora
   C. Obtain PW Doppler of hepatic veins, which will show marked decrease in diastolic forward flow with large reversals of flow in expiration
   D. Use sample volume between 3 and 4 mm (slow sweep speed between 25 and 50 mm/sec)

V. SVC (Figure A27)
   A. Obtain PW Doppler of SVC, which shows less marked respiratory changes in Doppler flows compared with hepatic vein flow
   B. Use sample volume between 3 and 4 mm placed 5 to 6 cm into SVC (slow sweep speed between 25 and 50 mm/sec)

A-2. Echocardiographic Approach to the Evaluation of CP

The following systematic approach is recommended:

I. PLAX (Figures A11 and A12): 2D and M-mode
   A. Increase depth to assess presence of PEff and pericardial thickening/calcification/conical compression/tubular deformity (decrease gain/turn off harmonics)
   B. Activate respirometer and evaluate by serial sweeping scans for the presence of a septal bounce by 2D and M-mode; use a slow sweep speed (25–50 mm/sec); adjust gain to clearly delineate the upward (onset of inspiration) and downward slopes (onset of expiration); if poor signal noted, adjust ECG wires cable box to be flush on patient's chest and diaphragm; respirometer should remain on throughout examination

II. PSAX (Figures A13 and A14): 2D and M-mode
   A. Repeat serial sweeping scans by 2D and M-mode to evaluate for a septal bounce from base to apex
   B. Modify view to evaluate location, size, and extent of PEff and pericardial thickening/calcification/conical compression/tubular deformity
   C. Obtain multiple-beat acquisitions with spontaneous breathing to assess for interventricular dependence

	Philips iCT 256-slice	
	3D (standard)	Four-dimensional (limited indication)
Mode	Axial/sequential	Helical/spiral
ECG referencing	Prospective triggering	Retrospective gating
Scan range	Heart	Heart
Tube voltage (kVp)	100, 120	100, 120
Rotation time (sec)	0.27	0.27
Pitch		0.18
Collimated detector row width (mm)	96, 112, 128 × 0.625	128 × 0.625
Reconstruction phase		

(Continued)

(*Continued*)

Philips iCT 256-slice		
	3D (standard)	Four-dimensional (limited indication)
Reconstructed slice thickness (mm)/ increment (mm)	1.5/0.75	1.5/0.75
Reconstruction kernel	Xres Standard (XCB)	Xres Standard (XCB)

Siemens Flash dual-source		
	3D	Four-dimensional
Mode	Axial/sequential	Helical/spiral
ECG Referencing	Prospective triggering	Retrospective gating
Scan range	Heart	Heart
Tube voltage (kVp)	100, 120	100, 120
Rotation time (sec)	0.28	0.28
Pitch		0.2–0.45
Collimated detector row width (mm)	128 × 0.625	128 × 0.625
Reconstruction phase		
Reconstructed slice thickness (mm)/ increment (mm	1.5/0.75	1.5/0.75
Reconstruction kernel	B26f	B26f

Philips 64-slice	
	3D/four-dimensional
Mode	Helical/spiral
ECG referencing	Retrospective gating
Scan range	Heart
Tube voltage (kVp)	100, 120
Rotation time (sec)	0.4
Pitch	0.2
Collimated detector row width (mm)	64 × 0.625
Reconstruction phase	
Reconstructed slice thickness (mm)/ increment (mm)	1.5/0.75
Reconstruction kernel	Xres Standard (XCB)

B. Computed Tomographic Protocol: System Settings in Evaluation of Pericardial Diseases

C. CMR Protocol for Evaluation of Pericardial Disease

I. Standard MRI sequences in pericardial diseases
   A. The sequences are described in the typical order of data acquisition
   B. Listed is a comprehensive, standard examination
   C. In clinical practice, the order and number of sequences should be tailored to the specific clinical question for each individual patient
   D. Also, the name of sequences varies between vendors and scanners

1. https://wiki.nci.nih.gov/display/CIP/MRI+pulse+sequence+cross-vendor+nomenclature+playbook
2. MRI_Cross_Vendor_Acronyms_508_compliant.pdf
3. http://radiographics.rsna.info/content/26/2/513.full

STEP-BY-STEP PROTOCOL

1. Nongated steady-state free precession (SSFP) localizer (Figure A28): sagittal
   - Acquire in inspiration
   - Use empiric values for coverage
2. ASSET calibration (Figure A29): axial
3. Nongated SSFP localizer (Figure A30): axial
   - Cover entire chest in one breath-hold
4. Nongated SSFP localizer (Figure A31): coronal
   - Cover entire chest in one breath-hold

These additional localizers are optional but may aid in prescribing standard planes:

5. Nongated single-shot fast spin-echo (FSE) localizer (half Fourier acquisition single-shot turbo spin-echo, etc.) (Figure A32): axial
   - Cover entire chest in one breath-hold

These additional localizers are optional but may aid in identifying mass lesions quickly:

6. Cine SSFP (Figure A33): paraseptal long-axis
   - Two slices left ventricle, 8-mm thickness, skip 0–2 mm
   - Prescribe off-axial scout images at level of ventricular septum, parallel to septum and through LV apex
7. PD/T2 dual echo FSE (Figure A34): short-axis
   - Prescribe off-paraseptal long-axis and axial images, orthogonal to LV long axis and to ventricular septum
   - Assess pericardial thickness
   - 8 mm thick, skip 2 mm, cover left ventricle from base to just above apex
   - May use dual-echo technique echo times minimum (∼4 msec), 80 if patient tolerates
   - This allows to get T2W images in addition to proton density
   - Otherwise, minimum (∼4 ms) echo time only
8. Cine SSFP (FIESTA) (Figure A35): four-chamber
   - Two slices mid left ventricle, single breath-hold
   - Prescribe off-short-axis views to intersect center of left ventricle and angle between RV anterior and inferior free walls (acute margin)
9. Cine SSFP (FIESTA) (Figure A36): three-chamber
   - Prescribe off-short-axis view at level of LV outflow tract; center to intersect LV cavity center and aortic valve
10. Tagged gradient-echo (for constriction only) (Figure A37): four-chamber
    - Six to eight slices to cover entire left ventricle
    - 8-mm slice thickness, zero skip
    - Tagged lines should be orthogonal to anterior wall
    - Allows to interrogate for pericardial adhesions
11. Tagged gradient echo (OPTIONAL) (Figure A38): paraseptal long-axis
    - Four to six slices to cover entire left ventricle
    - Tagged lines should be orthogonal to inferior wall
    - Allows to interrogate for pericardial adhesions
12. Double inversion-recovery T2 FSE (Figure A39): short-axis
    - TURN ON BODY COIL!
    - Four to five slices, slice thickness 9 mm, skip 1 mm
    - Dual echo if possible, with echo time 65 and maximum (100 – 120)
    - If breath-holds too long, single echo with echo time 65
    - Echo train length ∼ 20
    - For measurement of myocardial edema
13. T1 FSE (OPTIONAL) (Figure A40): short-axis
    - ONLY if pericardial thickening identified on FSE or cines
    - Cover atrium and ventricle
    - Slice thickness 10 mm, skip 0 mm
    - Echo train length = 16

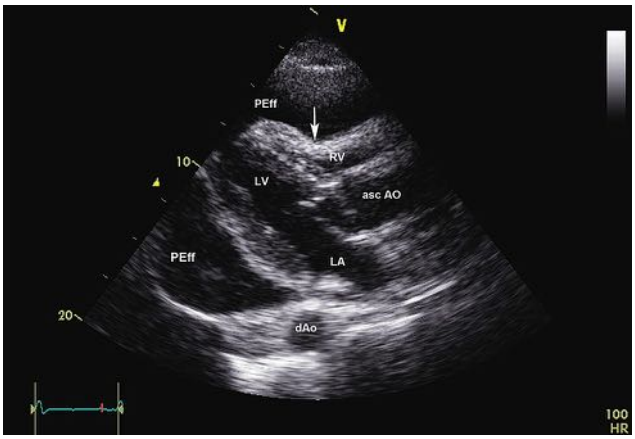

Figure A1 Cardiac tamponade: 2D parasternal long-axis view demonstrating a large circumferential, free-flowing PEff (Video A1). Diastolic collapse of the right ventricle is shown (*arrow*) consistent with cardiac tamponade.

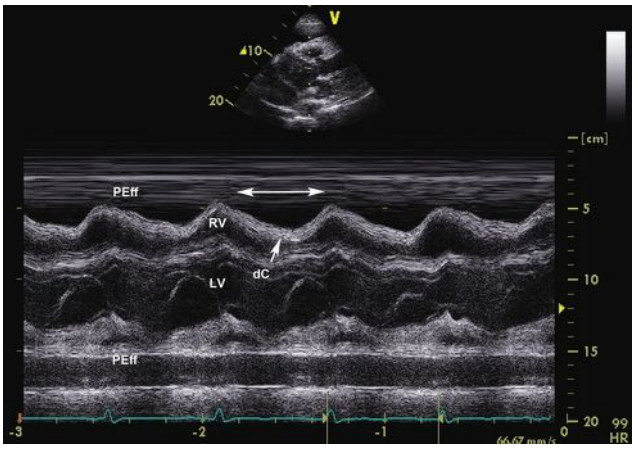

Figure A2 Cardiac tamponade: M-mode obtained from the parasternal long-axis view in a patient with cardiac tamponade (same patient as in Figure A1). The high temporal resolution of M-mode allows determination of the timing and duration of diastolic collapse (dC). The *two-sided arrow* shows the duration of diastole as determined by electrocardiography (end of the T wave to onset of QRS) or outward movement of the interventricular septum. The *one-sided arrow* demonstrates the duration of diastole during which dC is present. In this example, dC is occurring for more than half of diastole, excluding late diastole, which is specific for cardiac tamponade. Note that M-mode of the right ventricle can be obtained from other views, including the subxiphoid view.

14. Administer first (single-dose) gadolinium (0.1 mmol/kg)
15. T1 SE after gadolinium OPTIONAL (Figure A41): same view as prior sequence
    - ONLY if noncontrast T1 FSE performed!
    - DO NOT PRESCAN TO AVOID tuning/chimming (just do manual prescan, done)
    - Copy precontrast sequence prescription
    - Look for pericardial enhancement
16. Administer either second single-dose gadolinium (0.1 mmol/kg) or double-dose gadolinium (0.2 mmol/kg) if T1 FSE not performed
17. Cine SSFP (Figure A42): short-axis
    - Complete short-axis stack
    - 8 mm thick, skip 2 mm
    - Chamber volumes/function
    - Look for septal bounce
18. 3D MDE (Figure A43): four-chamber stack
    - Use best inversion time (TI) to null myocardium
19. 3D MDE (Figure A44): short-axis stack(s)
    - Find TI; repeat if necessary
20. 3D MDE (Figure A45): paraseptal long-axis stack
    - Use best TI
21. 2D MDE (Figure A46): short-axis, other obliquities as needed
    - Use best TI time (may vary from 3D)
22. Real-time MR echo SSFP (Figure A47): short axis
    - Try to include diaphragms
    - Several slow deep inspiration and expiration
    - To assess for respirophasic ventricular interdependence
23. Phase contrast: choose plane according to pericardial disease
    - Use if possibility of small effusion mimicking pericardial thickening needs to be excluded
    - Use slow velocity encoding (e.g., 30 cm/sec), as fluid motion within pericardium is slow

Other sequences

24. Double inversion-recovery T1 FSE (Figure A48): axial
25. Double inversion-recovery T1 FSE after contrast (Figure A49): axial

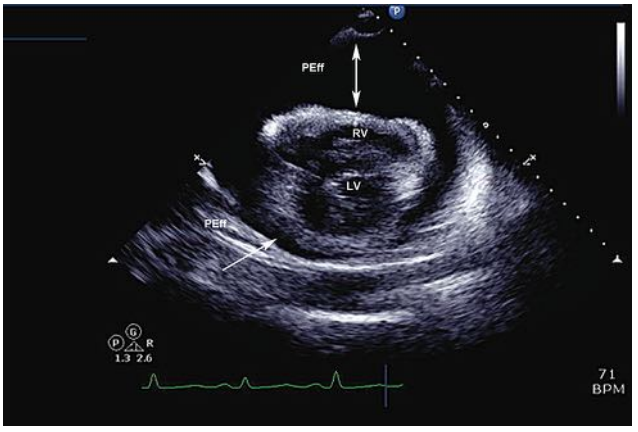

Figure A3 Cardiac tamponade: 2D parasternal short-axis view sweeping scan from base to apex (Video A2) is obtained in the same patient as in Figure A1 with cardiac tamponade. This view is obtained to determine the size and extent of the PEff in each region of the heart during diastole. In this example, the anterior effusion is >4 cm, as denoted by the large *double-headed arrow*, and the posterior effusion is small (<1 cm). Of note, the patient position should be noted when determining the size and location of the effusion, because it may vary with free-flowing effusions.

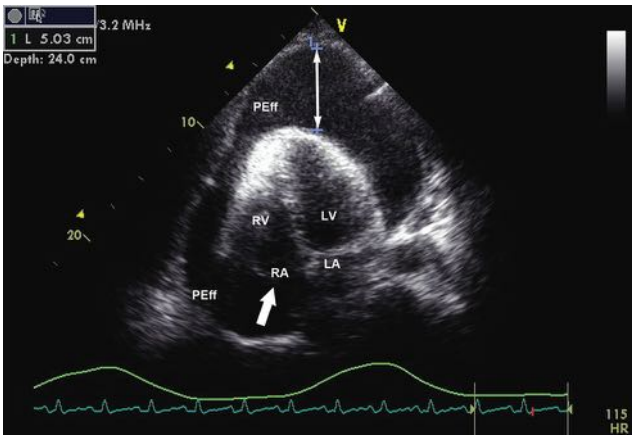

Figure A4 Cardiac tamponade: 2D apical four-chamber view of a patient with a large PEff and cardiac tamponade as evidenced by RA systolic collapse (Video A3). Of note, RA collapse (*one-headed arrow*) may occur in diastole or systole, and the longer the proportion of the cardiac cycle during which collapse is present, the greater the specificity that cardiac tamponade is present. In this example, the largest collection (~5 cm) of fluid is at the apex (*two-headed arrow*), and pericardiocentesis can be performed from this approach.

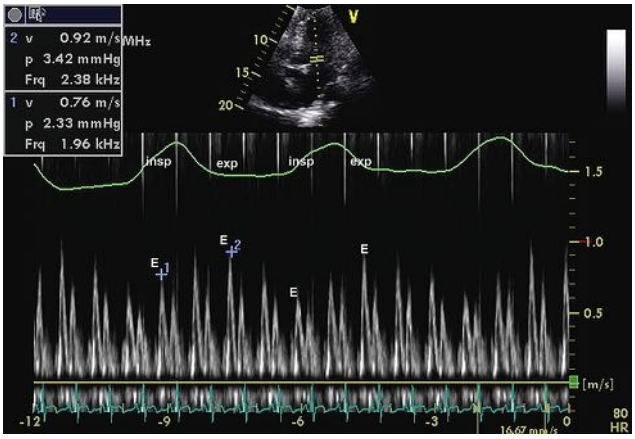

Figure A5 Cardiac tamponade: PW Doppler recording of mitral inflow assessing respiratory variation in a patient with cardiac tamponade. Note that the respirometer denotes the onset of inspiration (insp) and expiration (exp). The peak E-wave in inspiration (1 = 76 cm/sec) and expiration (2 = 92 cm/sec) are recorded. The method for determining respiratory variation of mitral inflow is from expiration with the formula (expiration − inspiration)/expiration or, in this example, (92 − 76)/92 = 17%. Several measurements should be made and averaged. Usually, >30% respiratory variation in mitral inflow is considered abnormal and likely present in this patient when averaging measurements over several cardiac cycles.

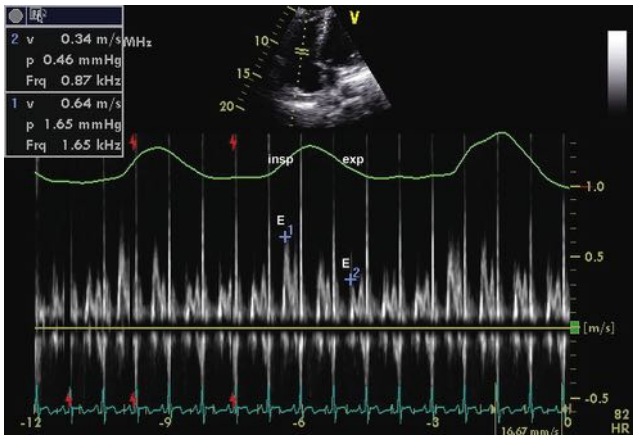

Figure A6 Cardiac tamponade: PW Doppler recording of tricuspid inflow assessing respiratory variation in a patient with cardiac tamponade. As in Figure A5, the respirometer denotes inspiration (insp) and expiration (exp). The peak E waves in inspiration (1 = 64 cm/sec) and exp (2 = 34 cm/sec) are noted. Respiratory variation from expiration is calculated by the formula (expiration − inspiration)/expiration or, in this example, (34 − 64)/34 = −87%. Generally, >60% tricuspid inflow variation is expected in presence of cardiac tamponade.

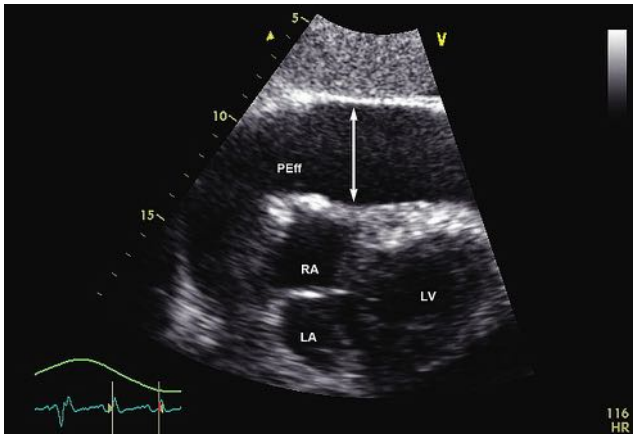

Figure A7 Cardiac tamponade: 2D subcostal view of a patient with a large PEff and cardiac tamponade (Video A4). Note that RV dC is present in this example. This view aids to demonstrate the size of the effusion in diastole and the distance from the transducer and the liver when considering pericardiocentesis using the subxiphoid approach.

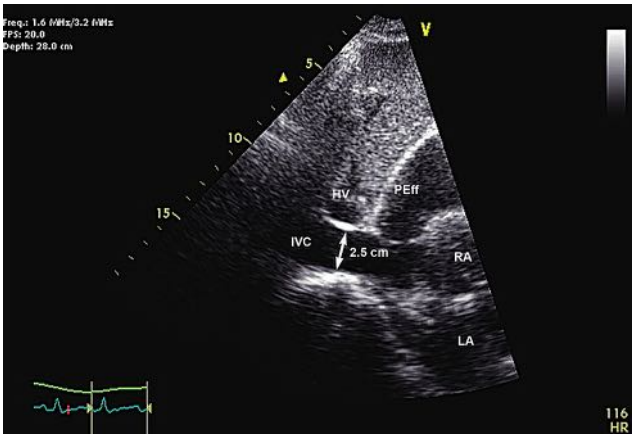

Figure A8 Cardiac tamponade: 2D subcostal view of the IVC in a patient with cardiac tamponade (Video A5). The IVC is dilated (>2.2 cm at the mouth) and has <50% collapse during inspiration as seen in the subsequent image (Figure A9). A dilated IVC with minimal collapse during respiration is referred to as IVC plethora and is an expected finding with cardiac tamponade.

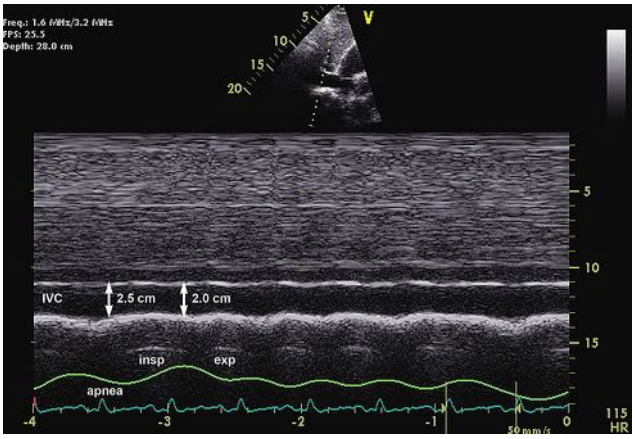

Figure A9 Cardiac tamponade: subcostal M-mode of a plethoric IVC in the same patient with cardiac tamponade as seen in Figure A8. The *two-headed arrows* demonstrate the IVC diameter at the beginning and end of inspiration. The percentage collapse is 20%, which is very abnormal (<50% is considered abnormal) and consistent with elevated RA pressure and cardiac tamponade.

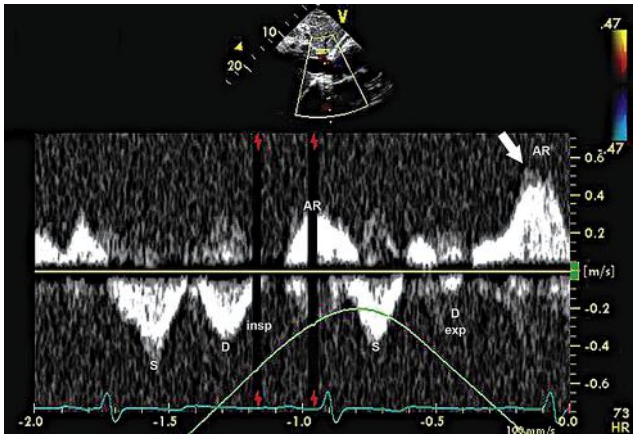

Figure A10 Cardiac tamponade: PW Doppler of the hepatic vein in a patient with cardiac tamponade. S and D are antegrade flow in systole and diastole, respectively, and AR is retrograde flow in diastole. A decrease in the diastolic flow or a large AR particularly during the first beat of expiration are hallmarks of cardiac tamponade. PW Doppler of the hepatic vein should be obtained in all patients with suspected cardiac tamponade if obtainable.

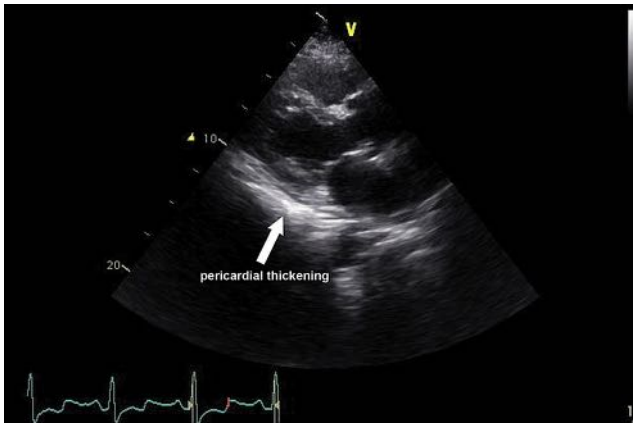

Figure A11 CP: 2D parasternal long-axis view in a patient with CP (Video A6). The *arrow* points to a focal region of pericardial calcification extending from the atrioventricular groove to the posterior LV wall. This finding, in conjunction with an interventricular septal bounce, is consistent with CP.

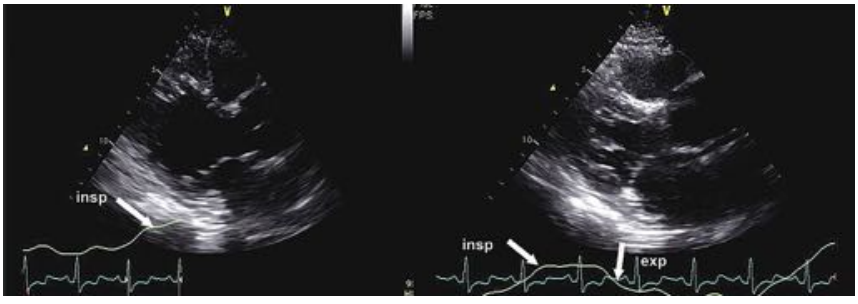

Figure A12 CP: 2D parasternal long-axis view demonstrating proper use of a respirometer in a patient with CP. A high-quality tracing demonstrating both inspiration and expiration is essential. The *left panel* and *arrow* point to upslope in inspiration only (Video A7). The *right panel* and *arrows* point to the peak of inspiration and expiration after an adjustment of the respirometer was made (Video A8).

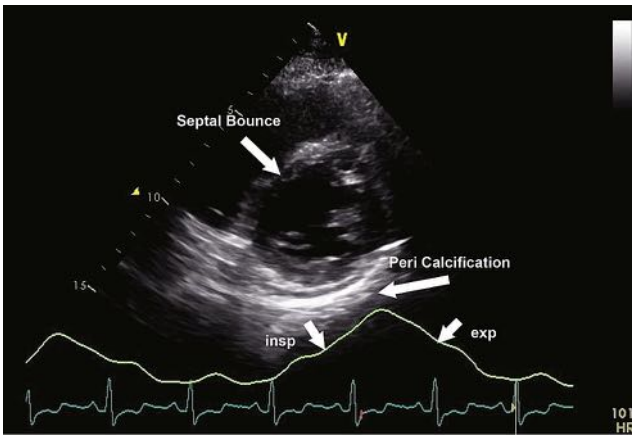

Figure A13 CP: 2D parasternal short-axis view in a patient with CP. *Arrows* point to the onset of inspiration and onset of expiration; pericardial calcification and the interventricular septum where flattening of the septum is apparent in diastole consistent with a septal bounce (Video A9). These are the features that are consistent with CP.

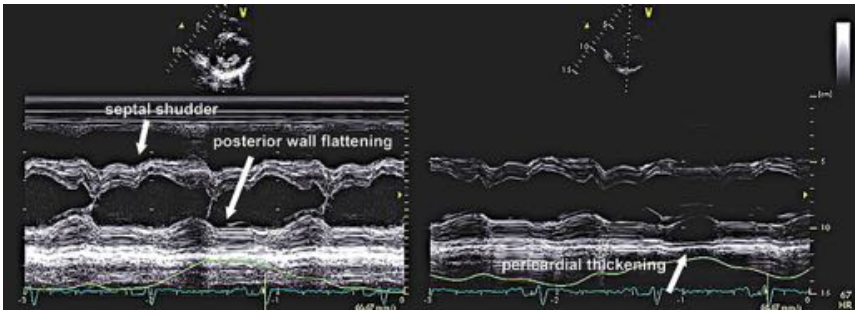

Figure A14 CP: M-mode of parasternal short-axis view in the same patient as in Figure A13. Several M-mode features of CP are seen, including diastolic flattening of the posterior wall, pericardial calcification (better seen in the *right panel* with a reduced 2D gain and fundamental imaging), a septal diastolic shudder consistent with the septal bounce seen by 2D imaging, and respiratory variation in LV cavity size.

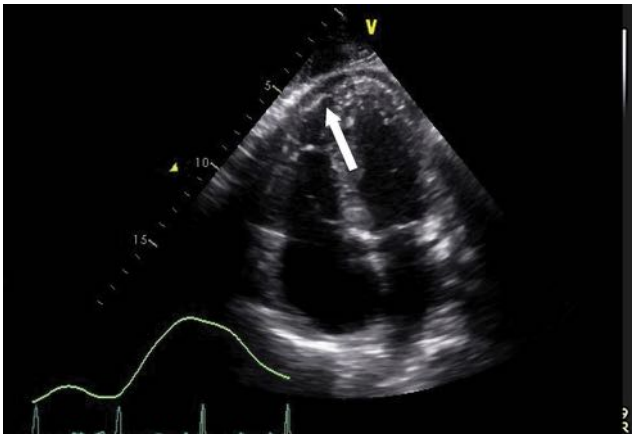

Figure A15 CP: 2D apical four-chamber view in a patient with CP (Video A10). The *arrow* points to pericardial thickening and an organized PEff at the LV and RV apex consistent with the diagnosis.

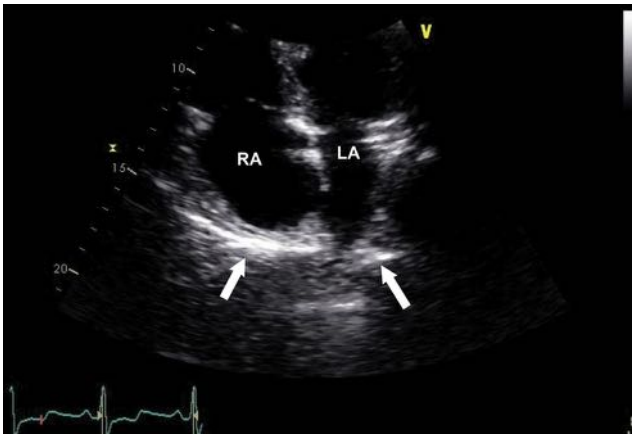

Figure A16 CP: apical four-chamber view in a patient with CP. *Arrows* point to pericardial calcification and thickening adjacent to the right and left atria, which result in tethering and constrictive physiology (Video A11).

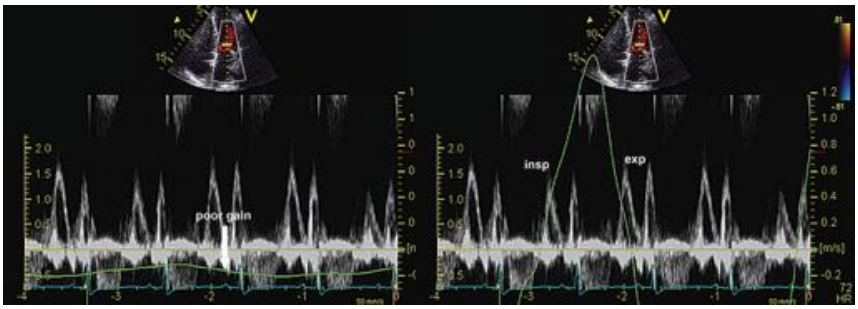

Figure A17 CP: apical four-chamber view with PW Doppler recording of the mitral inflow in a patient with CP. (*Left*) The respirometer waveform is indistinguishable because of poor gain. After adjustment (*right*) the respiratory waves are now able to clearly distinguish inspiration and expiration.

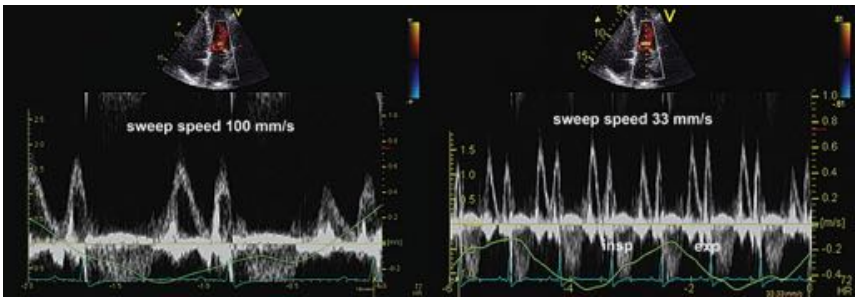

Figure A18 CP: apical four-chamber view with PW Doppler of the mitral inflow in a patient with CP. (*Left*) The sweep speed is set to 100 mm/sec, and the mitral inflow in inspiration and expiration cannot be distinguished on the same image. After adjustment to a sweep speed of 33 mm/sec (usually 25–50 mm/sec is suitable), the mitral inflow can be clearly distinguished to show onset of in inspiration and expiration.

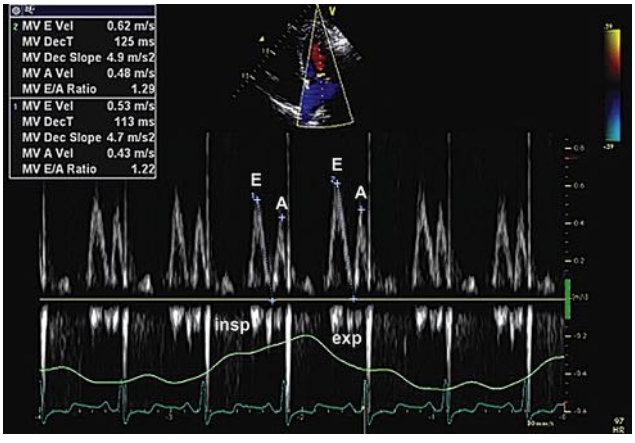

Figure A19 CP: apical four-chamber view with pulsed Doppler of mitral inflow in a patient with CP. The mitral E and A waves are labeled. The first beat of inspiration is recorded, and peak expiration beat is recorded and can be used to determine respiratory variation from expiration using the formula (expiration − inspiration)/expiration. At least three beats should be averaged. Significant respiratory variation is considered to be present when there is an inspiratory decrease of mitral inflow is >25%. However, maneuvers (preload reduction as in sitting up or increase in volume loading) may be required to demonstrate variation.

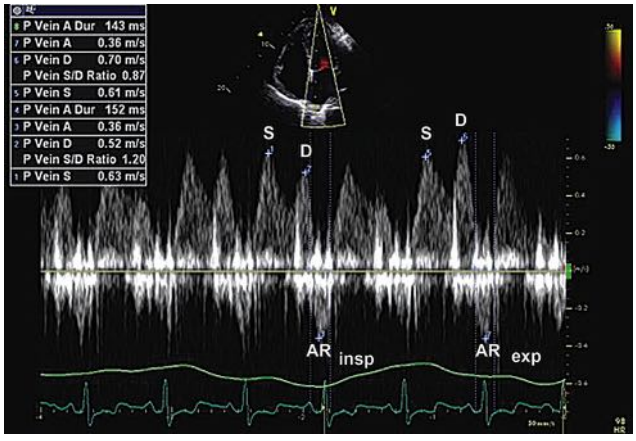

Figure A20 CP apical four-chamber view with PW Doppler of the right upper pulmonary vein in a patient with CP. The S (systolic), D (diastolic), and AR (atrial reversal waves) are noted. Respiratory variation of the D wave should be determined similar to the method used for the mitral E wave.

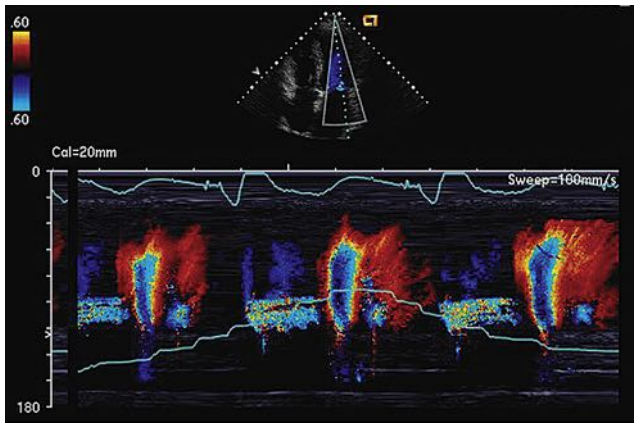

Figure A21 CP: apical four-chamber view with color M-mode through the mitral valve in a patient with CP. The slope of the propagation velocity of early diastolic flow is obtained by measuring the slope of the first aliasing velocity from the mitral coaptation 4 cm into the LV cavity. Typically, the Nyquist limit should be baseline shifted to about 30 to 40 cm/sec to demonstrate aliasing of propagation velocity (not done in this example). Note the rapid slope (100 cm/sec) in this patient.

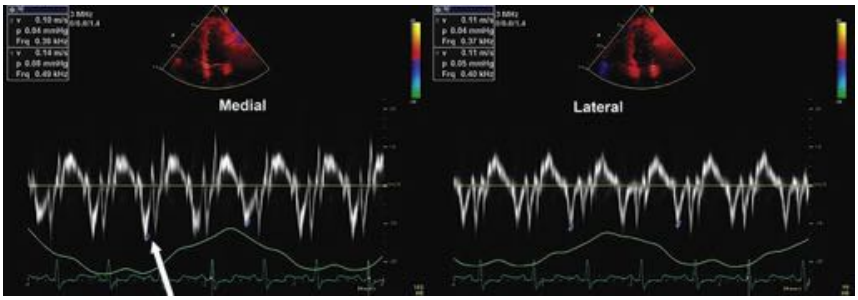

Figure A22 CP: PW Doppler tissue imaging from the apical four-chamber view in a patient with CP. Measurements of the peak e′ from medial and lateral annulus should be obtained. Note in this example that the medial e′ (*arrow*) is elevated (14 cm/sec) and greater than than the lateral e′. This finding (annulus reversus) is a typical feature of CP when the lateral annulus is involved with the constrictive process.

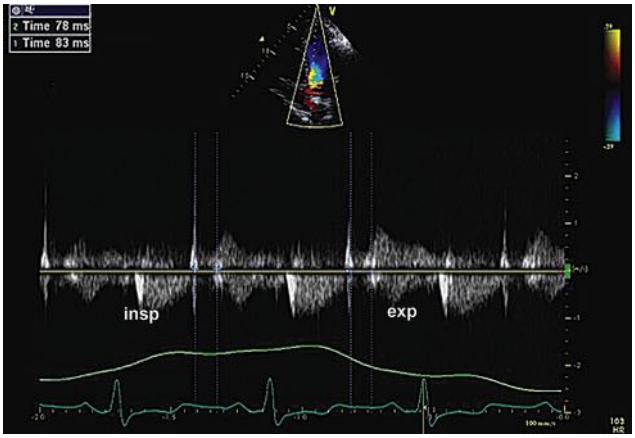

Figure A23 CP: apical four-chamber view in a patient with CP. The isovolumic relaxation time (IVRT) is obtained by continuous-wave Doppler but can alternatively be obtained with PW Doppler. The IVRT is the time from aortic valve closure to mitral valve opening and can be obtained in inspiration and expiration. Typically, the IVRT of the left ventricle will increase with inspiration; in this example, 83 msec in inspiration and 78 msec in expiration.

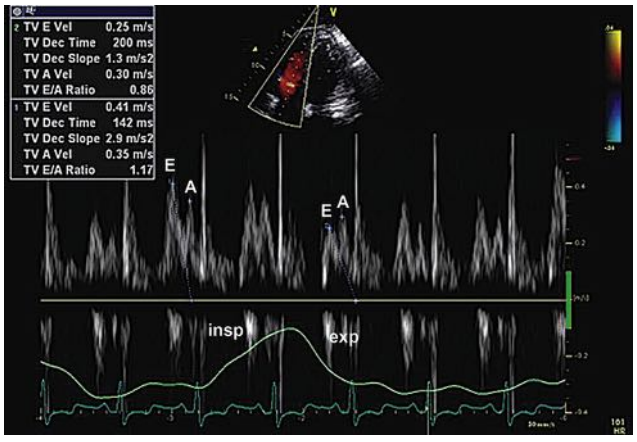

Figure A24 CP: apical 4-chamber view of the tricuspid inflow with PW Doppler in a patient with CP. Measurements of peak E-wave velocity in inspiration and expiration are made, similar to Figure A20. However, respiratory variation from expiration is determined by the formula (expiration − inspiration)/expiration or, in this example, (21 − 41)/21 = −95%. A >40% respiratory variation of tricuspid inflow is considered consistent with CP. Similar to mitral inflow respiratory variation, maneuvers may be required to demonstrate to demonstrate respiratory variation.

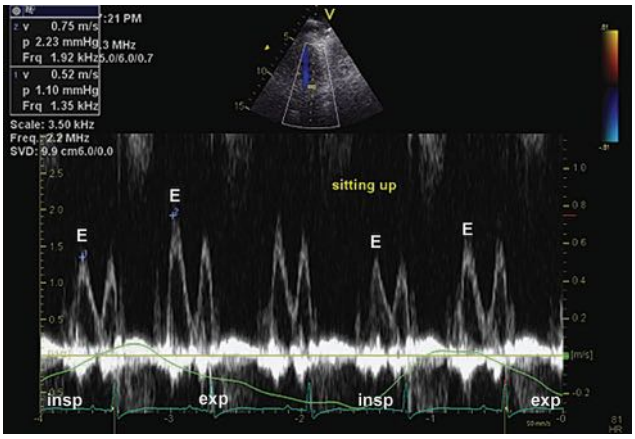

Figure A25 CP: apical four-chamber view with PW Doppler of the mitral inflow in a patient with CP. The study is performed with the patient in the upright position to decrease preload and increase respiratory variation. Marked respiratory variation of mitral inflow E wave is apparent. This maneuver should be performed if CP is suspected but not readily evident in the basal state.

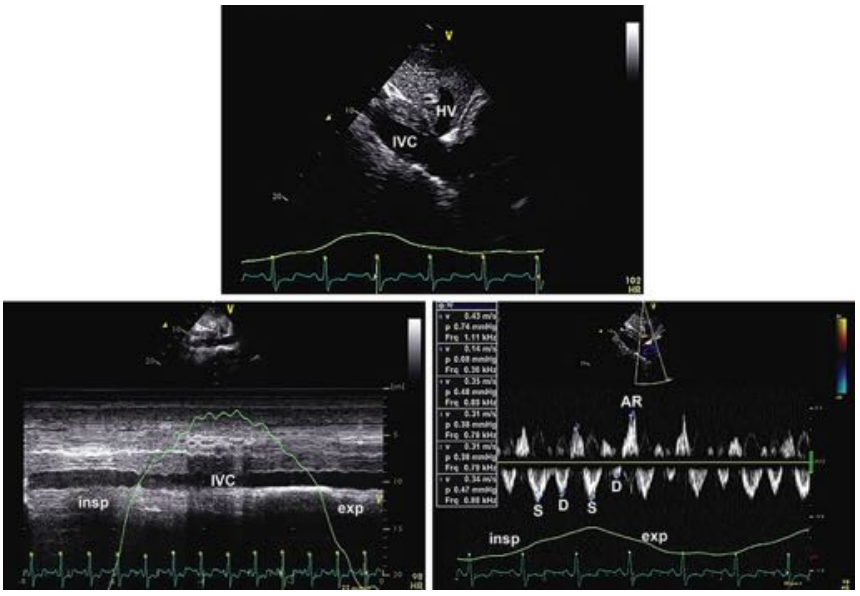

Figure A26 CP: subcostal view in a patient with CP. (*Top*) A dilated IVC and hepatic vein (HV) (Video A12); (*left*) M-mode demonstrating a dilated and plethoric IVC; (*right*) HV flow with reduced diastolic (D) flow during expiration and prominent AR reversals during expiration.

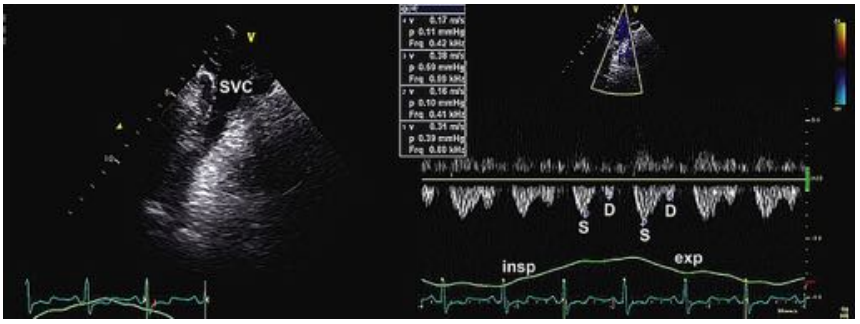

Figure A27 CP: SVC flow as obtained from the right subclavicular fossa in a patient with CP. (*Left*) A 2D image of the SVC (Video A13). (*Right*) S and D waves appearing similar to hepatic vein flow. Note the lack of significant respiratory variation of systolic flow in CP, which is different from the finding of marked respiratory variation of systolic flow noted in chronic obstructive pulmonary disease.

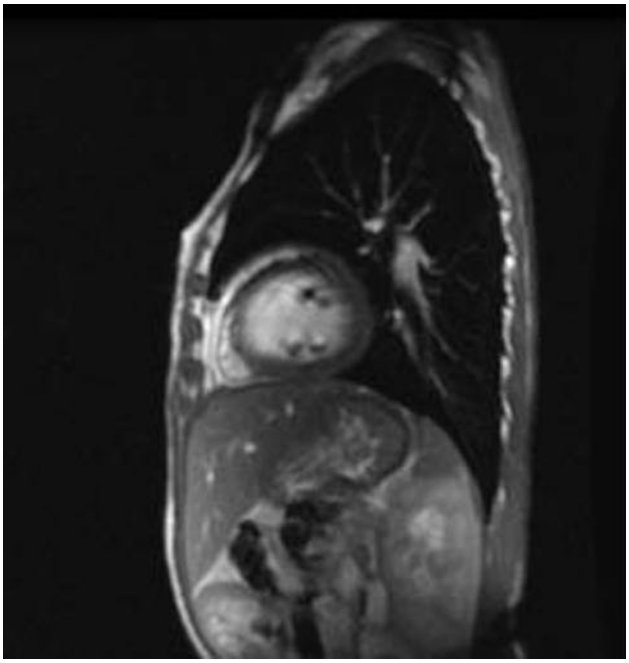

Figure A28 Nongated SSFP localizer.

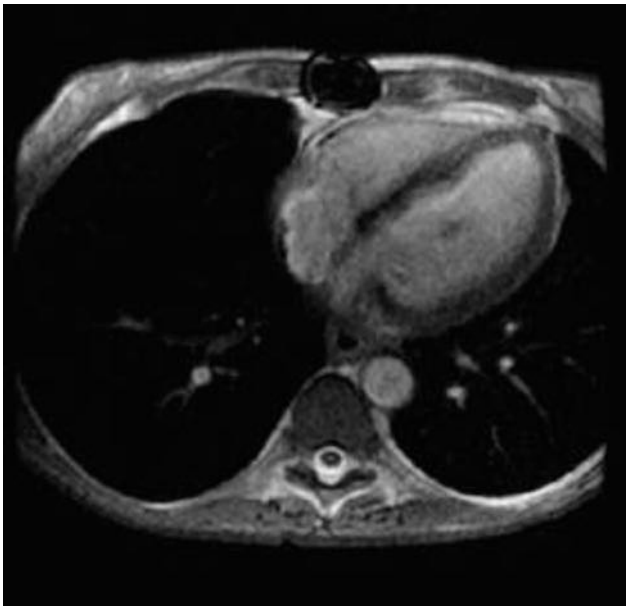

Figure A30 Nongated SSFP localizer.

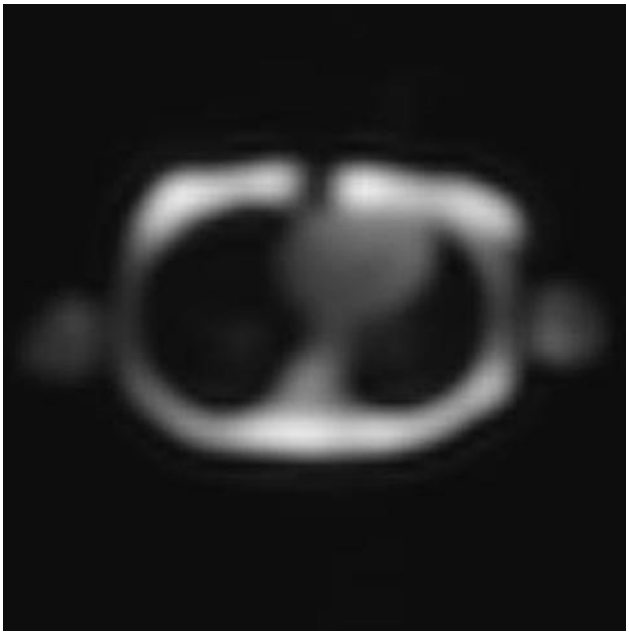

Figure A29 ASSET calibration.

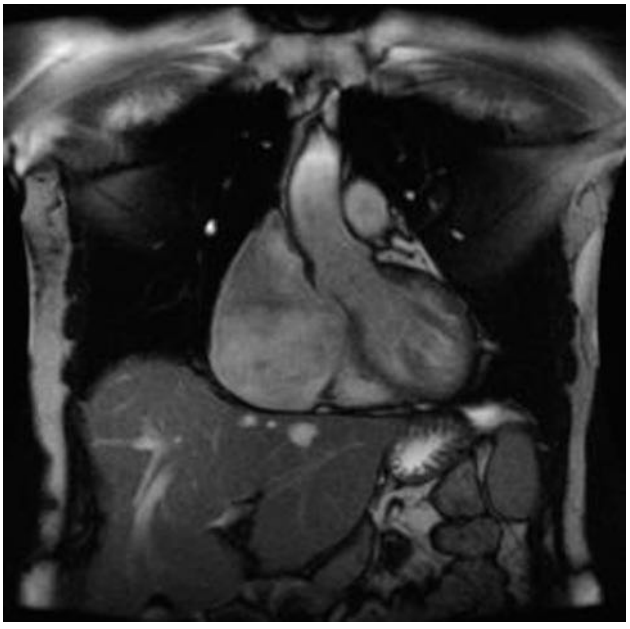

Figure A31 Nongated SSFP localizer.

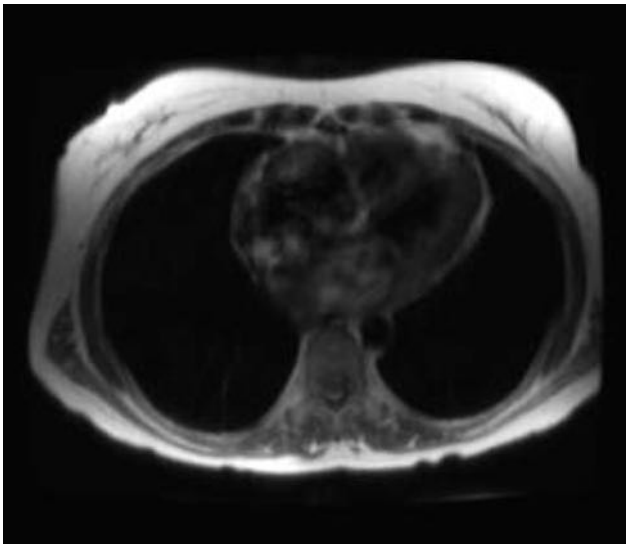

Figure A32 Nongated single-shot FSE localizer (half Fourier acquisition single-shot turbo spin-echo, etc.).

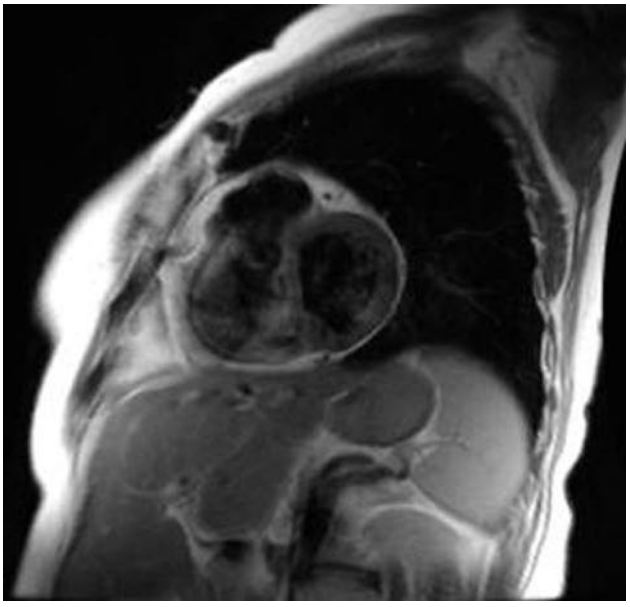

Figure A34 PD/T2 dual-echo FSE.

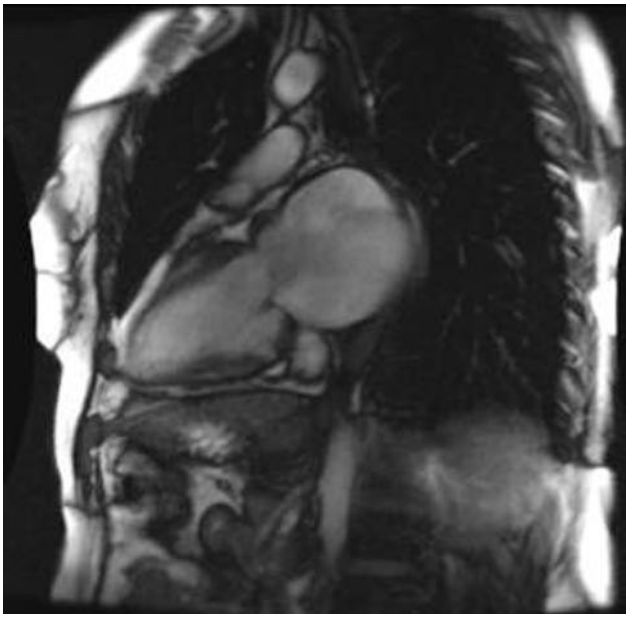

Figure A33 Cine SSFP.

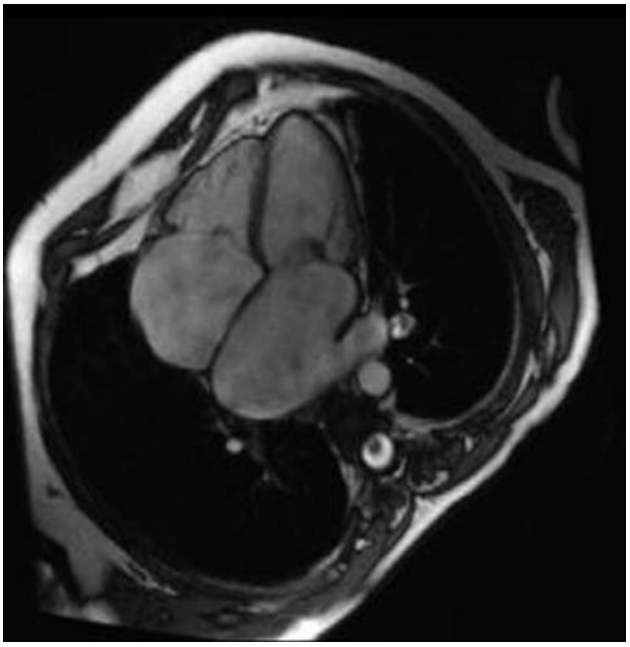

Figure A35 Cine SSFP (FIESTA).

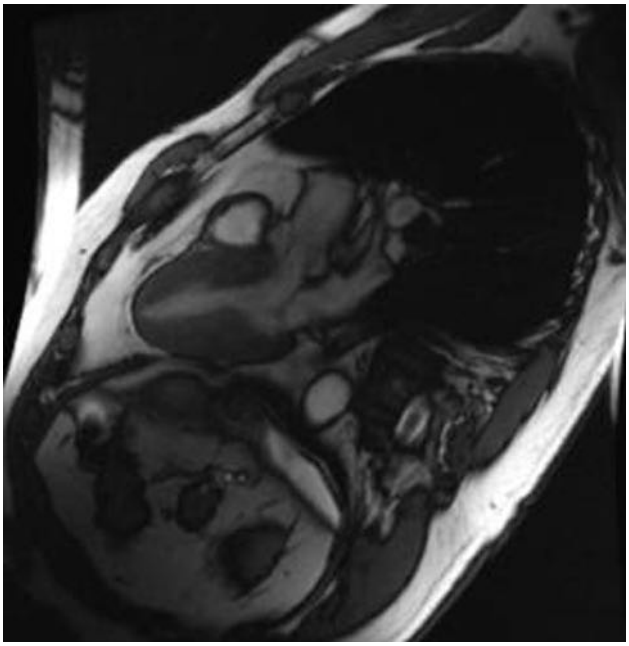

Figure A36 Cine SSFP (FIESTA).

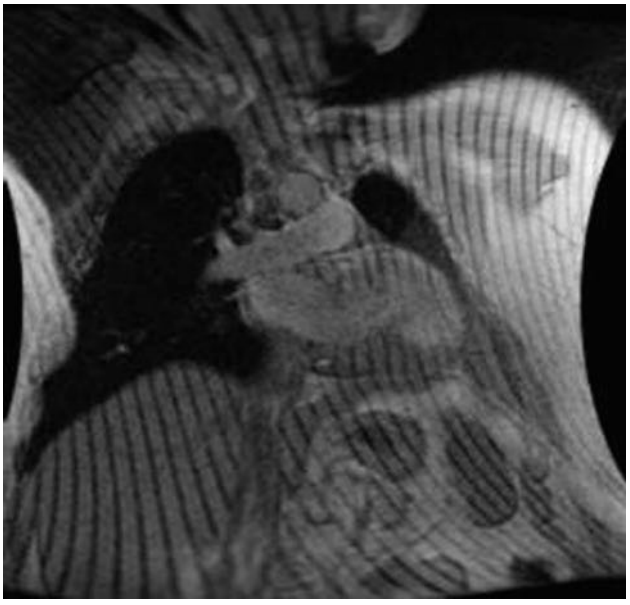

Figure A38 Tagged gradient echo (OPTIONAL).

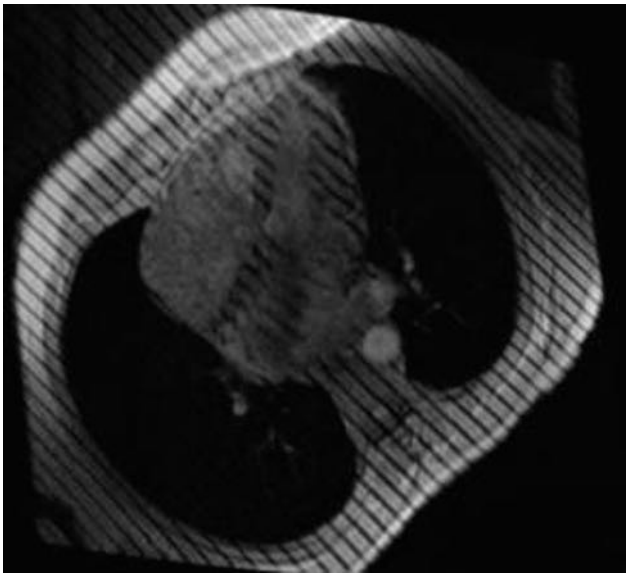

Figure A37 Tagged gradient echo (for constriction only).

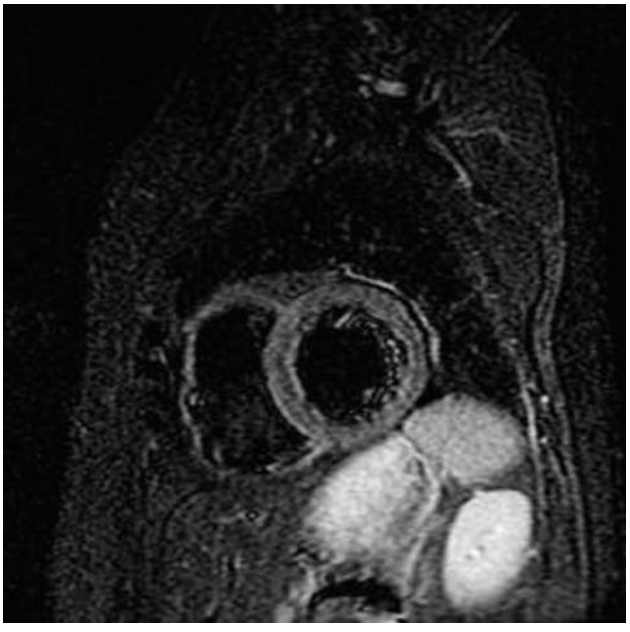

Figure A39 Double inversion-recovery T2 FSE.

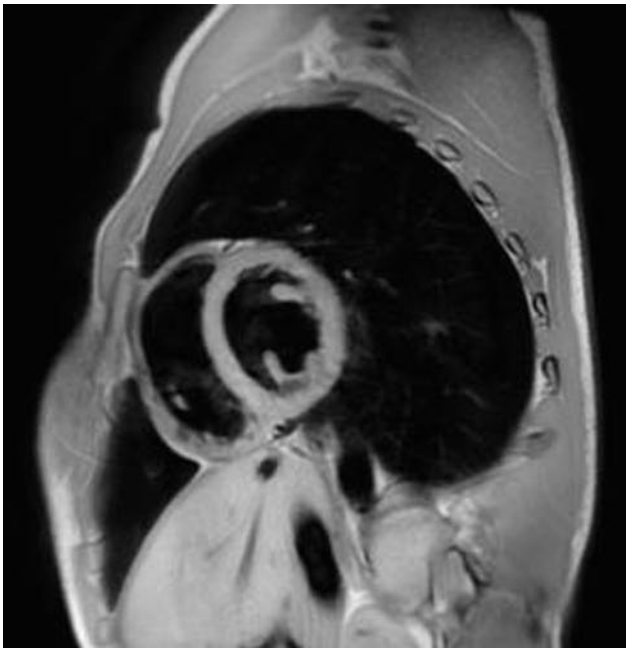

Figure A40 FSE (OPTIONAL).

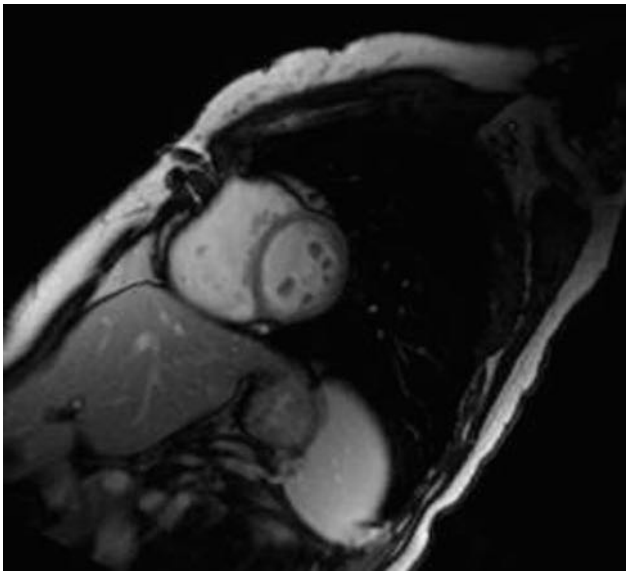

Figure A42 Cine SSFP.

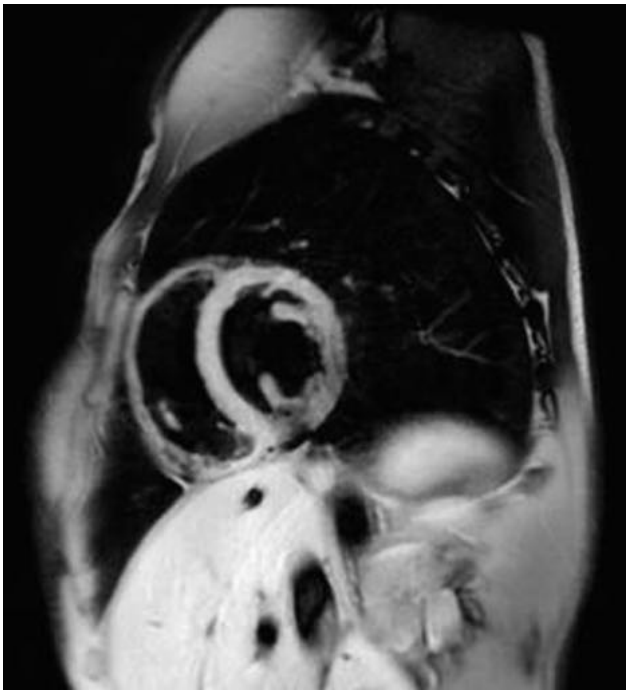

Figure A41 T1 SE after gadolinium (OPTIONAL).

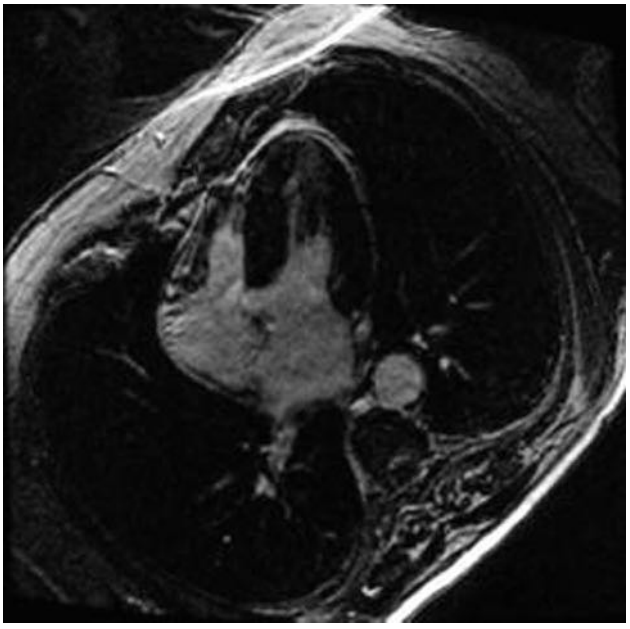

Figure A43 3D MDE.

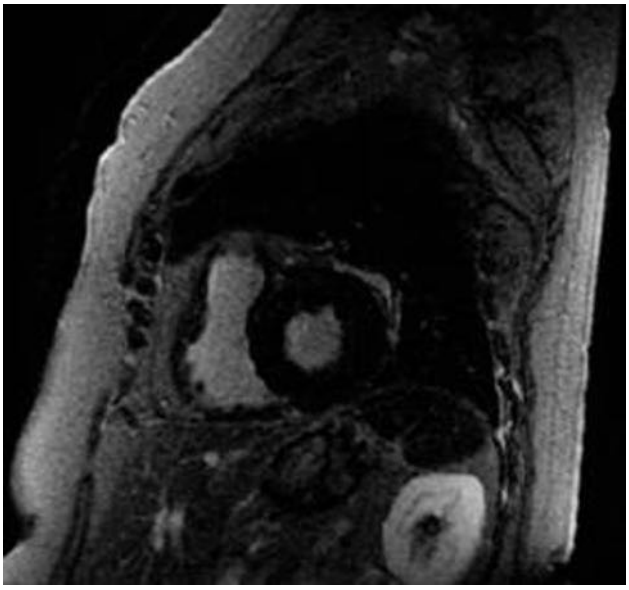

Figure A44 3D MDE.

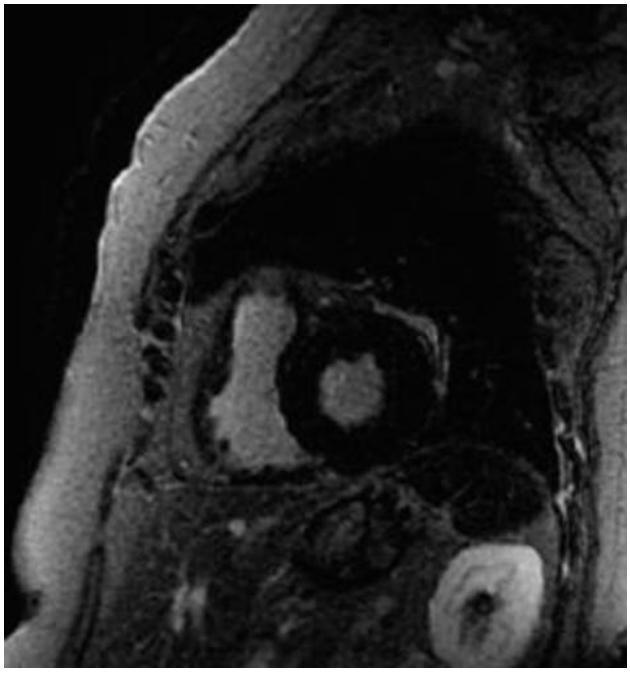

Figure A46 2D MDE.

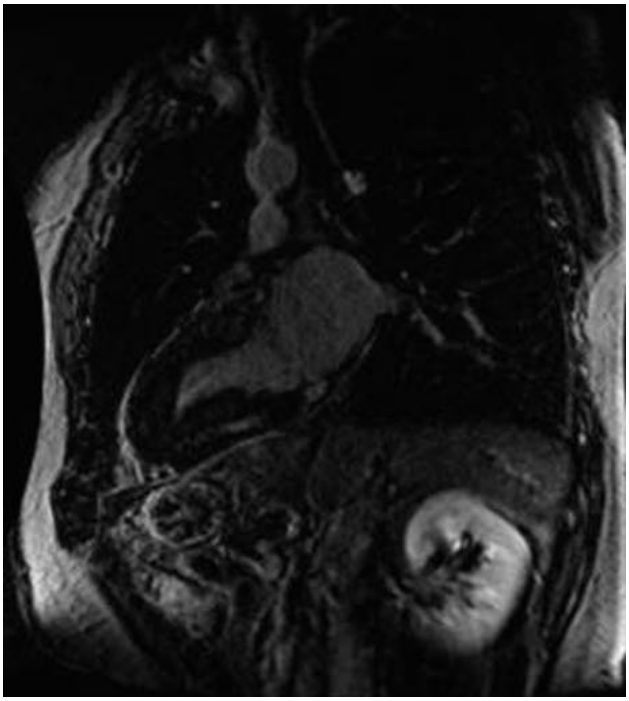

Figure A45 3D MDE.

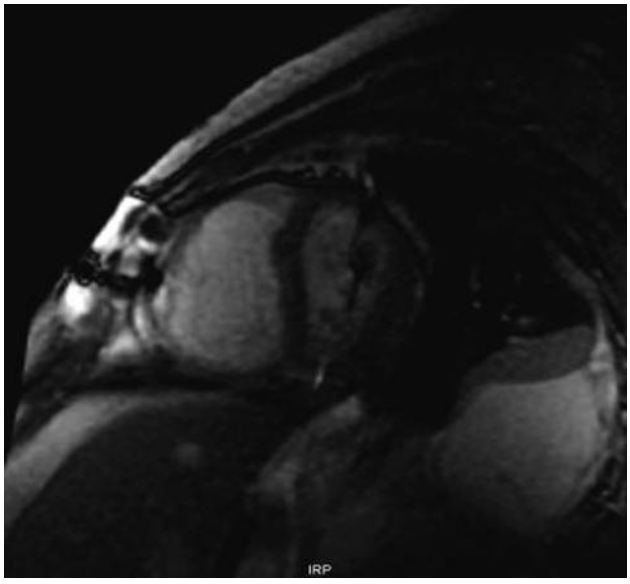

Figure A47 Real-time MR echo SSFP.

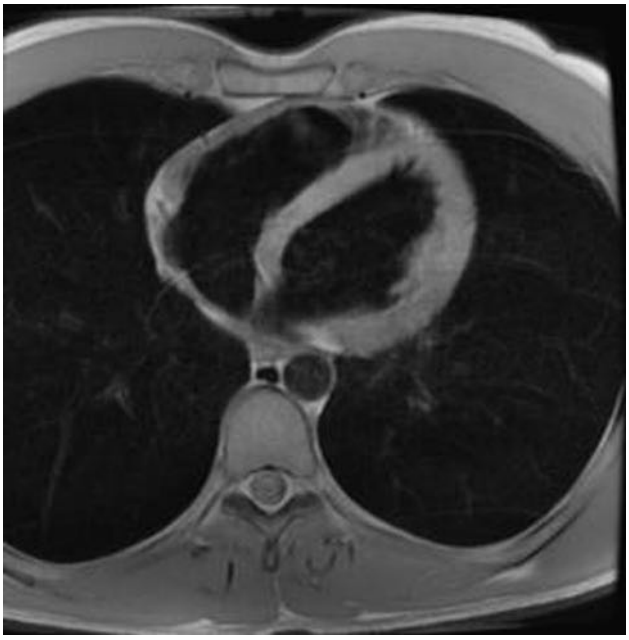

Figure A48 Double inversion-recovery T1 FSE.

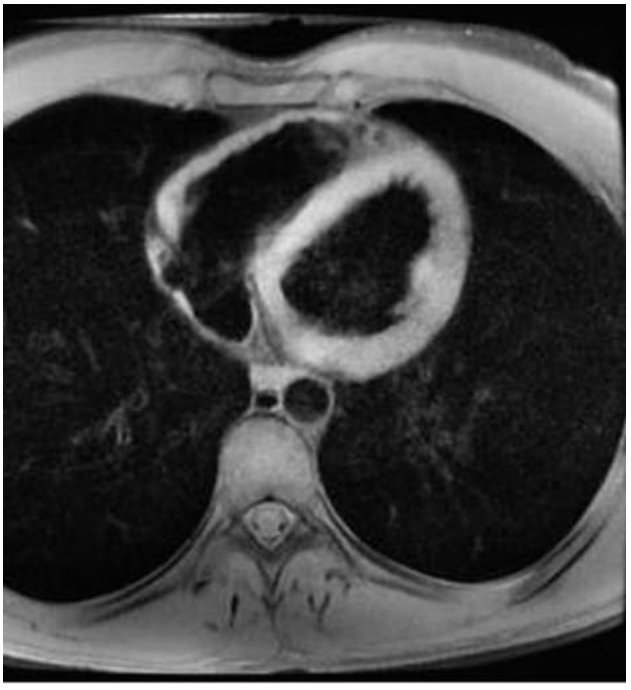

Figure A49 Double inversion-recovery T1 FSE postcontrast.